ELECTRON CORRELATION EFFECTS ON NUCLEAR MAGNETIC RESONANCE SPIN-SPIN COUPLING CONSTANT CALCULATIONS

By

S. AJITH D. PERERA

A DISSERTATION PRESENTED TO THE GRADUATE SCHOOL
OF THE UNIVERSITY OF FLORIDA IN PARTIAL FULFILLMENT
OF THE REQUIREMENTS FOR THE DEGREE OF
DOCTOR OF PHILOSOPHY

UNIVERSITY OF FLORIDA

1996

To my parents

ACKNOWLEDGMENTS

A great many people have contributed to the success of this dissertation.

I would especially like to thank my advisor, Rod Bartlett, for the role he played in my graduate student career. He is an inspirational teacher and continuous source of new ideas. His enthusiasm and constant encouragement of my research was a great inspiration, and his influence has changed my outlook significantly. Amidst a very busy schedule, he always had time to discuss my progress and offered help on problems. Once again my wholehearted thanks go to him.

Over the last few years, I have collaborated with many people in the Bartlett research group. Among them, first I would like to thank Dr. Marcel Nooijen. I enjoyed discussions with him, though they lasted long. He played a major role in the success of this dissertation not only by collaborating in some of the work described in this disserattion but also by carefully reading a preliminary version and suggesting improvements. A word of gratitude goes to Drs. Hideo Sekino, John D. Watts and David E. Bernholdt with whom I have had close collaborations on several research projects, for sharing their knowledge and offering me help without any reservation.

A special word of thanks goes to Dr. Keith Runge for leaving his door open for all my questions. I benefited enormously from discussions with him on many different subjects, and his encouragement and concern was a great inspiration.

His invaluable comments on a preliminary version of this dissertation contributed in many ways to its present form.

Drs. (Mrs.) Renee Peloquin Mattie, (Miss.) Anna Balkova, Nevin Oliphant, John Stanton, Leszek Meissner and Stanislaw Kucharski offered me help one time or another and my sincere thanks goes to them too.

My sincere gratitude goes to Mr. Sullivan Beck for his first few lessons on unix and for helping me on a great many other occasions. I had the luxury of being one of those whom he would not ask to read the manual, when I had questions concerning the computers. In my graduate student life, I was fortunate to meet Mr. Jorge Morales, Miss. Lynn Salemi, Mr. Steve Gwaltney, Mr. Piotr Rozyczcko, Dr. Junqiang Sun, Dr. Marshal Cory, Miss. Ya-Wen Hsiao, Mr. Cristian Cardenas-Lailhacar, Mr. Joaquim D. Motta, Mr. Juan Oreiro, Dr. Herbert Da Costa, Dr. Xuehe Zheng and Mr. Srinivasan Iyengar with whom I had shared office space or had many discussions about science and life in general. Steve and Piotr offered me help a great many times. Steve always suprised me in giving statistics on any point we argued. Lynn and Jorge are really true friends, being with me in good times and also in bad times. All of them have my deepest appreciation.

My mom and brothers Dhammika, Rohan and Chandana, offered me moral support throughout my studies and have shown utmost understanding. Mr. and

Mrs. Richard and Cynthia Newberg shared their warm hospitality and I always felt at home at their house. I enjoyed the company of Pathmalal, Thishya, Natalie and Ruvani and they helped me in many ways on many occasions. Words cannot express my gratitude to these wonderful people.

Mrs. Ewa Rozyzcko, Mr. Rodney and Richard Sarkees are very special friends and deserve a special word of thanks.

TABLE OF CONTENTS

ACKNOWLEDGMENTS iii

ABSTRACT ix

CHAPTERS

1. INTRODUCTION 1

2. MOLECULAR RELATIVISTIC HAMILTONIANS: AN OVERVIEW . 11

Introduction 11

Dirac's One-Fermion Theory 12

Relativistic Many-Fermion Hamiltonians 17

The Non-Relativistic Form of the Molecular Relativistic Hamiltonian. 28

The NMR Chemical Shifts and Indirect Nuclear Spin-Spin Coupling Operators 53

Conclusion 63

3. MOLECULAR STATIC SECOND-ORDER PROPERTIES 64

Introduction 64

Some Basic Preliminaries 70

Fock Space 70

Hartree-Fock Approximation 72

Second Quantization and Normal Order 74

Energy Derivatives 78

Spin Hamiltonian 78

The Hartree-Fock Analytical Energy Derivatives 81

Coupled Cluster Energy Derivatives and EOM-CCSD Models for Second-Order Properties 96

4. THEORETICAL CALCULATION OF INDIRECT NUCLEAR SPIN-SPIN COUPLING CONSTANTS: AN HISTORICAL PERSPECTIVE 108

Introduction 108

Theoretical Indirect Nuclear Spin-Spin Coupling Constants 108

Conclusions 113

5. A CRITICAL ASSESSMENT OF THE EOM-CCSD METHOD FOR INDIRECT NUCLEAR SPIN-SPIN COUPLING CONSTANT CALCULATIONS 5.116

Introduction 116

Basis Set Dependence and Electron Correlation Effects on Nuclear Spin-Spin Coupling Constants Within the EOM-CCSD Method. . . . 118

Direct Comparison of the EOM-CCSD Method with Other Theoretical Methods and Experiment 143

Conclusions 153

6. NMR SPECTRA OF ALKYL CARBOCATIONS 158

Introduction 158

The Ethyl Carbocation ($C_2H_5^+$) 160

2–Nobornyl Cation ($C_7H_{11}^+$) 170

Conclusions 182

7. APPLICATION OF EOM-CCSD NMR SPIN-SPIN COUPLING CONSTANTS IN CONFORMATIONAL ANALYSIS 185

Introduction 185

NMR Spin-Spin Coupling Constants of Formamide ($HCONH_2$) and N-methylacetamide ($CH_3NHCOCH_3$) 191

Conclusions 206

BIBLIOGRAPHY 209

BIOGRAPHICAL SKETCH 226

Abstract of Dissertation Presented to the Graduate School
of the University of Florida in Partial Fulfillment of the
Requirements for the Degree of Doctor of Philosophy

ELECTRON CORRELATION EFFECTS ON NUCLEAR MAGNETIC RESONANCE SPIN-SPIN COUPLING CONSTANT CALCULATIONS

By

S. AJITH D. PERERA
May, 1996

Chairman: Prof. Rodney J. Bartlett
Major Department: Chemistry

This work involves development and implementation of equation-of-motion coupled cluster singles and doubles (EOM-CCSD) quadratic and CI-like methods, in order to carry out quantitative NMR spin-spin coupling constant calculations for medium size molecules. The EOM-CCSD method for general second-order properties is derived within the so-called quadratic and CI-like approximation from coupled cluster (CC) energy derivative theory. Appropriate atomic basis integrals over Gaussian basis functions required for NMR spin-spin coupling constant calculations and the EOM-CCSD models for general second-order properties have been implemented and their performance is examined for a variety of molecules. In these calibration studies, we focus on the effects of the quadratic contribution, magnitude of the non Fermi-contact contributions, effects of the atomic basis set employed and electron correlation on NMR spin-spin coupling constant calcula-

tions within the EOM-CCSD quadratic and CI-like approximations. The results are found to be generally good, providing 13.9, 8.4, 7.3 and 7.6 mean absolute percent deviation from experiment, respectively, for DZP, TZP, Chipman and QZP basis sets. The overall mean absolute error of the EOM-CCSD results compared to experiment is 7%. The Fermi-contact contribution usually constitutes the largest portion of the total coupling constant. However, there are instances that the non-contact contributions are dominating, for example, HF and N_2 molecules. Moreover, for quantitative accuracy all four contributions need to be incorporated.

Several interesting applications of the EOM-CCSD method have been reported. First, we consider the NMR spin-spin coupling constants of alkyl carbocations. In some cases, the species under consideration is unstable and the direct measurement of the NMR spectrum is impossible, for example, $C_2H_5^+$. For such a situation, the EOM-CCSD results provides quantitative NMR spin-spin coupling constants to fill voids in the NMR data of carbocations and to offer "fingerprint" for detection. In other instances, our calculated results assist or corroborate experimental spectral assignments. Finally, the variation of NMR spin-spin coupling constants with the dihedral angle ϕ of N-methylacetamide ($CH_3NHCOCH_3$, the dihedral angle ϕ is the angle between hydrogen atoms in CH_3NH fragment) has been studied. N-methylacetamide has been widely used to mimic the peptide bond in proteins, and the resulting Karplus type relation will be useful for conformational analysis of peptides.

CHAPTER 1
INTRODUCTION

Nuclear magnetic resonance (NMR) spectroscopy, invented by Purcel and Bloch in 1946, has become one of the most valuable spectroscopic tools with a wide variety of applications in diverse areas such as biology, medicine and chemistry. In chemistry, NMR spectroscopy is mainly used for structure elucidations, compound identification, and conformational analysis. The relative shieldings (chemical shifts) and indirect nuclear spin-spin coupling constants measured in an NMR experiment correlate with the structure and conformation of molecules. The accurate measurement of chemical shifts and correlation of them with molecular structures is relatively easy compared to the use of spin-spin coupling constants and consequently, chemical shifts are more commonly used in structure elucidations. With the use of modern high resolution NMR spectrophotometers, nuclear spin-spin coupling constants can be measured increasingly accurately and on a wide variety of systems. As a result, their application in structure elucidations has witnessed a dramatic growth, particularly in the areas of conformational analysis of proteins, nucleic acids and polysaccharides. In some instances completely novel coupling phenomena have been observed [1]. Sophisticated theoretical analysis is required to sort out the subtleties involved in correlating the spin-spin coupling mechanisms to the electronic structure of molecules and also to find explanations for new coupling phenomena. There are instances in which the coupling constants of interest cannot be measured directly and the relevant information requires theoretical calculations.

In the last few decades, through an increase in computational power and methodological sophistication, theoretical chemists have been able to tackle increasingly complex systems with higher accuracy. As an example, rigorously gauge-origin-independent, quantitatively accurate, chemical shift calculations for medium-size molecules (up to eight to ten non-hydrogen atoms) can be done routinely today. In spite of the continuous effort from various theoretical research groups, quantitative calculations of NMR spin-spin coupling constants still present a challenge to theoreticians. Both theoretical and technical advances made in recent years led to methods which give quantitative NMR spin-spin coupling constants. However, their applications are limited to smaller molecules mainly due to limitations in the computer implementations.

Having reliable theoretically calculated NMR spin-spin coupling constants is an important component of using experimentally determined spin-spin coupling constants in spectral analysis. For example, consider the application of NMR spectroscopy in the structure elucidation of carbocations. The alkyl carbocations can exist in classical form (contain an sp^2 hybridized electron-deficient carbon atom) or nonclassical bridged form (contain penta or higher coordinated carbon atoms), and the preferred stable form has often led to controversies. NMR spectroscopy assisted by crude theoretical estimates of chemical shifts and spin-spin coupling constants has been used extensively to resolve this problem. However, the absence of reliable theoretical results sometimes led to ambiguities in spectral assignments and thus inconclusive results. In some cases neither form is stable enough to observe experimentally and a theoretical prediction of NMR parameters becomes essential. The NMR spectra of isomers quite usually are similar, and often it is difficult to assign a particular spectrum to one isomer or the other without theoretical support. In some cases the NMR spectrum is complicated and theoretically calculated results are required for correct assignments. For such applications the accuracy of the calculated results is crucial since there might be several coupling constants which differ by a few Hz.

The NMR chemical shifts and spin-spin coupling constants are in general sensitive only to the local environment of the nuclei of interest. This is a quite useful property since it allows the use of a small model system which mimics the local region of interest of a molecule. This strategy often can be exploited for large molecules which are not amenable to high-level theoretical calculations.

Another important application of theoretical NMR parameters is in conformational analysis, in particular conformational analysis of amino acids, proteins *etc.* For example, vicinal proton-proton coupling constants have been used to estimate the relative populations of the three staggered rotamers in $\alpha-$amino acids and derivatives [2]. The general idea stems from the fact that the NMR spectrum of a sample which consists of a mixture of conformers in dynamic equilibrium corresponds to an average of all the conformers over the NMR time scale. One important question in conformational analysis is the relative populations of the individual conformers in the mixture. We can relate the experimentally determined average coupling constants with the corresponding coupling constants in the individual conformers and their relative populations. The number of conformers should be small enough to define a solvable problem using the limited number of coupling constants avaliable. The individual conformers are thermally unstable to observe directly in an NMR experiment, hence one has to calculate them theoretically. Conformations of amino acid residues in proteins have been determined by measuring their NMR spin-spin coupling constants.

For example, the two dihedral angles ϕ_i and ψ_i depicted in Fig. 1.1 which describe the conformation of the peptide link can be related to the coupling constants such as $^3J(NH)$, $^3J(HH)$, $^1J(CN)$ *etc.*

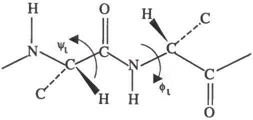

Figure 1.1. A fragment of a peptide chain.

These empirical relations usually are derived by studying model systems which can mimic the peptide linkages, for example, N-methylacetamide, alanine dipeptide *etc.* To establish such relations requires a knowledge of the spin-spin coupling constants of the model system for different values of dihedral angle. Quantitatively accurate theoretical methods are required to evaluate these since the individual conformers corresponding to different dihedral angles cannot be observed experimentally. Theory is the only recourse for information on such short lived species.

In non-relativistic theory, the NMR spin-spin coupling constant has four contributions: the Fermi-contact (FC), spin-dipole (SD), paramagnetic spin-orbit (PSO) and diamagnetic spin-orbit (DSO) contributions. Experimentally measured spin-spin coupling constants correspond to the sum of these four contributions. The individual contributions have no separate physical significance and are not observables. Nevertheless, knowledge of the magnitude of individual contributions can be useful to identify various coupling mechanisms and also to develop various qualitative interpretative tools.

Having discussed the possible application of theoretically calculated NMR spin-spin coupling constants, it is clear that to be truly useful, the theoretical methods employed to calculate NMR spin-spin coupling constants must be accurate and reliable and also applicable to medium-sized molecules. The subject of this dissertation, the effects of electron correlation nuclear magnetic resonance spin-spin coupling constant calculations, was undertaken in response to this need.

In chapter 1 a systematic development of the non-relativistic approximation of the relativistic many-electron Hamiltonian is presented. After introducing Dirac's one-fermion Hamiltonian, the starting point for our derivation, we discuss the problems associated with developing relativistic many-electron Hamiltonians. As will be discussed in chapter 1, a simple-minded extension of Dirac's one-particle picture to many-particle systems does not give a proper relativistic many-electron Hamiltonian. Next we review briefly recent developments for many-electron Hamiltonians based on quantum electrodynamics (QED). The resulting QED or no-pair Hamiltonians do not suffer from the problems associated with Hamiltonians derived from the direct extension of Dirac's equation. Next we discuss the development of the non-relativistic two-component form of the relativistic many-electron Hamiltonians. A comprehensive account of decoupling schemes, including the potential singularity problems in the expansion in terms of α^2 (where α is the fine structure constant) is also given. Finally we present the Hamiltonian we use to describe the NMR spectra with a thorough account of the origin of each term.

In chapter 2 the development of the computational methods pertinent to the present study is given. After introducing the necessary preliminaries (Fock space, Hartree-Fock theory, second-quantization) we proceed to discuss the spin-Hamiltonian which will introduce the chemical shift and indirect nuclear spin-spin coupling constant tensors. Next we consider the coupled perturbed Hartree-

Fock theory (CPHF) and equation-of-motion coupled cluster singles and doubles (EOM-CCSD) methods as means of evaluating NMR spin-spin coupling constants. Equations for general second-order properties at the HF level based on analytical energy derivative theory are presented. Similarly, expressions are derived for the coupled cluster singles and doubles (CCSD) model using analytical derivative theory. This led to a method for general second-order properties known as the EOM-CCSD quadratic method. In taking the derivative, orbital relaxation effects are neglected as they have shown to be relatively unimportant for coupled cluster (CC) reference state [3, 4]. This form lacks the convenient, familiar second-order perturbation theory expression. Alternatively, we can insist upon that form by reanalyzing the quadratic term in the CCSD energy derivative expression to obtain a convenient CI-like approximation. The ground and excited state wave functions that enter into a sum-over-state expression are eigenfunctions of the CCSD effective Hamiltonian and establish the connection to the EOM-CC methods for excited states [5]. The sum-over-state expression describes the EOM-CCSD CI-like approximation to the general second-order properties. Detailed equations which are being used for computer implementations are given.

In chapter 3 we review the existing literature on NMR spin-spin coupling constant calculations briefly. A chronological account of the development of computational methods and an assessment of the quality of the numerical results obtained by using these methods is given. The current state of the art in the theoretical calculation of NMR spin-spin couplings constants, and the exciting new experiments which require more elaborate theoretical analysis are discussed in chapter 3. We also identify both conceptual and technical problems associated with the theoretical calculation of NMR spin-spin coupling constants.

Chapter 4 is devoted to applications of EOM-CCSD methods to various molecules in order to calibrate the EOM-CCSD results with respect to the experimental results. A systematic study of the effects of the quadratic contribution, effects of the atomic basis set employed, and electron correlation on NMR spin-spin coupling constant calculations within the EOM-CCSD quadratic and CI-like approximations is presented. In chapter 4 we also consider direct comparison of the EOM-CCSD quadratic method and CI-like approximation with other quantitative correlated methods such as the polarization propagator and multiconfiguration linear response methods.

In chapter 5 we employ the EOM-CCSD method to calculate NMR spin-spin coupling constants of selected carbocations. The main focus of this chapter is on NMR spin-spin coupling constants of alkyl carbocations. However, for completeness, we also report the NMR chemical shifts based on gauge-independent atomic orbitals (GIAO) obtained at the second-order perturbation theory (MBPT(2)) level. Here, we have chosen two alkyl carbocations. First, the ethyl carbocation which is not stable enough to isolate, enabling our calculated results to provide much needed NMR data for this prototypical alkyl carbocation. The second sytem we consider is the 2–norbornyl carbocation which has been the focal point of the classical versus nonclassical ion controversy. In this case, we provide much needed theoretical support for the experimental NMR assignments reported by Olah *et al.* [6] and several other research groups, thereby reaffirming the stable nonclassical form of the norbornyl carbocation.

In chapter 6 application of the EOM-CCSD NMR spin-spin coupling constants in conformational analysis is considered. The variation of vicinal NMR spin-spin coupling constants with the dihedral angle between the coupled nuclei can be described by mathematical relations of the form

$$^3J = Acos^2\phi_i + Bcos\phi_i + C \tag{1.1}$$

commonly known as "Karplus-like relations" (where the dihedral angle ϕ_i is shown in Fig. 6.1). Given the experimentally measured ^3J and independently determined *A*, *B* and *C*, one can calculate the dihedral angle and hence the conformation. Such a technique has been used in the determination of the conformation of open chain and cyclic organic molecules, particularly polypeptides and other biologically interesting molecules. *A*, *B* and *C* usually are determined by employing approximate theoretical models to calculate the spin-spin coupling constant as a function of the dihedral angle of a small model system which can mimic the bonding situation of interest. The reliability of this approach depends on the accuracy of the calculated NMR spin-spin coupling constants and the transferability of "Karplus-like relations" based on a model to a molecule which has a completely different surrounding chemical environment from the model system. Systematic studies based on quantitatively accurate NMR spin-spin coupling constants are required to establish quantitatively accurate correlations that can be used reliably in conformational analysis. In chapter 6, we present an application of the EOM-CCSD method to investigate the variation of ${}^{3}J({}^{1}\mathrm{H}{}^{1}\mathrm{H})$ in N-methylacetamide ($CH_3NHCOCH_3$) as a function of the dihedral angle. N-methylacetamide is widely used to model peptide links and is accessible to high-level correlated calculations. In principle, the constants A, B and C reported in this work must be a significant improvement over the ones currently being used. The problems associated with employing relations similar to Eqn. 1.1 in conformational analysis are addressed, and that chapter. It also sets the stage for future systematic investigations of this interesting, synergistic application of the calculated and experimentally measured NMR spin-spin coupling constants.

CHAPTER 2
MOLECULAR RELATIVISTIC HAMILTONIANS: AN OVERVIEW

2.1 Introduction

In this chapter, a systematic development of relativistic molecular Hamiltonians and various non-relativistic approximations are presented. The discussion is mainly pedagogical and also establishes the notation used in subsequent chapters. Our starting point is the Dirac one-fermion Hamiltonian in the presence of an external electromagnetic field. The problems associated with generalizing "Dirac's one-fermion theory" smoothly to more than one fermion are discussed. The description of many-fermion systems within the framework of quantum electrodynamics (QED) will lead to Hamiltonians which do not suffer from the problems associated with the direct extension of "Dirac's one-fermion theory" to many-fermion systems. An exhaustive discussion of the recent QED developments in the relevent area is not presented, except for cursory remarks for completeness. The non-relativistic form of the many-electron relativistic Hamiltonian is developed as the working Hamiltonian. It is used to extract operators for the observables which represent the response of a molecule to an external electromagnetic radiation field. In this study our focus is mainly on the operators which eventually were used to calculate the nuclear magnetic resonace (NMR) chemical shifts and indirect nuclear spin-spin coupling constants.

2.2 Dirac's One-Fermion Theory

The relativistic one-fermion equation in the free field presented by Dirac in 1928 [7, 8] is usually written in the contravariant form, which illustrates the relativistic equivalence of space and time in an elegant way

$$i\frac{\partial\psi}{\partial t} = [c(\boldsymbol{\alpha}.\mathbf{P}) + \boldsymbol{\beta} mc^2]\psi \tag{2.2}$$

where *m* and *c* are the rest mass of the particle and the velocity of light in atomic units, respectively. Here, the bold face letters represent both matrices and vectors interchangeably. The linear momentum operator **P**, is given by

$$\mathbf{P} = -i\nabla = -i(\mathbf{i}\frac{\partial}{\partial x} + \mathbf{j}\frac{\partial}{\partial y} + \mathbf{k}\frac{\partial}{\partial z}) \tag{2.3}$$

The components of the $\boldsymbol{\alpha}$ and $\boldsymbol{\beta}$ operators are independent of space and time coordinates and satisfy the anticommutator relationship

$$[\boldsymbol{\alpha}_\mu, \boldsymbol{\alpha}_\nu]_+ = 2\delta_{\mu\nu} \qquad (\mu, \nu = \mathrm{o}, x, y, z) \tag{2.4}$$

where we have used

$$\boldsymbol{\beta} = \boldsymbol{\alpha}_\mathrm{o} \tag{2.5}$$

and *x*, *y* and *z* are the three components of the spatial coordinate vector **r**. The components of α and β operators in matrix representation are 4 X 4 matrices, and are usually written in the form

$$\alpha_x = \begin{bmatrix} 0 & \sigma_x \\ \sigma_x & 0 \end{bmatrix} \quad \alpha_y = \begin{bmatrix} 0 & \sigma_y \\ \sigma_y & 0 \end{bmatrix} \quad \alpha_z = \begin{bmatrix} 0 & \sigma_z \\ \sigma_z & 0 \end{bmatrix}$$
$$\beta = \alpha_o = \begin{bmatrix} \mathbf{I} & \mathbf{0} \\ \mathbf{0} & -\mathbf{I} \end{bmatrix} \tag{2.6}$$

where σ's are the Pauli spin matrices [9]; **I** and **0** are the 2 X 2 unit and null matrices respectively. The Dirac spinor

$$\psi = \psi(\mathbf{r}, t) = \begin{pmatrix} \phi_1(\mathbf{r}, t) \\ \phi_2(\mathbf{r}, t) \\ \phi_3(\mathbf{r}, t) \\ \phi_4(\mathbf{r}, t) \end{pmatrix} \tag{2.7}$$

is a function of spatial (**r**) and time (*t*) coordinates.

Lengthy accounts of the properties and physical interpretation of the Dirac equation can be found in several standard text books [10–12], and will not be repeated here. However, some important points will be addressed below.

The Dirac equation is invariant to Lorentz transformations [13], a necessary requirement of a relativistic equation. In the limit of large quantum numbers the Dirac equation reduces to the Klein-Gordon equation [14, 15]. The time-independent form of Dirac's Hamiltonian is given by

$$[c(\boldsymbol{\alpha}.\mathbf{P}) + \beta mc^2]\psi = \mathrm{E}\psi \tag{2.8}$$

This can be easily derived from Eqn. 2.2 by standard separation of variables technique where the quantity E is the total energy of the system. Note that in the time-independent Dirac equation the frame of reference is fixed. The energy spectrum of the Dirac equation is unbounded both from above and below, and has both positive and negative energy solutions. As an example, in the Dirac picture, a free fermion has both a positive and negative continuum of energies, above mc^2 and below $-mc^2$ respectively. However, in the presence of an external field, the Dirac equation has a discrete spectrum of bound state solutions for values of the total energy E in the range of E $< mc^2$, in addition to the continuum states above mc^2 and below $-mc^2$ [16].

The presence of a negative continuum of energies leads to conceptual difficulties: there is no ground-state energy as in the case of non-relativistic theory, which suggests that the fermion may fall into the negative continuum of energy and attain infinitely low energy. Dirac circumvented this problem by redefining the vacuum state as the situation in which all the negative energy states are fully occupied and all the positive energy states are unoccupied. The Pauli exclusion principle prevents additional fermions from occupying the fully occupied negative energy states. Excitation of a fermion from the negative energy state to a positive energy state implies a creation of a hole in the negative energy continuum and a particle in the positive energy continuum. The negative energy solutions are then interpreted as solutions for such hole particles having a positive charge,

$+e$, positrons, while the positive energy solutions are interpreted as solutions for particles having an equal magnitude but opposite charge to the hole particles, $-e$, electrons. However, this interpretation is not free of problems either. One has to deal with the interaction of fermions with the background charge of an infinite "sea of fermions." This leads to infinities in the actual calculation of electron properties. On the other hand, Dirac's hypothesis does not apply to spinless particles, which do not obey the Pauli principle but which do have negative energy solutions. The problem was ultimately solved by renormalized quantum electrodynamics introduced in the late 1940's by Feynman, Dyson, Schwinger, Tomonaga and others [17–21].

In the presence of an external electromagnetic radiation field the Dirac equation for a fermion takes the form

$$[i\frac{\partial}{\partial t} - q\phi]\psi = [c(\boldsymbol{\alpha}.\mathbf{\Pi}) + \beta mc^2]\psi \tag{2.9}$$

where q is the charge of the fermion, $\phi = \phi(\mathbf{r}, t)$ is the scalar potential and $\mathbf{\Pi}$ is the modified canonical momentum of the fermion. The modified canonical momentum is given by

$$\mathbf{\Pi} = \mathbf{P} - \frac{q}{c}\mathbf{A} \tag{2.10}$$

where $\mathbf{A} = \mathbf{A}(\mathbf{r}, t)$ is the vector potential. Thus the introduction of coupling between particles and the radiation field corresponds to the substitution $(\mathbf{P} - \frac{q}{c}\mathbf{A})$

in Eqn. 1 instead of $\mathbf{P}$, a relation which is often referred to as the principle of minimal electromagnetic coupling. This relationship can be derived rigorously using quantum electrodynamics [22]. The attractive features of the free field Dirac Hamiltonian remain intact in the external electromagnetic radiation field Dirac equation. Alternatively, we can write the time independent form of Eqn. 2.9,

$$[\mathbf{h}_{\mathrm{D}} + \mathbf{V}_{\mathrm{ext}}]\psi = \mathbf{h}_{\mathrm{D,ext}}\psi = \mathrm{E}\psi \tag{2.11}$$

where, $\mathbf{h}_{\mathrm{D}} = \left[c(\boldsymbol{\alpha}.\mathbf{P}) + \boldsymbol{\beta}mc^2\right]$ and $\mathbf{V}_{\mathrm{ext}} = q[\phi\mathbf{I} - (\boldsymbol{\alpha}.\mathbf{A})]$, in which the external, field-dependent terms are grouped in $\mathbf{V}_{\mathrm{ext}}$ and $\mathbf{I}$ is the identity operator. As we will see later, the external electromagnetic field Dirac one-fermion equation as written in Eqn. 2.11 is more convenient for the discussion of many-fermion relativistic Hamiltonians.

It is also common in the literature to write the time independent Dirac equation in terms of Pauli-spin matrices,

$$\begin{pmatrix} (mc^2 + q\phi)\mathbf{I} & c\boldsymbol{\sigma}.\boldsymbol{\Pi} \\ c\boldsymbol{\sigma}.\boldsymbol{\Pi} & (-mc^2 + q\phi)\mathbf{I} \end{pmatrix} \begin{pmatrix} \psi_{\mathrm{L}} \\ \psi_{\mathrm{S}} \end{pmatrix} = \mathrm{E} \begin{pmatrix} \psi_{\mathrm{L}} \\ \psi_{\mathrm{S}} \end{pmatrix} \tag{2.12}$$

Here, $\psi_{\mathrm{L}} = \begin{pmatrix} \phi_1^{\alpha}(\mathbf{r},t) \\ \phi_2^{\beta}(\mathbf{r},t) \end{pmatrix}$ and $\psi_{\mathrm{S}} = \begin{pmatrix} \phi_3^{\alpha}(\mathbf{r},t) \\ \phi_4^{\beta}(\mathbf{r},t) \end{pmatrix}$ are historically known as "large" and "small" components. They also are referred to as positive and negative energy components. The largest term in the Dirac Hamiltonian (Eqn. 2.11) is mc^2, the rest mass energy of the fermion. It will be useful to know an estimate of the magnitude of the other terms relative to this term. The order of magnitude of each of the other terms in the Hamiltonian, $c\boldsymbol{\alpha}.\mathbf{P}$, $q\phi$ and $qc\boldsymbol{\alpha}.\mathbf{A}$, can be expressed as $mc^2\alpha^n$, based on the magnitude of each of them in the ground state hydrogen atom [10]. As an example, the electron velocity (u) in the first Bohr radius is $c\alpha$ and the first Bohr radius (a_o) is given by $\frac{1}{mc^2\alpha^2}$. Thus, classically: $c\boldsymbol{\alpha}.\mathbf{P} \sim mcu = mc^2\alpha$, $q\phi \sim \frac{1}{a_o} = mc^2\alpha^2$ and $qc\boldsymbol{\alpha}.\mathbf{A} \sim \frac{u}{c^2 a_o} = mc^2\alpha^3$. Here α is the fine structure constant. The magnitude of the electric and magnetic field experienced by an electron in the first Bohr radius is much larger than the external electric or magnetic fields commonly encountered in the laboratory [10]. Hence, these qualitative estimates will not be altered materially in the presence of an applied external field. It will be seen later that the order of magnitude of any term arising in the relativistic many-fermion Hamiltonian can be estimated from these results as well as the order of magnitude of each term in the equivalent two-component form expanded in a power series.

So far our discussion is limited to a single fermion in the free field or in the presence of a electromagnetic radiation field. In the following section, we will generalize the discussion to relativistic many-fermion Hamiltonians.

2.3 Relativistic Many-Fermion Hamiltonians

Dirac's equation cannot be extended directly to many-fermion systems. The many-fermion Hamiltonians should be derived from first principles (QED). However, QED treatments of interacting many-fermion systems do not automatically lead to an eigenvalue problem. An eigenvalue problem has to be extracted from a perturbation expansion derived by QED for the frequency of the emitted radiation from a system. There is no universally accepted scheme for this process and consequently there is no unique, multi-purpose relativistic many-fermion Hamiltonian, but the Hamiltonians we are looking for should instead be "reasonable". To be "reasonable", we would like our many-fermion relativistic Hamiltonian (H) to satisfy criteria which are vital or desirable. The proper Hamiltonians should be based on sound theoretical concepts and should be amenable to systematic improvements. In the non-interacting limit they should be exact (ie. reduce to a sum of independent external electromagnetic field Dirac Hamiltonians). Relativistic many-fermion Hamiltonians H can be regarded as linear Hermitian operators which act on configuration state functions (CS), $\Psi = \Psi(\mathbf{r}_1, \mathbf{r}_2, \ldots, \mathbf{r}_N, t)$, the multi-Dirac spinors, in the Hilbert space which refers to a definite number N ($N > 0$) of fermions. Here, the $\mathbf{r}_i$ (i = 1, 2, . . . , N) are the position vector and the Dirac spin matrix of the i^{th} particle. Moreover, the eigenvalue problem

$$\mathrm{H}\Psi = \mathrm{E}\Psi \tag{2.13}$$

should have normalizable solutions, which can be associated with the energy levels of an N electron atomic or molecular system. An extensive list of criteria can be found in Sucher [23], and will not be repeated here.

The Dirac-Breit-Coulomb (DBC) Hamiltonian ($\mathbf{H}_{\mathrm{DBC}}$) is a good starting point for a discussion of many-fermion[1] relativistic Hamiltonians, not only because of its historical importance and widespread use in molecular relativistic calculations (in spite of its known failures) but also as an excellent example of a disastrous failure of an attempt to directly extend a relativistic "one-fermion theory" to a relativistic "many-fermion theory" without sound theoretical justification. It has the form

$$i\frac{\partial\Psi}{\partial t} = \left\{ \sum_{i=1}^{N} [\mathbf{h}_{\mathrm{D}}(i) + \mathbf{V}_{\mathrm{ext}}(i)] + \sum_{i<j}^{N} \mathbf{V}_{\mathrm{int}}(i,j) \right\} \Psi = \mathbf{H}_{\mathrm{DBC}}\Psi \tag{2.14}$$

or for stationary states,

$$\mathbf{H}_{\mathrm{DBC}}\Psi = \mathrm{E}\Psi \tag{2.15}$$

where $\mathbf{h}_{\mathrm{D}}(i)$,

$$\mathbf{h}_{\mathrm{D}}(i) = \left[c(\boldsymbol{\alpha}_i.\mathbf{P}_i) + \boldsymbol{\beta}_i m_i c^2\right] \tag{2.16}$$

is the free field Dirac Hamiltonian for the i^{th} particle and $\mathbf{V}_{\mathrm{ext}}(i)$,

$$\mathbf{V}_{\mathrm{ext}}(i) = q_i[\phi\mathbf{I} - (\boldsymbol{\alpha}_i.\mathbf{A}_i)] \tag{2.17}$$

is the external radiation field effects acting on the i^{th} particle and $\mathbf{V}_{\mathrm{int}}(i,j)$, represents the particle-particle interactions. Note that the first part of the DBC

---

[1] (The original form of the DBC Hamiltonian was proposed for molecules. Here, we use it for general many-fermion systems)

Hamiltonian (Eqn. 2.14) is a sum of external field one particle Dirac Hamiltonians. In the DBC Hamiltonian, the particle particle interacton effects are approximated by an instantaneous Coulombic and Breit interaction [24],

$$\mathbf{V}_{\mathrm{int}}(i,j) = \frac{q_i q_j(\mathbf{I}+\mathbf{B}_{ij})}{|\mathbf{r}_i - \mathbf{r}_j|} \tag{2.18}$$

where $\mathbf{B}_{ij}$,

$$\mathbf{B}_{ij} = -\frac{1}{2}[\boldsymbol{\alpha}_i.\boldsymbol{\alpha}_j + \frac{(\boldsymbol{\alpha}_i.\mathbf{r}_{ij})(\boldsymbol{\alpha}_j.\mathbf{r}_{ij})}{\mathbf{r}_{ij}^2}] \tag{2.19}$$

both of which are on the order of magnitude $mc^2\alpha^2$ in a molecular environment. The complete interaction cannot be written in a closed form but has to be obtained by (diagrammatic) perturbation theory. The Coulomb and the Breit interaction terms are the first two terms of an infinite series and the DBC Hamiltonian as written in Eqn. 2.14 is only an approximation (not a closed form equation). The original derivation of the Breit interaction was based on the classical magnetic dipole interactions of moving charged particles [24]. Since then it has been rederived using QED arguments [16]. The higher order ($>> mc^2\alpha^4$) terms in the series arise from the retarded interactions of particles via transverse virtual photons and, in principle, may be obtained to any order of accuracy based on QED arguments. The DBC Hamiltonian is not Lorentz invariant, but it can be systematically improved to any order and eventually in the limit it becomes Lorentz invariant. As we can see from Eq. 2.14, in the absence of particle-particle interactions the DBC Hamiltonian reduces to a sum of independent one-particle external radiation field Dirac equations. The DBC Hamiltonian is correct through order $mc^2\alpha^2$ and it can be shown that it is independent of the origin of the coordinate system choosen to represent the electromagnetic potentials (gauge-origin invariant) [10].

At this point it is interesting to discuss the solutions of the DBC Hamiltonian briefly. As Brown and Ravenhall pointed out in 1951 [25], the DBC Hamiltonian does not have bound state solutions. To illustrate this point, let us consider the stationary state DBC Hamiltonian of two non-interacting fermions in an external potential given by

$$\left\{\sum_{i=1}^{2}[\mathbf{h}_{\mathrm{D}}(i)+\mathbf{V}_{\mathrm{ext}}(i)]\right\}\Psi_o=\left\{\sum_{i=1}^{2}\mathbf{h}_{\mathrm{D,ext}}(i)\right\}\tilde{\Psi}=\tilde{\mathrm{E}}\tilde{\Psi} \tag{2.20}$$

As noted earlier, for each particle *i*, there is a discrete spectrum of positive energy bound states and positive and negative energy continuum states. Let us consider a product wave function of the form $\tilde{\Psi}=\psi_1(1)\psi_2(2)$, a normalizable stationary bound-state eigenfunction of

$$\sum_{i=1}^{2}\mathbf{h}_{\mathrm{D,ext}}(i) \tag{2.21}$$

with energy $\tilde{\mathrm{E}}=\sum\limits_{i=1}^{2}\varepsilon_i(i)$. Here, $\psi_i(i)$ for each *i*, are normalizable stationary state eigenfunctions of

$$\mathbf{h}_{\mathrm{D,ext}}\psi_i(i)=\varepsilon_i(i)\psi_i(i)\quad i=1,2 \tag{2.22}$$

To any bound state solution with energy $\tilde{E}$, we can associate an infinite number of states, one in the positive energy continuum and the other in the negative energy continuum having the same $\tilde{E}$ as the combined energy. As we turn on the particle-particle interaction, states from the negative energy continuum can mix with the positive energy continuum states so that their combined energy equal to $\tilde{E}$. This will add large contributions to the bound state wave function and extend it to infinite distances or dissolve into the continuum. This phenomenon is commonly known as "Brown and Ravenhall disease" or "continuum dissolution" (CD) [25]. As a consequence of the presence of negative energy continuum states, the positive energy bound state solutions of interest are highly excited, and the electrons that occupy the positive energy bound states can be excited to positive and negative energy continuum states. Thus it can be easily shown by using perturbation theory arguments, following Sucher [23], that the first-order correction to the bound state wave function is not normalizable. However, it is important to note that the zeroth-order state is highly excited and for a such a zeroth-order state, perturbation theory arguments break down. A solvable model problem has also been used to demonstrate the point in question, without relying on perturbation theory [26].

Obviously, the CD is related to the existence of unfilled negative energy (including rest mass energy) states, but arises only because fermions are interacting with each other regardless of the mechanism of interaction. In the one-fermion case, Dirac conceptually avoided this problem by assuming completely filled negative energy states commonly known as Dirac's "hole theory" but, there is nothing explicitly in the Dirac equation itself to enforce this constraint. As noted earlier, the DBC Hamiltonian is not derived from first principles; it is merely an intuitive extension of Dirac's "one-fermion" theory to many fermions. Hence, the DBC Hamiltonian does not incorporate the physical ideas of Dirac's "hole theory" in which the Pauli exclusion principle prevents transitions to filled negative energy states. This dilemma calls for the derivation of many-fermion Hamiltonians from QED, the mathematical formulation of the Dirac's "hole theory" which incoporates these ideas from the outset. As we will see later, such a derivation provides many-fermion Hamiltonians which are amenable to systematic improvements and do not suffer from CD.

The Dirac-Hartree-Fock (DHF) equation has been derived starting from the DBC Hamiltonian following similar arguments as was done in deriving its non-relativistic analogue, the Hartree-Fock (HF) equation [27–29]. The DHF equation has been severely numerically tested over the last few decades, and proven to be useful in a qualitative, and often quantitative, understanding of atomic structure and spectra of relativistic atoms, especially those involving inner-shell ionization in heavy atoms. It is not surprising that the DHF equation has bound state solutions, since the DHF equation is a one-body equation which does not suffer from CD. However, CD undermines the interpretation of these solutions, because the exact wave function for which the DHF wave function is supposed to be an approximation does not exist. Any attempt to improve upon the DHF solutions by including electron correlation effects proved to be a dismal failure [30, 31], just as one would expect since the DBC Hamiltonian does not have bound state solutions.

Apparently, a large number of successful relativistic configuration-interaction (RCI) and multireference Dirac-Hartree-Fock (MRDHF) calculations [32] reported over the last two decades are "supposedly" based on the DBC Hamiltonian. This apparent success seems to contradict the earlier claims of the CD. As shown by Sucher [23, 33], in fact the RCI and MRDHF calculations are not based on the DBC Hamiltonian, but on an approximation to a more fundamental Hamiltonian based on QED which does not suffer from the CD. At this point, let us defer further discussion until we review the many-fermion Hamiltonians derived from QED.

The underlying relativistic Hamiltonian for many-fermion systems is the Hamiltonian for quantum electrodynamics, $\mathbf{H}_{\mathrm{QED}}$. It acts on wave function in Fock-space and is capable of describing systems involving an arbitrarily large number of electrons, positrons and photons. $\mathbf{H}_{\mathrm{QED}}$ conserves only the total charge of the system, not the total number of electrons, positrons or photons. Irrespective of a particular partitioning, $\mathbf{H}_{\mathrm{QED}}$ will always have terms which couple different sectors of the Fock-space with the same total electric charge but with different number of electrons, positrons and photons. The Fock-space wave function is an infinite-order column matrix, consists of electrons, positrons and photons consistent with the total charge and quantum numbers of the system [34]. For example, the Fock-space wave function for an electron consists of a one-electron wave function, a one-electron and one-photon function, a one electron and electron-positron pair function, *etc.* The individual elements of the Fock-space wave function in a particular sector (Hilbert space) satisfy a set of infinite coupled linear partial differential equations and can be used to extract the form of the Fock-space wave function for the photons and electrons [34].

The first rigorous derivation of such a relativistic Hamiltonian for a two-fermion system that makes use of Feynman [18, 19] formalism of QED was due to Bethe and Salpeter [35, 36]. Recently Broyles has extended it to many-electron atoms and molecules [37]. A detailed account of Broyle's derivation can be found elsewhere [37, 38] and will not be repeated here. Following Broyles the stationary state many-fermion Hamiltonian based on QED can be written as

$$\left\{\sum_{i=1}^{N} \mathbf{h}_{\mathrm{D,ext}}(i) + \left[\prod_{k=1}^{N} \Lambda_{k+} - (-1)^{N} \prod_{k=1}^{N} \Lambda_{k-}\right] \sum_{i<j} \mathbf{V}_{\mathrm{int}}(i,j)\right\} \Psi = \mathrm{E}\Psi \quad (2.23)$$

where $\Lambda_{k\pm}$ are the projection operator into the positive and negative energy states of $\mathbf{h}_{\mathrm{D,ext}}$ namely

$$\Lambda_{k\pm}\psi_k(k) = \frac{1}{2}(\mathrm{p}^2 + m^2)^{-1/2}\left[(\mathrm{p}^2 + m^2)^{1/2} \pm \mathbf{h}_{\mathrm{D,ext}}\right]|\psi_{k\pm}(k)\rangle \quad (2.24)$$

where $\psi_i(i)$ is an eigenfunction of $\mathbf{h}_{\mathrm{D,ext}}$. As we can see from Eqn. 2.23, the form of the QED Hamiltonian is identical to that of the DBC Hamiltonian given in Eqn. 2.14 except for the presence of projection operators. For potentials ($\mathbf{V}_{\mathrm{int}}(i,j)$) which involve only pairwise interactions, Broyles has shown that the bound state wave functions of Eqn. 2.23 separate into two components. This in mathematical terms can be written as

$$\Psi = \Big[\prod_{k=1}^{N} \Lambda_{k+} - (-1)^N \prod_{k=1}^{N} \Lambda_{k-}\Big]\Psi \tag{2.25}$$

and consequently in no case does the wave function have a mixture of both positive and negative energy solutions. The positive and negative energy solutions correspond to two different equations. It is the presence of projection operators which decouple the positive and negative energy states that actually prevents the QED Hamiltonian from CD. As Broyles stated, if more than two-body interactions are present, this separation into two components still may hold, but in that case a more elaborate proof is required.

The no-pair Hamiltonian derived from QED principles [31] is equivalent to the Broyles Hamiltonian. It may be obtained in a more simple and transparent manner, without invoking the perturbational four-dimensional machinery associated with Broyles or Bethe and Salpeter's derivation. However, it should be noted that this derivation is less rigorous. In the Coulomb gauge $\mathbf{H}_{\mathrm{QED}}$ can be written in the form

$$\mathbf{H}_{\mathrm{QED}} = \mathbf{H}_{\mathrm{mat}} + \mathbf{H}_{\mathrm{rad}} + \mathbf{H}_{\mathrm{T}} \tag{2.26}$$

where $\mathbf{H}_{\mathrm{mat}}$ is the external field Hamiltonian for the particles (electrons and positrons) in terms of the quantized Dirac field. $\mathbf{H}_{\mathrm{rad}}$ is the free Hamiltonian for the radiation in terms of the quantized radiation field, and $\mathbf{H}_\mathrm{T}$ is the Hamiltonian for the interaction of particles with the quantized transverse radiation field. The interaction term $\mathbf{H}_\mathrm{T}$ is assumed to be small and is usually treated by perturbation theory. We can define a set of electron and positron creation and annihilation operators (see chapter 2) in terms of the solutions of the external field Dirac equation (Eqn. 2.11) or the free field Dirac equation (Eqn. 2.8). The two choices correspond to different definitions of creation and annihilation operators and hence lead to different "no-pair" Hamiltonians. Expand the quantized Dirac and the radiation field in terms of electron and positron field operators defined in terms of solution of the external field Dirac equation as in the *Furry* bound state picture or interms of solution of the free field Dirac equation as in the *free* picture. This leads to analytical expressions for $\mathbf{H}_\mathrm{mat}$, $\mathbf{H}_\mathrm{rad}$ and $\mathbf{H}_\mathrm{T}$ presented by Sucher [23, 31, 33]. The major difficulty with the operator $\mathbf{H}_\mathrm{mat}$ is that it does not conserve the number of particles. However, it is possible to split off from $\mathbf{H}_\mathrm{mat}$ a "pair part" which involves the creation or destruction of virtual electron-positron pairs and which can in many cases be treated as perturbations, along with $\mathbf{H}_\mathrm{T}$. The remaining part, the "no-pair part", then has a fixed number of electrons and positrons (commute with electron and positron number operators) so that the eigenvalue problem it poses is equivalent to the problem of solving for the relativistic many-fermion wave equation. Thus we can write

$$\mathbf{H}_\mathrm{mat} = \mathbf{H}_\mathrm{mat}^\mathrm{np} + \mathbf{H}_\mathrm{mat}^\mathrm{pair} \qquad (2.27)$$

The definition of the "pair" part or, equivalently the "no-pair part" of $\mathbf{H}_{\mathrm{mat}}$ is not unique. The precise meaning of "no-pair" implicitly depends on the choice of external potential, so that the operator $\mathbf{H}^{\mathrm{np}}_{\mathrm{mat}}$ depends implicitly on the external potential, whereas the sum $\mathbf{H}_{\mathrm{mat}} = \mathbf{H}^{\mathrm{np}}_{\mathrm{mat}} + \mathbf{H}^{\mathrm{pair}}_{\mathrm{mat}}$ is independent of the choice of external potential. Since the no-pair part conserves the number of particles (electrons, positrons and photons) we can look for eigenstates Ψ of $\mathbf{H}^{\mathrm{np}}_{\mathrm{mat}}$ in the sector of Fock space with N fermions and no photons or positrons. Following Sucher [31, 33, 23], the resulting no-pair Hamiltonian in configuration space can be written as

$$\left\{\sum_{i=1}^{N} \mathbf{h}_{\mathrm{D,ext}}(i) + \prod_{k=1}^{N} \mathbf{L}_{k+}(k)\left(\sum_{i<j}^{N} \mathbf{V}_{\mathrm{int}}(i,j)\right)\prod_{k=1}^{N} \mathbf{L}_{k+}(k)\right\}\Psi = \mathrm{E}\Psi \qquad (2.28)$$

where the positive energy projection operators are defined in terms of positive energy eigenfunctions $\psi_{k+}(k)$ of $\mathbf{h}_{\mathrm{D,ext}}$ (both discrete and continuous) or $\mathbf{h}_{\mathrm{D}}$ (continuous) such that

$$\mathbf{L}_{k+} = \sum_{k} |\psi_{k+}(k)\rangle\langle\psi_{k+}(k)| \qquad (2.29)$$

Depending on the choice of $\psi_{k+}(k)$; eigenfunctions of the external field Dirac equation $\mathbf{h}_{\mathrm{D,ext}}$ or the free field Dirac equation $\mathbf{h}_{\mathrm{D}}$, Eqn. 2.28 represent the *Furry* bound state molecular Hamiltonian or the *free* molecular Hamiltonian.

2.4 The Non-Relativistic Form of the Molecular Relativistic Hamiltonian.

Instead of a two-component equation as in the non-relativistic case, for fully relativistic calculations one has to solve a four-component equation. Conceptually, fully relativistic calculations are no more complicated than non-relativistic calculations, but they are computationally demanding, in particular, for correlated molecular relativistic calculations. Unless taken care of at the outset, spurious solutions can occur in variational four-component relativistic calculations. In practice, this problem is handled by employing kinetically balanced basis sets. The kinetic balance relation is

$$\psi_{\mathrm{S}} = -\frac{1}{2mc}\boldsymbol{\sigma}.\mathbf{P}\psi_{\mathrm{L}} \tag{2.30}$$

This relation becomes exact only in the non-relativistic limit. If a basis set is chosen in which the small and large components do not fulfil this condition, convergence to the non-relativistic limit upon enlarging the value of c is not possible. Such a lack of balance between the large and small components manifests itself by giving too small a value for the kinetic energy in that limit. Consequently, two different atomic orbital basis functions for the large and small components is required. This result in large storage requirements and expensive two electron integral evaluation. However, Dirac Hartree-Fock (DHF) (four component) calculations of atoms and simple diatomics are routine today and correlated fully relativistic molecular calculations are rapidly emerging [32].

An attractive alternative is to use a two-component equation derived from a decoupling of the “large” and “small” components of the four-component equation. By decoupling of the “large” and “small” components (equivalently positive and negative solutions) the Dirac equation would in effect be reduced to the non-relativistic form (NRF). Furthermore, the decoupling would allow us to focus on a particular component, basically the positive energy component, since the processes that we are interested in studying does not involve positrons or positron-electron pair creation. At least in principle, the decoupled equations can be expanded in terms of powers of α^2 which in turn can be used to obtain the non-relativistic limit (NRL) by taking the limit $\alpha \rightarrow 0$.

First, we consider the NRF and NRL of the one-electron external field Dirac equation. Before we continue any further, let us rewrite the Eqn. 2.12, for a fermion in an external radiation field

$$\mathrm{h}_{\mathrm{D,ext}}\psi = \begin{pmatrix} q\phi\mathbf{I} & c\boldsymbol{\alpha}.\boldsymbol{\Pi} \\ c\boldsymbol{\alpha}.\boldsymbol{\Pi} & (-2mc^2 + q\phi)\mathbf{I} \end{pmatrix}\psi = \mathrm{E}\psi \tag{2.31}$$

where, $\psi = \begin{pmatrix} \psi_{\mathrm{L}} \\ \psi_{\mathrm{S}} \end{pmatrix}$, $\langle\psi|\psi\rangle = \mathbf{I}$ and ψ_{L} and ψ_{S} are the large and small component respectively. Note, that Eqn. 2.31 is written for stationary states and also the whole energy spectrum is shifted by $-mc^2$, so that a direct comparison with the non-relativistic result is feasible. It is important to note that decompostion into small and large components is strictly valid only for the one-electron case.

Since the introduction of the Dirac equation [7, 8], there have been numerous studies on the problem of decoupling it into a two-component equation and its NRL. The problem is that the Dirac equation does not have an obvious NRF or NRL. In order to write the Dirac equation in NRF or to establish the NRL one must first manipulate the Dirac equation. A recent review by Kutzelnigg [39, 40] gives a detailed exposition of various approaches and the difficulties that arise in the form of divergent terms and singularities. In these approaches, usually, one first derives an effective Hamiltonian which acts on two-component wave functions and which is supposed to have the same eigenvalues as the original four component Hamiltonian, before one takes the non-relativistic limit or formulates a perturbation series in terms of α^2. We can classify all of these approaches into three broad categories.

First, the method for the large component of the Dirac spinor. In this category, the elimination of the small component (ESC) is the simplest and most straightforward [41]. It simply involves an elimination of the "small" component in order to derive a Hamiltonian for the "large" component. The resulting Hamiltonian is Hermitian, energy-dependent and acts on two component spinors. Its eigenfunctions are identical to the large component $\psi_{\rm L}$ of the Dirac spinor ψ. In the second category, the Foldy-Wouthuysen (FW) or related transformations convert the Hamiltonian in Eqn. 2.31 into a block diagonal form by a unitary transformation [42]. This results in an energy-independent, Hermitian Hamiltonian which acts on a two component spinor, but the eigenfunctions of this Hamiltonian are no longer the large component of the Dirac spinor. The methods in the third category leave the four-component form of the equation intact, but treat the positive and negative energy states differently by different choices of the metric. They can be derived from the direct perturbation theory approach (DPT) of Kutzelnigg [39]. In the following discussion, all of the above three categories are presented as special cases of the general theory of effective Hamiltonians [43]. This procedure will help us to identify elements common in each method, problems, and possible soultions.

Let us rewrite the Dirac equation (Eqn. 2.31), with an added arbitrary real parameter z,

$$\mathbf{h}\psi = \begin{pmatrix} (q\phi + z)\mathbf{I} & c\boldsymbol{\sigma}.\boldsymbol{\Pi} \\ c\boldsymbol{\sigma}.\boldsymbol{\Pi} & [-2mc^2 + (q\phi + z)]\mathbf{I} \end{pmatrix} \psi = (\mathrm{E} + z)\psi \qquad (2.32)$$

where the use of z will become clear later on.

Now, consider an arbitrary but non-singular transformation $\mathbf{U}$, as yet unspecified, of the old basis ψ, into a new basis $\tilde{\psi}$, such that $\tilde{\psi} = \mathbf{U}^{-1}\psi$. Then Eqn. 2.32 becomes

$$(\mathbf{U}^{\dagger}\mathbf{h}\mathbf{U})\mathbf{U}^{-1}\psi = \mathrm{E}(\mathbf{U}^{\dagger}\mathbf{U})\mathbf{U}^{-1}\psi \qquad (2.33)$$

Let us define a transformed Hamiltonian as $\tilde{\mathbf{h}}$,

$$\tilde{\mathbf{h}} = \mathbf{U}^{\dagger}\mathbf{h}\mathbf{U} = \begin{pmatrix} \mathbf{h}_{11} & \mathbf{h}_{12} \\ \mathbf{h}_{21} & \mathbf{h}_{22} \end{pmatrix} \qquad (2.34)$$

and define the metric S,

$$\mathbf{S} = \mathbf{U}^{\dagger}\mathbf{U} \qquad (2.35)$$

and rewrite Eqn. 2.33,

$$\tilde{\mathbf{h}}\mathbf{U}^{-1}\psi = \mathrm{E}\mathbf{S}\mathbf{U}^{-1}\psi \qquad (2.36)$$

As we can see from Eqn. 2.36, $\tilde{\psi}$ is an eigenfunction of the transformed Hamiltonian $\tilde{\mathbf{h}}$ with the normalization $\langle\tilde{\psi}|\mathrm{S}|\tilde{\psi}\rangle$ and the eigenvalues remain unchanged. Basically this implies that instead of diagonalizing the full Hamiltonian for the whole energy spectrum, one can diagonalize the effective Hamiltonian to obtain a subset of eigenvalues. The form of **U** needs to be determined such that both $\tilde{\mathbf{h}}$ and S are block-diagonal. The transformed Hamiltonian is Hermitian, but in general corresponds to a non-unit metric.

Alternatively we may use a similarity transformation

$$(\mathrm{U}^{-1}\mathbf{h}\mathrm{U})\mathrm{U}^{-1}\psi = \mathrm{E}\mathrm{U}^{-1}\psi \tag{2.37}$$

and define a similarity transformation $\bar{\mathbf{h}}$, $\bar{\mathbf{h}} = \mathrm{U}^{-1}\mathbf{h}\mathrm{U}$ which does not involve a metric. The similarity transformed Hamiltonian is not necessarily Hermitian, but a Hermitian effective Hamiltonian can be derived from it by an additional transformation commonly known by the name des Cloizeaux [44]. When **U** is chosen to be unitary, the similarity transformed Hamiltonian is automatically Hermitian and the unitary similarity transformations are commonly known in the literature as Hermitian Similarity transformations.

The FW transformation is in effect equivalent to a Hermitian similarity transfomation. Following van Lenthe *et al.* [45], we can parametrize the unitary transformation **U**, as follows

$$\mathrm{U} = \begin{pmatrix} (\mathbf{I}+\mathbf{X}^{\dagger}\mathbf{X})^{-1/2} & (\mathbf{I}+\mathbf{X}^{\dagger}\mathbf{X})^{-1/2}\mathbf{X}^{\dagger} \\ -\mathbf{X}(\mathbf{I}+\mathbf{X}\mathbf{X}^{\dagger})^{-1/2} & (\mathbf{I}+\mathbf{X}\mathbf{X}^{\dagger})^{-1/2} \end{pmatrix} \tag{2.38}$$

Here, $\mathbf{X}$ is to be determined by imposing that the resulting transformed Dirac Hamiltonian is block diagonal. It is fairly easy to see that this leads to an equation for $\mathbf{X}$

$$\mathrm{X}(z) = \frac{1}{2mc^2}(c\mathrm{X}\ \boldsymbol{\sigma}.\boldsymbol{\Pi}\mathrm{X} - c\boldsymbol{\sigma}.\boldsymbol{\Pi}\ + [(q\phi + z)\mathrm{I}, \mathrm{X}]) \tag{2.39}$$

and the effective Hamiltonian $\mathbf{h}_{11}$ and wave function ψ^{eff}

$$\begin{aligned} \mathbf{h}_{11}\psi^{\text{eff}} &= \left[(\mathrm{I}+\mathrm{X}^{\dagger}\mathrm{X})^{1/2}((q\phi+z)\mathrm{I} - c\boldsymbol{\sigma}.\mathbf{P}\mathrm{X})(\mathrm{I}+\mathrm{X}^{\dagger}\mathrm{X})^{-1/2}\right]\psi^{\text{eff}} \\ &= (\mathrm{E}+z)\psi^{\text{eff}} \end{aligned} \tag{2.40}$$

The FW Hamiltonian $\mathbf{h}^{\text{FW}}$,

$$\begin{aligned} \mathbf{h}^{\text{FW}}\psi^{\text{FW}} &= \left[(\mathrm{I}+\mathrm{X}^{\dagger}\mathrm{X})^{1/2}(q\phi\mathrm{I} - c\boldsymbol{\sigma}.\mathbf{P}\mathrm{X})(\mathrm{I}+\mathrm{X}^{\dagger}\mathrm{X})^{-1/2}\right]\psi^{\text{FW}} \\ &= \mathrm{E}\psi^{\text{FW}} \end{aligned} \tag{2.41}$$

follows directly from Eqns. 2.39 and 2.40 by putting the arbitrary parameter z to zero. Here, ψ^{FW} is the FW two-component wave function. As we can see from Eqn. 2.41, the FW Hamiltonian is energy independent and Hermitian. It is also important to note that the Hermiticity of $\mathbf{h}^{\text{FW}}$ is guaranteed only for exact $\mathbf{X}$. Now, we can write the FW wave function in terms of the solutions of the original Dirac Hamiltonian. Since $\begin{pmatrix}\psi^{\text{FW}} \\ 0\end{pmatrix}$ is an eigenfunction of the similarity transformed Hamiltonian, one can write

$$\begin{pmatrix}\psi^{\text{FW}} \\ 0\end{pmatrix} = \begin{pmatrix}(\mathrm{I}+\mathrm{X}^{\dagger}\mathrm{X})^{-1/2} & -\mathrm{X}^{\dagger}(\mathrm{I}+\mathrm{X}^{\dagger}\mathrm{X})^{-1/2} \\ \mathrm{X}(\mathrm{I}+\mathrm{X}\mathrm{X}^{\dagger})^{-1/2} & (\mathrm{I}+\mathrm{X}\mathrm{X}^{\dagger})^{-1/2}\end{pmatrix}\begin{pmatrix}\psi_{\mathrm{L}} \\ \psi_{\mathrm{S}}\end{pmatrix} \tag{2.42}$$

We can use the Eqn. 2.42, to write an expression for ψ^{FW}, in terms of ψ_{L} as,

$$\psi^{\text{FW}} = \left(\mathrm{I}+\mathrm{X}^{\dagger}\mathrm{X}\right)^{1/2}\psi_{\mathrm{L}} \tag{2.43}$$

As we can see, the FW two-component wave function is not the large component of the Dirac spinor, but it is related to it by an expression involving **X**.

Consider a similarity transformation based on **U** parametrized as

$$\mathrm{U} = \begin{pmatrix} \mathrm{I} & 0 \\ -\mathrm{X} & \mathrm{I} \end{pmatrix} \qquad \mathrm{U}^{-1} = \begin{pmatrix} \mathrm{I} & 0 \\ \mathrm{X} & \mathrm{I} \end{pmatrix} \tag{2.44}$$

In this case, **X** is to be determined by requiring that the off-diagonal blocks of the resulting transformed Dirac Hamiltonian vanishes. It can be shown that the equation for **X** is identical to the one we obtained in the case of a unitary transformation as given in Eqn. 2.39. In this case the effective Hamiltonian $\mathbf{h}_{11}$ and wave function ψ^{eff}, can be written as

$$\begin{aligned} \mathbf{h}_{11}\psi^{\text{eff}} &= [((q\phi + z)\mathbf{I} - c\boldsymbol{\sigma}.\mathbf{PX})]\psi^{\text{eff}} \\ &= (\mathrm{E} + z)\psi^{\text{eff}} \end{aligned} \tag{2.45}$$

The ESC Hamiltonian is obtained by substituting $z = -\mathrm{E}$ in Eqn. 2.45,

$$\begin{aligned} \mathbf{h}^{\text{ESC}}\psi^{\text{ESC}} &= (q\phi\mathbf{I} - c\boldsymbol{\sigma}.\mathbf{PX})\psi^{\text{ESC}} \\ &= \mathrm{E}\psi^{\text{ESC}} \end{aligned} \tag{2.46}$$

Similar to the FW case, one can write

$$\begin{pmatrix} \psi^{\text{ESC}} \\ 0 \end{pmatrix} = \begin{pmatrix} \mathrm{I} & 0 \\ \mathrm{X} & \mathrm{I} \end{pmatrix} \begin{pmatrix} \psi_{\mathrm{L}} \\ \psi_{\mathrm{S}} \end{pmatrix} \tag{2.47}$$

resulting in $\psi^{\text{ESC}} = \psi_{\mathrm{L}}$. That is, in contrast to the FW Hamiltonian, the large component of the Dirac spinor is an eigenfunction of the two component ESC Hamiltonian. Let us rewrite Eqn. 2.39 when $z = -\mathrm{E}$ and rearrange to obtain

$$\left(1 - \frac{(q\phi - \mathrm{E})}{2mc^2}\right)\mathbf{X} = \frac{1}{2mc^2}[c\mathbf{X}\boldsymbol{\sigma}.\boldsymbol{\Pi}\mathbf{X} - c\boldsymbol{\sigma}.\boldsymbol{\Pi} - \mathbf{X}(q\phi - \mathrm{E})\mathbf{I}] \tag{2.48}$$

Rearranging Eqn. 2.46 we get

$$(q\phi - \mathrm{E})\psi^{\mathrm{ESC}} = c\boldsymbol{\sigma}.\mathbf{P}\mathbf{X}\psi^{\mathrm{ESC}} \tag{2.49}$$

Multiply Eqn. 2.49 on left by **X**. Then, the result is true for all ψ^{ESC}, we can substitute for $\mathbf{X}(q\phi - \mathrm{E})\mathbf{I}$ in Eqn. 2.48 to get a simplified expression for **X**,

$$\begin{aligned} \left(1 - \frac{(q\phi - \mathrm{E})}{2mc^2}\right)\mathbf{X} &= \frac{-c\boldsymbol{\sigma}.\boldsymbol{\Pi}}{2mc^2} \\ \mathbf{X} &= \frac{-c\mathrm{k}\ \boldsymbol{\sigma}.\boldsymbol{\Pi}}{2mc^2} \end{aligned} \tag{2.50}$$

where $\mathrm{k} = (1 - \frac{(q\phi - \mathrm{E})}{2c^2})^{-1}$. Now substitute for **X** in Eqn. 2.46 to get the ESC Hamiltonian $\mathbf{h}^{\mathrm{ESC}}$,

$$\mathbf{h}^{\mathrm{ESC}}\psi_{\mathrm{L}} = [q\phi\mathbf{I} + \frac{(\boldsymbol{\sigma}.\boldsymbol{\Pi})\mathrm{k}(\boldsymbol{\sigma}.\boldsymbol{\Pi})}{2}]\psi_{\mathrm{L}} = \mathrm{E}\psi_{\mathrm{L}} \tag{2.51}$$

As seen from Eqn. 2.51, the ESC Hamiltonian is energy dependent and Hermitian. For a fixed value of E, the ESC Hamiltonian can be diagonalized and the resulting solutions, in principle, form a complete orthonormal set. The eigenfunctions of $\mathbf{h}^{\mathrm{ESC}}$ are identical to the large component of the Dirac spinor.

When $z = 0$, Eqns. 2.39 and 2.45 gives us the similarity transformed Hamiltonian $\mathbf{h}^{\mathrm{ST}}$,

$$\mathbf{h}^{\mathrm{ST}}\psi_{\mathrm{L}} = (q\phi\mathbf{I} - c\boldsymbol{\sigma}.\mathbf{P}\mathbf{X})\psi_{\mathrm{L}} \tag{2.52}$$

Note that the $\mathbf{h}^{\mathrm{ST}}$ is non-Hermitian and energy independent. Moreover, the large component of the Dirac spinor is an eigenfunction of $\mathbf{h}^{\mathrm{ST}}$. The Hamiltonians

$\mathbf{h}^{\mathrm{ST}}$ and $\mathbf{h}^{\mathrm{ESC}}$ are equivalent insofar as they have the same eigenvalues and eigenfunctions. They are indeed grouped together as derived from the methods for large components. The des Cloizeaux [44] transformation of $\mathbf{h}^{\mathrm{ST}}$ will give us a Hermitian similarity transformed Hamiltonian which is identical to the FW Hamiltonian given in Eqn. 2.41.

So far our derivations leading to the FW, ESC and ST Hamiltonians are formally rigorous. However, to be useful, the FW, ESC and ST Hamiltonians given in Eqns. 2.41, 2.51 and 2.52 need to be rewritten with appropriate **X** given in Eqn. 2.39. Conveniently, we can solve for **X** by iterating Eqn. 2.39 with the outcome an expansion in terms of α^2:

$$\mathbf{X} = -\frac{\alpha}{2m}\boldsymbol{\sigma}.\boldsymbol{\Pi} - \frac{\alpha^3}{4m}[q\phi\mathbf{I},\, \boldsymbol{\sigma}.\boldsymbol{\Pi}] + \frac{\alpha^3}{8m}(\boldsymbol{\sigma}.\boldsymbol{\Pi})(\boldsymbol{\sigma}.\boldsymbol{\Pi})(\boldsymbol{\sigma}.\boldsymbol{\Pi}) + \cdots \tag{2.53}$$

Now, substituting for **X** in Eqn. 2.41 we get the FW or equivalent Hermitian similarity transformed Hamiltonian which is an expansion in terms of α^2

$$\begin{aligned}\mathbf{h}^{\mathrm{FW}} = {} & q\phi + \frac{1}{2m}(\boldsymbol{\sigma}.\boldsymbol{\Pi})^2 - \frac{\alpha^2}{8m^3}(\boldsymbol{\sigma}.\boldsymbol{\Pi})^4 + \frac{\alpha^2}{8m^2}[(\boldsymbol{\sigma}.\boldsymbol{\Pi})\,,[q\phi,\,(\boldsymbol{\sigma}.\boldsymbol{\Pi})]] \\ & + \mathcal{O}(mc^2\alpha^6)\end{aligned} \tag{2.54}$$

and the corresponding wave function

$$\psi^{\mathrm{FW}} = \psi_{\mathrm{L}} + \frac{\alpha^2}{4m^2}(\boldsymbol{\sigma}.\boldsymbol{\Pi})^2\psi_{\mathrm{L}} + \cdots \tag{2.55}$$

Here, order of magnitude of the terms in the expansion being determined on the basis of orders of magnitude of $\phi \sim mc^2\alpha^2$ and $\boldsymbol{\sigma}.\boldsymbol{\Pi} \sim mc^2\alpha^2$. We only retain the terms up to order of magnitude $mc^2\alpha^4$ or simply speaking expand through first-order in α^2. Higher order terms quickly become cumbersome to evaluate. However, this is not a serious disadvantage, since higher order corrections are not very often observed to be important at present. In addition, at higher orders radiative corrections become important and QED treatments become essential.

In case of the Coulomb potential ($\phi \propto 1/|\mathbf{r}|$, where $\mathbf{r}$ is the position vector of the fermion with respect to an arbitrary origin) commutators such as $[\phi,\ (\boldsymbol{\sigma}.\boldsymbol{\Pi})^2]$ would give us terms which are proportional to $1/|\mathbf{r}^n|$ (here n is an integer greater than 1) in the expansion for $\mathbf{h}^{\mathrm{FW}}$ in Eqn. 2.54. When such operators act on well-behaved wave functions they may give terms which are proportional to $1/|\mathbf{r}|$, and singular when $|\mathbf{r}| \rightarrow 0$. Terms such as $(\boldsymbol{\sigma}.\boldsymbol{\Pi})^4$ in the expansion lead to a higher-order differential equations and there may not be enough constraints in the problem to find quantized solutions. These terms also become very large for the particles with higher momentum and for such cases the above expansion is not justified. Similar problems arises in the FW wave function too. As shown in Eqn. 2.55, the FW wave function can also be written as an expansion in α^2 in terms of the large component of the Dirac spinor which is a well behaved function. For Coulomb potentials, as in the case for the Hamiltonian, there will be terms in the expansion which are proportional to $\frac{1}{|\mathbf{r}^n|}\psi_{\mathrm{L}}$ (n is a positive integer). This clearly shows that the FW wave function truncated at some finite order in α^2 can be divergent. The zeroth-order wave function is, of course, well-behaved.

In conclusion, the perturbation expansion in Eqn. 2.54 is not valid for Coulomb potentials for small values of **r**.

As shown by Chang, Pelisser and Durand (CPD) [46] a regular expansion, however, can be deduced by isolating the Coulomb singularity by infinite summations. Let us rewrite the Eqn. 2.39, when $z = 0$

$$\begin{aligned} \left(1 - \frac{q\phi}{2mc^2}\right)\mathrm{X} &= \frac{1}{2mc^2}[c\mathrm{X}\boldsymbol{\sigma}.\Pi\mathrm{X} - c\boldsymbol{\sigma}.\Pi - \mathrm{X}q\phi] \\ \mathrm{X} &= \frac{\mathrm{f}}{2mc^2}[c\mathrm{X}\boldsymbol{\sigma}.\Pi\mathrm{X} - c\boldsymbol{\sigma}.\Pi - \mathrm{X}q\phi] \end{aligned} \tag{2.56}$$

where $\mathrm{f} = (1 - \frac{q\phi}{2mc^2})^{-1}$. An iterative solution of Eqn. 2.56 leads to a regular expansion for **X** in terms of f

$$\mathrm{X} = \frac{\mathrm{f}\alpha}{2m}\boldsymbol{\sigma}.\Pi - \frac{\mathrm{f}^2\alpha^2}{4m}(\boldsymbol{\sigma}.\Pi)\, q\phi - \frac{\mathrm{f}^2\alpha^3}{8m}(\boldsymbol{\sigma}.\Pi)(\boldsymbol{\sigma}.\Pi)\mathbf{f}(\boldsymbol{\sigma}.\Pi) + \cdots \tag{2.57}$$

It is clear from Eqn. 2.57, that the CPD expansion is free from potentially problematic commutators in FW or ESC. Now, substituting for **X** in Eqn. 2.41 we get an expansion similar to the one given in Eqn. 2.54. Although the CPD expansion is free from Coulombic singularities, it is divergent for particles with large momenta and should in principle only be used for slow moving particles. Application of CPD or related expansions to atomic and molecular relativistic calculations have been reported [47, 48, 45].

As we can see from Eqn. 2.50, in the case of ESC the expression for **X** is much simpler and iterative solution gives an expansion in terms of α^2

$$\mathrm{X} = -\frac{\boldsymbol{\sigma}.\Pi}{2m}\alpha\,\mathrm{I} - \frac{(q\phi - \mathrm{E})\boldsymbol{\sigma}.\Pi}{4m^2}\alpha^3\mathrm{I} - \frac{(q\phi - \mathrm{E})^2\boldsymbol{\sigma}.\Pi}{8m^3}\alpha^5\mathrm{I} + \cdots \tag{2.58}$$

This expansion is valid only when $(q\phi - \mathrm{E}) < 2mc^2$. For the Coulomb potentials when $|\mathbf{r}| \rightarrow 0$ this assumption breaks down and the expansion is unjustified. Clearly, the expansion above is valid only for regular potentials such that the classical velocity of the particle is everywhere small compared to the velocity of light. On the assumption that such an expansion is justified, substitution in Eqn. 2.51 gives the ESC Hamiltonian as an expansion of α^2

$$\begin{aligned}\mathbf{h}^{\mathrm{ESC}} = {} & q\phi\mathrm{I} + \frac{(\boldsymbol{\sigma}.\boldsymbol{\Pi})^2}{2m} + \frac{(\boldsymbol{\sigma}.\boldsymbol{\Pi})(q\phi - \mathrm{E})(\boldsymbol{\sigma}.\boldsymbol{\Pi})}{4m^2}\alpha^2 \\ & + \frac{(\boldsymbol{\sigma}.\boldsymbol{\Pi})(q\phi - \mathrm{E})^2(\boldsymbol{\sigma}.\boldsymbol{\Pi})}{8m^3}\alpha^4 + \cdots\end{aligned} \tag{2.59}$$

The ESC Hamiltonian is energy dependent and not very useful for higher orders.

The FW Hamiltonian (Eqn. 2.54) or identical Hermitian similarity transformed Hamiltonian truncated at order α^2 gives the widely used Pauli Hamiltonian. The resulting Hamiltonian has terms up to order of magnitude $mc^2\alpha^4$ as one can see from Eqn. 2.54, since the order of magnitude of both $q\phi$ and $\boldsymbol{\sigma}.\boldsymbol{\Pi}$ are proportional to $mc^2\alpha^2$. The Pauli Hamiltonian can also be derived from truncating the ESC Hamiltonian Eqn. 2.59, at order α^2. The Pauli Hamiltonian often regarded as a valid approximation to the exact FW Hamiltonian (not expanded in powers of α^2). However, as we have already seen in the previous analysis, the expansion of the FW Hamiltonian in terms of α^2 is singular for small $|\mathbf{r}|$ and in fact the Pauli Hamiltonian is a very poor approximation to the exact FW Hamiltonian in this region. Consequently, an assessment of the accuracy of the Pauli Hamiltonian is necessary before it can be used in electronic structure calculations.

This is usually done by comparison of the numerical results obtained by using the Pauli form with the full four-component relativistic calculations.

However, it is more appropriate to provide theoretical justifications for such use. In this respect, first, we introduce the third category of decoupling of positive and negative states commonly known as the "direct perturbation theory" (DPT). This approach does not suffer from the singularity problems described previously. However, the four-component form of the Dirac equation remains intact. The new Hamiltonian requires identical computational effort as for the Dirac equation itself, hence is not an attractive alternative to the Dirac equation. However, it is useful to assess the accuracy of approximate two-component forms derived from the Dirac equation such as the Pauli Hamiltonian.

Consider the transformation matrix **U**

$$\mathbf{U} = \begin{pmatrix} \mathbf{I} & \mathbf{0} \\ \mathbf{0} & c^{-1}\mathbf{I} \end{pmatrix} \tag{2.60}$$

and corresponding metric **S**

$$\mathbf{S} = \mathbf{U}^{\dagger}\mathbf{U} = \begin{pmatrix} \mathbf{I} & \mathbf{0} \\ \mathbf{0} & c^{-2}\mathbf{I} \end{pmatrix} \tag{2.61}$$

and the transformed wave function $\tilde{\psi}$

$$\tilde{\psi} = \begin{pmatrix} \psi_{\mathrm{L}} \\ c\psi_{\mathrm{S}} \end{pmatrix} = \begin{pmatrix} \mathbf{I} & \mathbf{0} \\ \mathbf{0} & c\mathbf{I} \end{pmatrix} \begin{pmatrix} \psi_{\mathrm{L}} \\ \psi_{\mathrm{S}} \end{pmatrix} \tag{2.62}$$

Next, use the general transformation defined in Eqn. 2.33, since we have a non-zero metric. Substituting for $\mathbf{U}^\dagger$, $\mathbf{U}$ and $\mathbf{S}$ in Eqn. 2.33 with $z = 0$ yields

$$\left[\begin{pmatrix} q\phi\mathbf{I} & \sigma.\Pi \\ \sigma.\Pi & -2m \end{pmatrix} + \frac{1}{c^2}\begin{pmatrix} 0 & 0 \\ 0 & q\phi\mathbf{I} \end{pmatrix}\right]\begin{pmatrix} \psi_L \\ c\psi_S \end{pmatrix} = \mathrm{E}\begin{pmatrix} \mathbf{I} & 0 \\ 0 & 0 \end{pmatrix}\begin{pmatrix} \psi_L \\ c\psi_S \end{pmatrix} + \frac{\mathrm{E}}{c^2}\begin{pmatrix} 0 & 0 \\ 0 & \mathbf{I} \end{pmatrix}\begin{pmatrix} \psi_L \\ c\psi_S \end{pmatrix} \tag{2.63}$$

Hence, the non-relativistic limit of the Dirac equation with c-dependent metric is

$$\begin{pmatrix} q\phi\mathbf{I} & \sigma.\Pi \\ \sigma.\Pi & -2m \end{pmatrix}\begin{pmatrix} \psi_L \\ c\psi_S \end{pmatrix} = \mathrm{E}\begin{pmatrix} \mathbf{I} & 0 \\ 0 & 0 \end{pmatrix}\begin{pmatrix} \psi_L \\ c\psi_S \end{pmatrix} \tag{2.64}$$

This non-relativistic equation in terms of four-component spinors has been studied in detail by Lévy-Leblond [49, 50], who has shown that it results automatically from a study of the irreducible representations of the Galilei group and that it gives a correct description of spin. It is easy to see that in the absence of an external magnetic field Eqn. 2.64 is equivalent to the Schrödinger equation in the sense that after elimination of the 'small component'

$$\begin{aligned} q\phi\psi_L + c\sigma.\mathbf{P}\psi_S &= \mathrm{E}\psi_L \\ \psi_S &= \frac{\sigma.\mathbf{P}\psi_L}{2mc} \end{aligned} \tag{2.65}$$

we get the Schrödinger equation

$$q\phi\psi_L + \frac{(\sigma.\mathbf{P})^2\psi_L}{2m} = \mathrm{E}\psi_L \tag{2.66}$$

Assuming $1/c^2$ as the perturbation parameter the first-order energy can be written as

$$\mathrm{E}^{(1)}(\mathrm{DPT}) = \langle\begin{pmatrix} \psi_L^{(0)} \\ c\psi_S^{(0)} \end{pmatrix}|\begin{pmatrix} 0 & 0 \\ 0 & (q\phi - \mathrm{E}^{(0)})\mathbf{I} \end{pmatrix}|\begin{pmatrix} \psi_L^{(0)} \\ c\psi_S^{(0)} \end{pmatrix}\rangle \tag{2.67}$$

or in two-component form

$$\mathrm{E}^{(1)}(\mathrm{DPT}) = \langle\psi_{\mathrm{L}}^{(0)}\frac{\boldsymbol{\sigma}.\boldsymbol{\Pi}}{2m}|(q\phi - \mathrm{E}^{(0)})|\frac{\boldsymbol{\sigma}.\boldsymbol{\Pi}}{2m}\psi_{\mathrm{L}}^{(0)}\rangle \tag{2.68}$$

We can use the relation

$$\left\{\frac{(\boldsymbol{\sigma}.\boldsymbol{\Pi}).(\boldsymbol{\sigma}.\boldsymbol{\Pi})}{2m} + q\phi\right\}|\psi_{\mathrm{L}}^{(0)}\rangle = \mathrm{E}^{(0)}|\psi_{\mathrm{L}}^{(0)}\rangle \tag{2.69}$$

to rewrite Eqn. 2.68

$$\begin{aligned}\mathrm{E}^{(1)}(\mathrm{DPT}) &= \langle\psi_{\mathrm{L}}^{(0)}\frac{\boldsymbol{\sigma}.\boldsymbol{\Pi}}{2m}|(q\phi - \frac{(\boldsymbol{\sigma}.\boldsymbol{\Pi})(\boldsymbol{\sigma}.\boldsymbol{\Pi})}{2m} - q\phi)|\psi_{\mathrm{L}}^{(0)}\rangle \\ &= \langle\psi_{\mathrm{L}}^{(0)}|\frac{q(\boldsymbol{\sigma}.\boldsymbol{\Pi})\phi(\boldsymbol{\sigma}.\boldsymbol{\Pi})}{4m^2} - \frac{(\boldsymbol{\sigma}.\boldsymbol{\Pi})^4}{8m^3} - \frac{q(\boldsymbol{\sigma}.\boldsymbol{\Pi})^2\phi}{4m^2}|\psi_{\mathrm{L}}^{(0)}\rangle \\ &= \langle\psi_{\mathrm{L}}^{(0)}|\mathbf{h}_1^{\mathrm{DPD}}|\psi_{\mathrm{L}}^{(0)}\rangle\end{aligned} \tag{2.70}$$

where $\mathbf{h}_1^{\mathrm{DPD}} = \frac{q(\boldsymbol{\sigma}.\boldsymbol{\Pi})\phi(\boldsymbol{\sigma}.\boldsymbol{\Pi})}{4m^2} - \frac{(\boldsymbol{\sigma}.\boldsymbol{\Pi})^4}{8m^3} - \frac{q(\boldsymbol{\sigma}.\boldsymbol{\Pi})^2\phi}{4m^2}$. Similarly, the first-order energy obtained from the Pauli Hamiltonian given in Eqn. 2.54 can be written as

$$\begin{aligned}\mathrm{E}^{(1)}(\mathrm{FW}) &= \langle\psi_{\mathrm{L}}^{(0)}|\frac{q(\boldsymbol{\sigma}.\boldsymbol{\Pi})\phi(\boldsymbol{\sigma}.\boldsymbol{\Pi})}{4m^2} - \frac{(\boldsymbol{\sigma}.\boldsymbol{\Pi})^4}{8m^3} - \frac{q[(\boldsymbol{\sigma}.\boldsymbol{\Pi})^2,\phi]_+}{8m^2}|\psi_{\mathrm{L}}^{(0)}\rangle \\ &= \langle\psi_{\mathrm{L}}^{(0)}|\mathbf{h}_1^{\mathrm{FW}}|\psi_{\mathrm{L}}^{(0)}\rangle\end{aligned} \tag{2.71}$$

where $\mathbf{h}_1^{\mathrm{FW}} = \frac{q(\boldsymbol{\sigma}.\boldsymbol{\Pi})\phi(\boldsymbol{\sigma}.\boldsymbol{\Pi})}{4m^2} - \frac{(\boldsymbol{\sigma}.\boldsymbol{\Pi})^4}{8m^3} - \frac{q[(\boldsymbol{\sigma}.\boldsymbol{\Pi})^2,\phi]_+}{8m^2}$. The $\mathbf{h}_1^{\mathrm{DPD}}$ is a non-Hermitean operator. Noting that the expectation value of a real non-Hermitean operator is equal to the expectation value of its Hermitean part, the equivalence of the two first-order energies is obvious. The difference in two Hamiltonians $\mathbf{h}_1^{\mathrm{FW}} - \mathbf{h}_1^{\mathrm{DPD}} = \frac{1}{4}[(\boldsymbol{\sigma}.\boldsymbol{\Pi})^2, \phi]$ is responsible for the singularities in $\mathbf{h}_1^{\mathrm{FW}}$ higher orders of perturbation theory. But as shown above this fact does not affect the first-order energy in Eqn. 2.71.

So far our discussion of the NRF and the NRL of the relativistic Hamiltonians has been limited to the one-fermion external field Dirac equation. For the many-fermion case the picture is not so simple. For example, in the case of two fermions, the wave function has sixteen components: four components representing both particles having positive energy states, another eight components representing one particle having positive energy states and the other particle having negative energy states and the other four components representing both particles having negative energy states. Consequently, we can not decompose the full wave function into two group of components, one having only positive energy states and the other having only negative energy states or equivalently, we cannot write the many-fermion Hamiltonian in the form given in Eqn. 2.31 contrary to what has been done in the literature in some occasions [51]. The decoupling of positive energy components from negative and mixed (both positive and negative) components to establish the NRF or NRL of many-fermion Hamiltonian is conceptually similar to the one-fermion case but the mathematics involved is laborious. The two-fermion problem is manageable but tedious.

Consequently, we have to adopt an intelligent, and at the same time accurate, scheme to obtain the NRF of the many electron-Hamiltonian. Two such schemes have been used in the literature. The first one involves a rigorous derivation of the NRF of the two-fermion DBC Hamiltonian and directly extends the resulting non-relativistic Hamiltonian to many-fermion systems. The advantage of this scheme is that the order of each term in terms of $mc^2\alpha^n$ (n is a postive integer) can be determined without any ambiguties. However, the physical significance of the individual terms is not quite clear from the way they are derived. In the other scheme, the NRF of the one-fermion Hamiltonian (Eqn. 2.54) is extended directly to the many-fermion case. The Coulomb and Breit interaction terms are added later on recognizing the fact that they are formally of order $mc^2\alpha^2$ in a molecular environment. The effect of other moving charged particles to the vector potential has to be taken into account in the derivation. Contrary to the former procedure, there are ambiguities in the order of certain terms in the expansion [10]. For this reason the latter approach is not entirely satisfatory, but it does have the advantage of exhibiting the origin of the each term in the Hamiltonian and it allows physical interpretation to be given to each. Here, we adopt the first approach.

Both FW and ESC methods have been applied to decouple the positive energy states from the negative and mixed states of the two-fermion DBC Hamiltonian [52–54]. Since we are only interested in positive energy solutions, we may start from the original two-fermion DBC Hamiltonian without positive and negative energy projection operators. The two-fermion DBC Hamiltonian for stationary states can be written as

$$\left\{\sum_{i=1}^{2} c\sigma_i.\mathbf{\Pi}_i + \sum_{i=1}^{2} q_i\phi_i\mathbf{I} + \frac{q_1q_2(\mathbf{I}+\mathbf{B}_{12})}{r_{12}}\right\}\Psi = \mathrm{E}\Psi \tag{2.72}$$

where

$$\mathbf{B}_{12} = -\frac{1}{2}[\boldsymbol{\alpha}_1.\boldsymbol{\alpha}_2 + \frac{(\boldsymbol{\alpha}_1.\mathbf{r}_{12})(\boldsymbol{\alpha}_2.\mathbf{r}_{12})}{r_{12}^2}] \tag{2.73}$$

As in the one-fermion case, the whole energy spectrum is shifted by $-(m_1+m_2)c^2$, so that the direct comparison with the non-relativistic results is feasible. Following the notation introduced by Foldy and Wouthuysen one can write

$$\begin{aligned} \mathcal{E}\mathcal{E} &= \sum_{i=1}^{2} q_i\phi_i\mathbf{I} + \frac{q_1q_2}{r_{12}}\mathbf{I} \\ \mathcal{E}\mathcal{O} &= \boldsymbol{\alpha}_1.\boldsymbol{\Pi}_1 \\ \mathcal{O}\mathcal{E} &= \boldsymbol{\alpha}_2.\boldsymbol{\Pi}_2 \\ \mathcal{O}\mathcal{O} &= -\frac{1}{2}[\boldsymbol{\alpha}_1.\boldsymbol{\alpha}_2 + \frac{(\boldsymbol{\alpha}_1.\mathbf{r}_{12})(\boldsymbol{\alpha}_2.\mathbf{r}_{12})}{r_{12}^2}] \end{aligned} \tag{2.74}$$

Here, $\mathcal{E}$ represents an even operator, that is one that has no matrix elements between positive and negative energy components while $\mathcal{O}$ is an odd operator having only matrix elements between positive and negative energy components. The conditions for an operator to be even or odd can be expressed more formally; an even operator must commute with β: $[\mathcal{E}, \beta] = 0$ while an odd operator must anticommute with β: $[\mathcal{E}, \beta]_+ = 0$.

As mentioned earlier, the concepts involved in the two-fermion case are essentialy the same and also the expansion in terms of α^2 have the similar problems as in the one-fermion case. Consequently, we have chosen to give only the final form of the Hamiltonian and refer to Barker and Glover [54] for mathematical details. The NRF of the two-fermion Hamiltonian can be written in terms of the operators defined in Eqn. 2.74 as

$$\begin{aligned} \mathrm{H} = &+ \frac{1}{2m_1}(\mathcal{E}\mathcal{O})^2 + \frac{1}{2m_2}(\mathcal{O}\mathcal{E})^2 - \frac{\alpha^2}{8m_1^3}(\mathcal{E}\mathcal{O})^4 - \frac{\alpha^2}{8m_2^3}(\mathcal{O}\mathcal{E})^4 + (\mathcal{E}\mathcal{E}) \\ &+ \frac{\alpha^2}{8m_1^2}\sum_i^N [\mathcal{O}\mathcal{E},\ [\mathcal{E}\mathcal{E}, \mathcal{O}\mathcal{E}]] + \frac{\alpha^2}{8m_1^2}\sum_i^N [\mathcal{E}\mathcal{O},\ [\mathcal{E}\mathcal{E}, \mathcal{E}\mathcal{O}]] \\ &+ \frac{\alpha^2}{4m_1 m_2}\sum_i^N [\mathcal{E}\mathcal{O},\ [\mathcal{O}\mathcal{E}, \mathcal{O}\mathcal{O}]_+]_+ + O\big(mc^2\alpha^5\big) \end{aligned} \tag{2.75}$$

Here, we only keep terms having order of magnitude $mc^2\alpha^4$. One can compare this expansion with the one-fermion Pauli expansion presented in Eqn. 2.54, given the fact that in the one-fermion case $\mathcal{E} = q\phi\mathrm{I}$ and $\mathcal{O} = \boldsymbol{\sigma}.\boldsymbol{\Pi}$. We can simplify this expression by expanding the commutators and with the extensive use of vector algebra. The resulting two-fermion Hamiltonian can be extended to many-fermions quite trivially and the NRF of the many-fermion Hamiltonian can be written as

$$\begin{aligned} \mathrm{H} = &+ \sum_i q_i\phi_i + \sum_i \frac{(\boldsymbol{\Pi}_i.\boldsymbol{\Pi}_i)}{2m_i} + \frac{1}{2}\sum_{ij}\frac{q_i q_{\mathrm{j}}}{r_{\mathrm{ij}}} - \alpha\sum_i \frac{q_i \mathbf{S}_i.(\nabla \times \mathbf{A}_i)}{m_i} \\ &- \frac{\alpha^2}{8}\sum_i \frac{q_i(\nabla.\mathbf{E}_i)}{m_i^2} - \frac{\alpha^2}{8}\sum_i \frac{(\boldsymbol{\Pi}_i.\boldsymbol{\Pi}_i)^4}{m_i^3} + \frac{\alpha^2}{2}\sum_i \frac{q_i \mathbf{S}_i.(\nabla \times \mathbf{A}_i)(\boldsymbol{\Pi}_i.\boldsymbol{\Pi}_i)}{m_i^3} \\ &+ \frac{\alpha^2}{4}\sum_i \frac{q_{\mathrm{i}}\mathbf{S}_i.(\boldsymbol{\Pi}_i \times \mathbf{E}_i - \mathbf{E}_i \times \boldsymbol{\Pi}_i)}{m_i^2} - \frac{\alpha^2}{2}\sum_{i,j}\frac{q_{\mathrm{i}} q_{\mathrm{j}}\mathbf{S}_i.(\mathbf{r}_{ij} \times \boldsymbol{\Pi}_i)}{m_i^2 r_{ij}^3} \end{aligned} \tag{2.76}$$

$$
\begin{aligned}
&-\alpha^2\sum_{i,j}\frac{q_iq_{\mathbf{j}}\mathbf{S}_i.(\mathbf{r}_{ij}\times\mathbf{\Pi}_j)}{m_i^2r_{ij}^3}-\frac{\alpha^2\pi}{2}\sum_{i,j}\frac{q_iq_j}{m_im_j}\delta(\mathbf{r}_{ij})\\
&-\frac{\alpha^2}{4}\sum_{i,j}q_iq_j\left(\frac{\mathbf{\Pi}_i.(r_{ij}^{-1}\mathbf{\Pi}_j)\ +(\mathbf{\Pi}_i.\mathbf{r}_{ij})r_{ij}^{-3}(\mathbf{r}_{ij}.\mathbf{\Pi}_j)}{m_im_j}\right)\\
&+\frac{\alpha^2}{2}\sum_{i,j}\frac{q_iq_j}{m_im_j}\left(\frac{(\mathbf{S}_i.\mathbf{S}_j)}{r_{ij}^3}-3\frac{(\mathbf{S}_i.\mathbf{r}_{ij})(\mathbf{S}_i.\mathbf{r}_{ij})}{r_{ij}^5}-\frac{8\pi\delta(\mathbf{r}_{ij})(\mathbf{S}_i.\mathbf{S}_j)}{3}\right)\\
&+O\left(mc^2\alpha^5\right)
\end{aligned}
$$

It is important to note once again that ϕ_i and $\mathbf{A}_i$ in Eqn. 2.76 are the scalar and vector potential resulting from the external electromagnetic radiation field. Also note that here, $\mathbf{E}_i = \nabla\phi_i$ and $\mathbf{S}_i$ is the spin of the i^{th} particle. We can identify each term in Eqn. 2.76 as corresponding to a certain type of physical interaction of moving charged particles. The list of physical interpretations of terms follows, in the same order as the terms in Eqn. 2.76.

1. Interaction of the charged particles with the external electric field.
2. Kinetic energy of the moving charged particle.
3. Particle-particle electrostatic interaction.
4. Interaction of particle spin magnetic moment with the external magnetic field (Zeeman term).
5. Relativiastic correction to the first term (Darwin term).
6. Relativistic correction to the second term.
7. Relativistic correction to the third term.

8. Interaction of an electron's spin magnetic moment with the magnetic field it experiences by virtue of its motion relative to the external electric field (spin-orbit term).
9. Interaction of the spin-magnetic moment of an electron with its own orbital motion due to the electric field of another electron.
10. Interaction of the spin magnetic moment of one electron with the orbital motion of another (spin-other-orbit term).
11. Relativistic correction to the third term.
12. Retarded orbit-orbit interaction of one electron with the electromagnetic field due to the relative motion of another.
13. Dipole-dipole interaction between the spin magnetic moments of two electrons and a Fermi-contact type interaction.

So far in the derivation of the Hamiltonian given in Eqn. 2.76 we have not placed any restriction on the type of particles except that they are fermions. If we limit our many-fermion systems to be molecules whose nuclei are point charges with spin one-half entities with proper nuclear masses and charges, Eqn. 2.76 describes a proper molecular Hamiltonian when we introduce the appropriate notation to distinguish the nuclei from electrons. In the case of electrons, the mass (m_e and electronic charge (e) both are unity in terms of Hartree atomic units. The mass of nucleus N in atomic units is denoted by M_N. Similarly, the electron spin $\mathbf{S}_i$ is replaced by $\mathbf{I}_N$, the spin of the nucleus N and $Z_N e$ is used in place of charge

q, where Z_N is the atomic number of nucleus N. However, this approach is not problem free either. It has been shown from QED arguments that the resulting molecular Hamiltonian is valid only if we neglect all the terms which involve M_N^{-2} and smaller [16]. As we can see from Eqn. 2.76, in fact all these terms are formally of order $mc^2\alpha^4$ to begin with and at least 10^{-6} smaller than the corresponding electron terms.

Another potential problem which can arise can be seen by estimating the order of magnitude of the terms on the basis of an electron in a Bohr orbit of the hydrogen atom. In general, when higher nuclear charges ($Z_N e$) are involved it is no longer appropriate to express the magnitude of terms in the Hamiltonian in terms of $mc^2\alpha^n$. Instead the terms $c\boldsymbol{\alpha}$.P, $q\phi$ and $qc\boldsymbol{\alpha}$.A in the Dirac Hamiltonian are of order $mc^2(Z_N\alpha)$, $mc^2(Z_N\alpha)^2$ and $mc^2(Z_N\alpha)^3$ respectively, so that $Z_N\alpha$ should be used as the expansion parameter rather than the fine structure constant itself. However, since α is very small number, these comments only become important for atoms or molecules with large atomic numbers, and then only for the inner electrons, since the outer electrons are screened from the nuclei.

Another subtlety is that the assumption nuclei behave as Dirac particles, amounts to assuming that all nuclei have spin 1/2. However, it is not uncommon to have nuclei with spin as high as 9/2: worse nuclei with integer spins are bosons and do not obey Fermi-Dirac statistics. The only justification to use Eqn. 2.76 for such a case is that the resulting theory agrees with experiment.

Under the assumption, we are in a position to extend our many-fermion Hamiltonian to molecules assuming that the nuclei are Dirac particles with anomalous spin. The molecular Hamiltonian may then be written as

$$\mathrm{H} = \mathrm{H}_e + \mathrm{H}_N + \mathrm{H}_{eN} \tag{2.77}$$

where $\mathrm{H}_e = \mathrm{H}_e^1 + \mathrm{H}_e^2 + \mathrm{H}_e^3 + \mathrm{H}_e^4 + \mathrm{H}_e^5 + \mathrm{H}_e^6 + \mathrm{H}_e^7 + \mathrm{H}_e^8 + \mathrm{H}_e^9 + \mathrm{H}_e^{10} + \mathrm{H}_e^{11} + \mathrm{H}_e^{12} + \mathrm{H}_e^{13}$, $\mathrm{H}_N = \mathrm{H}_N^1 + \mathrm{H}_N^2 + \mathrm{H}_N^3 + \mathrm{H}_N^4$ and $\mathrm{H}_{eN} = \mathrm{H}_{eN}^1 + \mathrm{H}_{eN}^2 + \mathrm{H}_{eN}^3 + \mathrm{H}_{eN}^4 + \mathrm{H}_{eN}^5 + \mathrm{H}_{eN}^6 + \mathrm{H}_{eN}^7$ are, respectively, the electronic, nuclear and the electron-nuclear interaction Hamiltonian. Expressions for individual terms in Eqn. 2.77 can easily be written by substitution of appropriate masses and charges in Eqn. 2.76. In doing so it is helpful to keep in mind the interpretation of the individual terms in Eqn. 2.76 and which particle is responsible for quantities such as mass and charge in individual terms. The electronic terms

$$\begin{aligned}
\mathrm{H}_e^1 &= -\sum_i \phi_i \\
\mathrm{H}_e^2 &= \sum_i \frac{(\mathbf{\Pi}_i.\mathbf{\Pi}_i)}{2} \\
\mathrm{H}_e^3 &= \frac{1}{2}\sum_{i,j} \frac{1}{r_{ij}} \\
\mathrm{H}_e^4 &= \alpha \sum_i \mathbf{S}_i.(\nabla \times \mathbf{A}_i) \\
\mathrm{H}_e^5 &= \frac{\alpha^2}{8} \sum_i \nabla.\mathbf{E}_i
\end{aligned} \tag{2.78}$$

$$\begin{aligned}
\mathrm{H}_e^6 &= -\frac{\alpha^2}{8}\sum_i (\mathbf{\Pi}_i.\mathbf{\Pi}_i)^4 \\
\mathrm{H}_e^7 &= -\frac{\alpha^2}{2}\sum_i \mathrm{S}_i.(\nabla \times \mathrm{A}_i)(\mathbf{\Pi}_i.\mathbf{\Pi}_i) \\
\mathrm{H}_e^8 &= -\frac{\alpha^2}{2}\sum_{i,j} \frac{\mathbf{S}_i.(\mathbf{r}_{ij}\times\mathbf{\Pi}_i)}{\mathrm{r}_{ij}^3} \\
\mathrm{H}_e^9 &= -\alpha^2\sum_{i,j} \frac{\mathbf{S}_i.(\mathbf{r}_{ij}\times\mathbf{\Pi}_j)}{\mathrm{r}_{ij}^3} \\
\mathrm{H}_e^{10} &= -\frac{\alpha^2}{4}\sum_i \mathbf{S}_i.(\mathbf{\Pi}_i\times\mathbf{E}_i - \mathbf{E}_i \times \mathbf{\Pi}_i) \\
\mathrm{H}_e^{11} &= -\frac{\alpha^2}{4}\sum_{i,j} \mathbf{\Pi}_i.(r_{ij}^{-1}\mathbf{\Pi}_j) + (\mathbf{\Pi}_i.\mathbf{r}_{ij})r_{ij}^{-3}(\mathbf{r}_{ij}.\mathbf{\Pi}_j) \\
\mathrm{H}_e^{12} &= \frac{\alpha^2}{2}\sum_{i,j}\left(\frac{(\mathbf{S}_i.\mathbf{S}_j)}{r_{ij}^3} - 3\frac{(\mathbf{S}_i.\mathbf{r}_{ij})(\mathbf{S}_i.\mathbf{r}_{ij})}{r_{ij}^5} - \frac{8\pi\delta(\mathbf{r}_{ij})(\mathbf{S}_i.\mathbf{S}_j)}{3}\right) \\
\mathrm{H}_e^{13} &= -\frac{\alpha^2\pi}{2}\sum_{i,j}\delta(\mathbf{r}_{ij})
\end{aligned}$$

nuclear terms

$$\begin{aligned}
\mathrm{H}_N^1 &= \sum_N Z_N\phi_N \\
\mathrm{H}_N^2 &= \sum_N \frac{(\mathbf{\Pi}_N.\mathbf{\Pi}_N)}{2} \\
\mathrm{H}_N^3 &= \frac{1}{2}\sum_{N,N'} \frac{Z_N Z_{N'}}{r_{NN'}} \\
\mathrm{H}_N^4 &= -\alpha\sum_N \frac{Z_N\mathbf{I}_N.(\nabla \times \mathbf{A}_N)}{M_N}
\end{aligned} \tag{2.79}$$

and electronic-nuclear coupling terms

$$
\begin{aligned}
\mathrm{H}^1_{Ne} &= -\sum_{i,N} \frac{Z_N}{r_{iN}} \\
\mathrm{H}^2_{Ne} &= \frac{\alpha^2}{2} \sum_{i,N} \frac{Z_N \mathbf{S}_i.(\mathbf{r}_{iN} \times \mathbf{\Pi}_i)}{M_N r_{iN}^3} \\
\mathrm{H}^3_{Ne} &= \frac{\alpha^2}{2} \sum_{i,N} \frac{Z_N \mathbf{S}_i.(\mathbf{r}_{iN} \times \mathbf{\Pi}_N)}{M_N r_{iN}^3} \\
\mathrm{H}^4_{Ne} &= \frac{\alpha^2}{2} \sum_{i,N} \frac{Z_N \mathbf{I}_N.(\mathbf{r}_{iN} \times \mathbf{\Pi}_i)}{M_N r_{iN}^3} \\
\mathrm{H}^5_{Ne} &= \frac{\alpha^2}{2} \sum_{i,N} \frac{Z_N [\mathbf{\Pi}_N.(r_{iN}^{-1} \mathbf{\Pi}_N) + (\mathbf{\Pi}_N.\mathbf{r}_{iN}) r_{iN}^{-3} (\mathbf{r}_{iN}.\mathbf{\Pi}_N)]}{M_N} \\
\mathrm{H}^6_{Ne} &= -\frac{\alpha^2}{2} \sum_{i,N} \frac{Z_N}{M_N} \left(\frac{(\mathbf{S}_i.\mathbf{I}_N)}{r_{iN}^3} - 3 \frac{(\mathbf{S}_i.\mathbf{r}_{iN})(\mathbf{I}_N.\mathbf{r}_{iN})}{r_{iN}^5} - \frac{8\pi\delta(\mathbf{r}_{iN})(\mathbf{S}_i.\mathbf{I}_N)}{3} \right) \\
\mathrm{H}^7_{Ne} &= \frac{\alpha^2 \pi}{2} \sum_{i,N} Z_\alpha \delta(\mathbf{r}_{iN})
\end{aligned}
\tag{2.80}
$$

2.5 The NMR Chemical Shifts and Indirect Nuclear Spin-Spin Coupling Operators

The preceding discussion was intended to present a general survey of molecular Hamiltonians, in both their relativistic and non-relativistic forms. We focused mainly on the approximations involved in their derivations and also their limitations, with the hope that such a focus eventually will be helpful in using them intelligently for problems of interest and also in assessing the results obtained. In this respect, the Hamiltonian presented in Eqn. 2.77 is general and can be used in non-relativistic or relativistic (within limitations) calculations of energetics, dynamics and spectra of molecules and atoms. Similarly, Eqn. 2.28 can be used in four-component, fully relativistic calculations of such molecular properties.

We can make further approximations to simplify the NRF of the Hamiltonian presented in Eqn. 2.76 for non-dynamical properties. For such properties, we can freeze the nuclear movements and study only the electronic problem. This is commonly known as the clamped nuclei approximation, and it usually is quite good because of the fact that the nuclei of a molecule are about 1836 times more massive than the electrons, so we can usually think of the nuclei moving slowly in the average field of the electrons, which are able to adapt almost instantaneously to the nuclear motion. Invocation of the clamped nuclei approximation to Eqn. 2.76, causes all the nuclear contributions which involve the nuclear momentum operator to vanish and the others to become constants (nuclear repulsion *etc.*). These constant terms will only shift the total energy of the system. The remaining terms in the Hamiltonian are electronic terms and nuclear-electronic interaction contributions which do not involve the nuclear momentum operator.

Generally, it is not required to retain all the terms in the resulting approximate Hamiltonian need to be retained. Only those operators which describe the actual physical processes involved in the problem. For example, in the absence of an external electromagnetic field, the non-relativistic energy calculations only requires retaining the terms H_e^1, H_e^2, H_e^3 and H_N^3. Perturbative relativistic energy calcualtions can be carried out by including H_e^5, H_e^6 in addition to the terms retained for non-relativistic energy calculations. The electron coupled interaction of nuclear magnetic moments with themselves and also with an external magnetic field is responsible for NMR spectroscopy. Since the focus of this study is calculation of NMR spectra within the non-relativistic framework, we will take a closer look at the Hamiltonian derived from Eqn. 2.77 to describe NMR processes.

In this regard, we retain all the terms which depend on nuclear magnetic moments of nuclei in the molecule and the external magnetic field through its vector potential in addition to the usual non-relativistic Hamiltonian. The result is

$$\begin{aligned} \mathrm{H} = {} & \sum_{i} \frac{(\mathbf{\Pi}_i.\mathbf{\Pi}_i)}{2} + \frac{1}{2}\sum_{i,j}\frac{1}{r_{\mathrm{ij}}} - \sum_{i,N}\frac{Z_N}{r_{\mathrm{i}N}} + \sum_{N,N'}\frac{Z_N Z_{N'}}{R_{NN'}} \\ & + \frac{1}{c}\sum_{i,N}\gamma_N \frac{\mathbf{I}_N.(\mathbf{r}_{iN}\times\mathbf{\Pi}_i)}{r_{iN}^3} - \frac{1}{c}\sum_{i,N}\gamma_N\left(\frac{(\mathbf{S}_i.\mathbf{I}_N)}{r_{iN}^3} - 3\frac{(\mathbf{S}_i.\mathbf{r}_{iN})(\mathbf{I}_N.\mathbf{r}_i)}{r_{iN}^5}\right) \\ & + \frac{8\pi}{3c}\sum_{i,N}\gamma_N\delta(\mathbf{r}_{iN})(\mathbf{S}_i.\mathbf{I}_N) \end{aligned} \tag{2.81}$$

Here, we have introduced the notation $\boldsymbol{\mu}_N = \gamma_N\mathbf{I}_N = g_N\beta_N\mathbf{I}_N = (\frac{gZ_N m_p}{M_N})(\frac{1}{2m_p c})\mathbf{I}_N$ and $\beta = \frac{1}{2c}$ where β is the Bohr magneton and β_N, γ_N and $\boldsymbol{\mu}_N$ are nuclear magneton, nuclear magnetogyric ratio and nuclear magnetic moments of the nuclei *N* respectively. Substitute for $\mathbf{\Pi}_i$,

$$\mathbf{\Pi}_i = \mathbf{P}_i + \frac{\mathbf{A}_i}{c} = \mathbf{P}_i + \frac{1}{2c}\sum_i \mathbf{B}\times(\mathbf{r}_i - \mathbf{G}) \tag{2.82}$$

where **B** and **G** are the external magnetic field strength and the gauge origin of the external vector potential respectively. Substitute for $\mathbf{\Pi}_i$ in Eqn. 2.81 and then simplify assuming the Coulomb gauge ($\nabla.\mathbf{A} = 0$) to obtain

$$\begin{aligned}
\mathrm{H} = \; & -\sum_{i} \frac{\nabla_i^2}{2} + \frac{1}{2}\sum_{i,j} \frac{1}{r_{ij}} - \sum_{i,N} \frac{Z_N}{r_{iN}} + \sum_{N,N'} \frac{Z_N Z_{N'}}{R_{NN'}} \\
& + \frac{1}{ic}\sum_{i}\big((\mathbf{r}_i - \mathbf{G}) \times \nabla_i\big).\mathbf{B} + \frac{1}{ic}\sum_{i,N} \gamma_N \mathbf{I}_N.\left(\frac{(\mathbf{r}_{iN} \times \nabla_i)}{\mathbf{r}_{iN}^3}\right) \\
& + \frac{1}{2c^2}\sum \gamma_N \mathbf{I}_N.\left(\frac{(\mathbf{r}_{iN}.(\mathbf{r}_i - \mathbf{G}))(\mathbf{B})}{r_{iN}^3} - \frac{(\mathbf{r}_{iN}.\mathbf{B})(\mathbf{r}_i - \mathbf{G})}{r_{iN}^3}\right) \\
& - \frac{1}{c}\sum_{i,N} \gamma_N \left(\frac{(\mathbf{S}_i.\mathbf{I}_N)}{r_{iN}^3} - 3\frac{(\mathbf{S}_i.\mathbf{r}_{iN})(\mathbf{I}_N.\mathbf{r}_{iN})}{r_{iN}^5}\right) \\
& + \frac{8\pi}{3c}\sum_{i,N} \gamma_N \delta(\mathbf{r}_{iN})(\mathbf{S}_i.\mathbf{I}_N) + \sum_{i} \frac{(\mathbf{B}.\mathbf{B})[(\mathbf{r}_i - \mathbf{G}).(\mathbf{r}_i - \mathbf{G})]}{4c^2}
\end{aligned} \tag{2.83}$$

We can assign a formal order to each term in Eqn. 2.83 assuming **B** and γ_N as ordering parameters. First, let us consider the first-order field independent terms in Eqn. 2.83

$$\begin{aligned}
H(\mathrm{FC}) &= \frac{16\pi\beta}{3}\sum_{i,N} \gamma_N \delta(\mathbf{r}_{iN})(\mathbf{S}_i.\mathbf{I}_N) \\
H(\mathrm{SD}) &= 2\beta \sum_{i,N} \gamma_N \left(\frac{3(\mathbf{S}_i.\mathbf{r}_{iN})(\mathbf{I}_N.\mathbf{r}_{iN})}{r^5{}_{iN}} - \frac{(\mathbf{S}_i.\mathbf{I}_N)}{r_{iN}^5}\right) \\
H(\mathrm{PSO}) &= -2i\beta \sum_{i,N} \gamma_N \mathbf{I}_N.\left(\frac{\mathbf{r}_{iN} \times \nabla_i}{\mathbf{r}^3{}_{iN}}\right)
\end{aligned} \tag{2.84}$$

where $\beta = \frac{1}{2c}$. Historically, these operators are known as Fermi-contact (FC), spin-dipole (SD) and paramagnetic spin-orbit (PSO) operators and their forms were originally derived by Ramsey [55]. As we shall see, a collection of second-order properties, each of which involves a pair of the these various first-order external field independent operators, contributes to the indirect nuclear spin-spin coupling constant tensor. According to Ramsey, the indirect nuclear spin-coupling tensor also consists of a second-order contribution involving the diamagnetic spin-orbit contribution (DSO) given by

$$H(\mathrm{DSO}) = \frac{2\beta}{c} \sum_{N,N'} \gamma_N \gamma_{N'} \sum_i \frac{(\mathbf{I}_N.\mathbf{I}_{N'})(\mathbf{r}_{kN}.\mathbf{r}_{kN'}) - (\mathbf{I}_N.\mathbf{r}_{kN'})(\mathbf{I}_{N'}.\mathbf{r}_{kN})}{r^3_{kN} r^3_{kN'}} \tag{2.85}$$

The DSO term involves a product of γ_N ordering parameters and formally a second-order term. As seen from Eqn. 2.83, the DSO term does not arise in our derivation and requires further investigation. In this regard, first, we will present another derivation which will eventually lead to the DSO term in addition to all the other terms given in Eqn. 2.83.

In principle, this additional derivative also starts from the many-fermion Hamiltonian given in Eqn. 2.76. As discussed earlier, extension of this equation to molecules usually is done by imposing the requirement that some of these particles are nuclei which are assumed to be fermions. An alternative, but less rigorous approach to introduce nuclei is to consider them as an external perturbation which modifies the external vector and scalar potential in Eqn. 2.76. Further approximations can be made for non-dynamical properties by invoking the clamped nuclei approximation. For such a situation the external vector potential **A** can be written as

$$\mathbf{A}_i = \frac{1}{2} \sum_i \mathbf{B} \times (\mathbf{r}_i - \mathbf{G}) + \sum_{i,N} \frac{\boldsymbol{\mu}_{iN} \times \mathbf{r}_{iN}}{r^3_{iN}} \tag{2.86}$$

Retain the following terms in Eqn. 2.76,

$$\mathrm{H} = \sum_i \frac{(\boldsymbol{\Pi}_i.\boldsymbol{\Pi}_i)}{2} + \frac{1}{2}\sum_{i,j}\frac{1}{r_{ij}} - \sum_{i,N}\frac{Z_N}{r_{iN}} + \sum_{N,N'}\frac{Z_N Z_{N'}}{R_{NN'}} + \frac{1}{c}\sum_i \mathbf{S}_i.(\nabla \times \mathbf{A}_i) \tag{2.87}$$

and substitute for $\boldsymbol{\Pi}_i$ where $\boldsymbol{\Pi}_i = \mathbf{P}_i + \frac{\mathbf{A}_i}{c}$ and $\mathbf{A}_i$ is given in Eqn. 2.86. Expand the first term assuming the Coulomb gauge in order to obtain

$$\begin{aligned} \boldsymbol{\Pi}_i.\boldsymbol{\Pi}_i &= (\mathbf{P}_i + \frac{\mathbf{A}_i}{c}).(\mathbf{P}_i + \frac{\mathbf{A}_i}{c}) \\ &= \mathbf{P}_i{}^2 + \frac{2}{c}\mathbf{A}_i.\mathbf{P}_i + \frac{1}{c^2}\mathbf{A}_i.\mathbf{A}_i \end{aligned} \tag{2.88}$$

and then the last two terms

$$\begin{aligned} \frac{2}{c}\mathbf{A}_i.\mathbf{P}_i &= \frac{1}{ci}\Big[\sum_i \frac{\mathbf{B}\times(\mathbf{r}_i - \mathbf{G})}{2} + \sum_{i,N}\frac{\boldsymbol{\mu}_N \times \mathbf{r}_{iN}}{r^3_{iN}}\Big].\nabla_i \\ &= \frac{1}{ci}\sum_i((\mathbf{r}_i - \mathbf{G})\times\nabla_i).\mathbf{B} + \frac{1}{ic}\sum_{i,N}\frac{\boldsymbol{\mu}_N.(\mathbf{r}\times\nabla_i)}{r^3_{iN}} \end{aligned} \tag{2.89}$$

and

$$\begin{aligned} \frac{1}{c^2}\mathbf{A}_i.\mathbf{A}_i = {} & \frac{1}{4c^2}\sum_i(\mathbf{B}.\mathbf{B})(\mathbf{r}_i - \mathbf{G}).(\mathbf{r}_i - \mathbf{G}) + \frac{1}{2c^2}\sum_{i,N}\frac{(\mathbf{B}.\boldsymbol{\mu}_N)(\mathbf{r}_i - \mathbf{G}).\mathbf{r}_i}{r^3_{iN}} \\ & - \frac{1}{2c^2}\sum_{i,N}\frac{(\mathbf{B}.\mathbf{r}_i)(\mathbf{r}_i - \mathbf{G}).\boldsymbol{\mu}_N}{r^3_{iN}} \\ & + \frac{1}{c^2}\sum_{N,N'}\sum_i\frac{(\boldsymbol{\mu}_N.\boldsymbol{\mu}_{N'})(\mathbf{r}_{iN}.\mathbf{r}_{iN'}) - (\boldsymbol{\mu}_N.\mathbf{r}_{iN'})(\boldsymbol{\mu}_{N'}.\mathbf{r}_{iN})}{r^3_{iN}r^3_{iN'}} \end{aligned} \tag{2.90}$$

Substitute for $\mathbf{A}_i$ from Eqn. 2.86, in the last term of Eqn. 2.87 and then simplify to obtain

$$\begin{aligned}\frac{1}{c}\sum_i \mathbf{S}_i.(\nabla\times\mathbf{A}_i) &= \frac{1}{2c}\sum_i \mathbf{S}_i.\nabla\times(\mathbf{B}\times(\mathbf{r}_i-\mathbf{G})) \\ &\quad+\frac{1}{c}\sum_{i,N}\mathbf{S}_i.\nabla\times\left(\frac{\boldsymbol{\mu}_N\times\mathbf{r}_{\mathrm{iN}}}{r^3{}_{iN}}\right) \\ &= \frac{1}{c}\sum_{i,N}\left(\frac{3(\mathbf{S}_i.\mathbf{r}_{iN})(\boldsymbol{\mu}_N.\mathbf{r}_{iN})}{r_{iN}^5}-\frac{(\mathbf{S}_i.\boldsymbol{\mu}_N)}{r_{iN}^3}\right) \\ &\quad+\frac{1}{c}\sum_{i,N}\frac{8\pi\delta(\mathbf{r}_{iN})(\mathbf{S}_i.\boldsymbol{\mu}_N)}{3}\end{aligned} \tag{2.91}$$

The final molecular Hamiltonian

$$\begin{aligned}\mathrm{H}= &-\sum_i\frac{\nabla_i^2}{2}+\frac{1}{2}\sum_{i,j}\frac{1}{r_{ij}}-\sum_{i,N}\frac{Z_N}{r_{iN}}+\sum_{N,N'}\frac{Z_NZ_{N'}}{R_{NN'}} \\ &+\frac{1}{ic}\sum_i((\mathbf{r}_i-\mathbf{G})\times\nabla_i).\mathbf{B}+\frac{1}{ic}\sum_{i,N}\gamma_N\mathbf{I}_N.\left(\frac{(\mathbf{r}_{iN}\times\nabla_i)}{r_{iN}^3}\right) \\ &+\frac{1}{2c^2}\sum_{i,N}\gamma_N\mathbf{I}_N.\left(\frac{(\mathbf{r}_{iN}.(\mathbf{r}_i-\mathbf{G}))(\mathbf{B})}{r_{iN}^3}-\frac{(\mathbf{r}_{iN}.\mathbf{B})(\mathbf{r}_i-\mathbf{G})}{r_{iN}^3}\right) \\ &-\frac{1}{c}\sum_{i,N}\gamma_N\left(\frac{(\mathbf{S}_i.\mathbf{I}_N)}{r_{iN}^3}-3\frac{(\mathbf{S}_i.\mathbf{r}_{iN})(\mathbf{I}_N.\mathbf{r}_{iN})}{r_{iN}^5}\right) \\ &-\frac{8\pi}{3c}\sum_{i,N}\gamma_N\delta(\mathbf{r}_{iN})(\mathbf{S}_i.\mathbf{I}_N)+\sum_i\frac{(\mathbf{B}.\mathbf{B})[(\mathbf{r}_i-\mathbf{G}).(\mathbf{r}_i-\mathbf{G})]}{4c^2} \\ &+\frac{1}{c^2}\sum_{N,N'}\gamma_N\gamma_{N'}\sum_i\frac{(\mathbf{I}_N.\mathbf{I}_{N'})(\mathbf{r}_{iN}.\mathbf{r}_{iN'})-(\mathbf{I}_N.\mathbf{r}_{iN'})(\mathbf{I}_{N'}.\mathbf{r}_{iN})}{r_{iN}^3r_{iN'}^3}\end{aligned} \tag{2.92}$$

is formulated by collecting the expressions derived in Eqns. 2.88, 2.89, 2.90 and 2.91. The first-order field independent operators collected from this Hamiltonian are identical with the operators given in Eqn. 2.84. The second-order field-independent contribution is identical to the DSO operator given in Eqn. 2.85.

As shown from this derivation, the DSO contribution arises from A.A type contributions to the molecular Hamiltonian. Formally, this term has an order of magnitude $mc^2\alpha^8$ in a molecular environment. It is not all that suprising that the DSO term does not arise in our first derivation since it is based on a truncated Pauli expansion of the Hamiltonian in which the magnitude of all the terms is $mc^2\alpha^4$ or less. It seems, based on our estimation ($mc^2\alpha^8$), that the magnitude of the DSO term is very small. However, as we will see latter, the DSO contribution is significant for certain coupling constants and cannot be discarded. Note that our criterion to estimate the order of magnitude of the individual terms is based on an electron in a Bohr orbit of the hydrogen atom. On some occasions this estimate may not give a good indication of the actual magnitude.

For example, the DSO contribution involves a product of two gyromagnetic ratios of the pair of coupled nuclei which can be larger for lighter atoms and hence, can result in a large overall DSO contribution. Ultimately, these complications are results of the expansion of the Hamiltonian in terms of α^2 and terms which are supposedly higher order in the expansion and, can sometimes, be numerically significant. In such occasions the only guidance we have is the experimental results, and we arbitrarily incorporate higher-order terms in the expansion to improve the agreement with experiment.

At this point, it is appropriate to present a brief discussion on the origin of the FC operator ($\delta-$function) in the two-component form (Pauli form) of the molecular relativistic Hamiltonian. Many textbooks adopt the point of view that the FC is a relativistic effect, which must be derived from the Dirac equation [56, 57]. In other textbooks or review articles it is stressed that the FC is not a relativistic effect and that it can be derived from classical electrodynamics [58, 59], disregarding the origin of the gyromagnetic factor $g = 2$. In some textbooks both derivations are presented [60]. The relativistic derivations suffer from the inherent drawbacks in the Pauli expansion, in particular that the Pauli Hamiltonian can only be used in the context of the first-order perturbation theory. Moreover, the origin of the FC term appears to be different depending on whether one uses the ESC method or FW transformation.

Earlier we mentioned briefly that the electron spin is perfectly consistent with the non-relativistic four-component Lévy-Leblond theory [49, 50]. The FC type interaction is not manifests in Dirac or Lévy-Leblond theory. We shall show that on reducing the four component Lévy-Leblond equation into two component form the FC contribution arise naturally. A non-relativistic electron in an electromagnetic radiation field is described by the Lévy-Leblond equation given by

$$\begin{pmatrix} -\phi \mathrm{I} & \sigma.\Pi \\ \sigma.\Pi & -2m \end{pmatrix} \begin{pmatrix} \psi_{\mathrm{L}} \\ c\psi_{\mathrm{S}} \end{pmatrix} = \mathrm{E} \begin{pmatrix} \mathrm{I} & 0 \\ 0 & 0 \end{pmatrix} \begin{pmatrix} \psi_{\mathrm{L}} \\ c\psi_{\mathrm{S}} \end{pmatrix} \tag{2.93}$$

where ϕ is the scalar potential and $\Pi = \mathbf{p} - \frac{\mathbf{A}}{c}$. We can rewrite Eqn. 2.93 such that

$$\left[\begin{pmatrix} -\phi \mathrm{I} & \sigma.\mathrm{P} \\ \sigma.\mathrm{P} & -2m \end{pmatrix} - \frac{1}{c} \begin{pmatrix} 0 & \sigma.\mathrm{A} \\ \sigma.\mathrm{A} & 0 \end{pmatrix} \right] \begin{pmatrix} \psi_{\mathrm{L}} \\ c\psi_{\mathrm{S}} \end{pmatrix} = \mathrm{E} \begin{pmatrix} \mathrm{I} & 0 \\ 0 & 0 \end{pmatrix} \begin{pmatrix} \psi_{\mathrm{L}} \\ c\psi_{\mathrm{S}} \end{pmatrix} \tag{2.94}$$

which led to the perturbing operator $h_1 = -\frac{1}{c}\begin{pmatrix} 0 & \sigma.A \\ \sigma.A & 0 \end{pmatrix}$. Hence, the first-order perturbed energy can be written as

$$E^{(1)} = -\frac{1}{c}\langle\begin{pmatrix}\psi_L^{(0)} \\ c\psi_S^{(0)}\end{pmatrix}|\begin{pmatrix} 0 & \sigma.A \\ \sigma.A & 0 \end{pmatrix}|\begin{pmatrix}\psi_L^{(0)} \\ c\psi_S^{(0)}\end{pmatrix}\rangle \qquad (2.95)$$

or in two component form

$$E^{(1)} = -\frac{1}{2mc}\left\{\langle\sigma.\mathbf{P}\psi_L^{(0)}|\sigma.\mathbf{A}\psi_L^{(0)}\rangle + \langle\psi_L^{(0)}|(\sigma.\mathbf{A})(\sigma.\mathbf{P})|\psi_L^{(0)}\rangle\right\} \qquad (2.96)$$

One can use the "turnover-rule" for $\sigma.\mathbf{P}$ and get

$$E^{(1)} = -\frac{1}{2mc}\left\{\langle\psi_L^{(0)}|[\sigma.\mathbf{P},\sigma.\mathbf{A}]_+|\psi_L^{(0)}\rangle\right\} \qquad (2.97)$$

which is straightforward if **A** is regular at the origin, and which is still valid for singular **A** if the derivative implicit in **p** is taken in the "distribution sense" [61]. This can be further simplified to obtain

$$E^{(1)} = -\frac{1}{2mc}\left\{\langle\psi_L^{(0)}|\mathbf{P}.\mathbf{A}+\mathbf{A}.\mathbf{P}+i\sigma.(\mathbf{P}\times\mathbf{A}) + i\sigma.(\mathbf{A}\times\mathbf{P})|\psi_L^{(0)}\rangle\right\} \qquad (2.98)$$

The vector potential created by spin of a nucleus with a magnetic moment μ,

$$\mathbf{A} = \frac{\mu\times\mathbf{r}}{r^3} \qquad (2.99)$$

is singular at the origin. As a result we must take the derivatives, implicit in Eqn. 2.98, in the "distribution sense". This means that $\nabla \times \mathbf{A}$ consists of two terms, one in which the derivatives are taken in usual function sense, and an extra term

$$\nabla \times \mathbf{A} = -\frac{\mu}{r^3} + \frac{3(\mu.\mathbf{r})\mathbf{r}}{r^3} + \frac{2\mu\delta(\mathbf{r})}{3r^3} \qquad (2.100)$$

This shows that the FC operator arises as an artifact if one wants to describe the hyperfine interaction by first-order perturbation theory in terms of two-component spinors. In other words, when singular functions are involved, the boundary conditions cannot be ignored. These give rise to the FC operator.

2.6 Conclusion

In this chapter we have presented a detailed discussion of relativistic and non-relativistic forms of molecular Hamiltonians. We have focused on the problems associated with extending "Dirac's one fermion theory" smoothly to many-fermion systems. A brief discussion of QED many-fermion Hamiltonians also was given. A comprehensive account of the problem of decoupling Dirac's four-component equation into two-component form and the serious drawbacks of the Pauli expansion were presented. The origins of the DSO and FC operators have been addressed. In conclusion, the working Hamiltonian which we will use in the following chapters to describe NMR spectra is given in Eqn. 2.92.

CHAPTER 3
MOLECULAR STATIC SECOND-ORDER PROPERTIES

3.1 Introduction

The subject of molecular properties in principle involves all observable associated with isolated molecules, clusters, and solids. This study is concerned with isolated molecules. The molecular properties can be static or dynamic (frequency or time dependent); first, second, or higer order; and one- or two-particle type. First-order one-particle properties include dipole moments, electric-field gradients, spin densities and so forth. Polarizabilities and certain contributions to the NMR chemical shifts and spin-spin coupling constants are examples of one-particle, second-order properties. The two-particle spin-orbit contribution is a two-particle, first-order property. For convenience, we can classify them broadly into three rough but somtimes overlapping categories

1. External properties.
2. Internal properties and fine structure.
3. Energy properties.

The first category describes the response of a molecule to externally applied fields. This category of properties are of pivotal importance, since they include a response of a molecule to an external electromagnetic radiation, and hence all of spectroscopy is within its scope. It also includes, multipole moments, polarizabilities and susceptibilities, *etc.* A less obvious example in this category would be intermolecular interactions of molecules due to induced fields in the absence of external fields. Intermolecular forces are usually considered as an example in the third category, however.

The second category includes the fine structure terms which arise because of (usually small) relativistic interactions. They involve the coupling of electronic and nuclear spins, both with each other and with other terms. Examples are spin-orbit and spin-spin interactions. Sometimes there are couplings between electron spin and external fields. Such couplings are important in the study of electron paramagnetic resonance (EPR) and NMR spectroscopy.

The final category, energy properties, includes potential surfaces, together with their features such as minima and saddle points which are important in the study of molecular reactions and stability. Energy properties also include transition energies between electronic states and related quantities such as ionization and attachment energies.

It is well known that since the beginning of molecular quantum mechanics, observables can be evaluated as expectation values

$$\langle \hat{O} \rangle = \langle \Psi | \hat{O} | \Psi \rangle \tag{3.101}$$

where $\hat{O}$ is a Hermitian operator representing the physical quantity in question, and $|\Psi\rangle$ is a normalized eigenfunction of the stationary state Schrödinger equation

$$H_o\Psi = E\Psi \tag{3.102}$$

H is usually the non-relativistic Born-Oppenheimer [62] Hamiltonian for the system under consideration. For exact normalized $|\Psi\rangle$, there is an exact equivalence between the expectation value and the energy derivative

$$\langle\hat{O}\rangle = \left(\frac{\partial E}{\partial\lambda}\right)_{\lambda=0} \tag{3.103}$$

which is commonly known as the Hellmann-Feynman theorem [63]. Here λ is an ordering parameter and the perturbed Hamiltonian for the system under consideration is given by $\hat{H} = \hat{H}_o + \lambda\hat{O}$.

In terms of time-independent perturbation theory, the expectation value given in Eqn. 3.101 also can be interpreted as the first-order correction to the energy assuming that the solution to the non-relativistic Born-Oppenheimer Hamiltonian is considered zeroth-order. As a consequence of the Hellmann-Feynman theorem, the first-order correction to the energy is identical to the energy derivative. Similarly, we can talk about second- and higher order corrections which are proportional to second and corresponding higher energy derivatives. A similar, but more general concept is the response of a molecule to an applied field. In this respect, we define a time-dependent Hermitian operator of the form

$$\hat{O}(t) = F(t)\hat{V} \tag{3.104}$$

where the time-independent operators V are Hermitian, and the time factors have the Fourier decomposition

$$F(t) = \frac{1}{2\pi} \int_{-\infty}^{\infty} F(\omega) exp(-i\omega t) d\omega \tag{3.105}$$

in terms of the frequency ω, and the inverse Fourier transform

$$F(\omega) = \int_{-\infty}^{\infty} F(t) exp(i\omega t) dt \tag{3.106}$$

The change in expectation value of $\langle \hat{O} \rangle = \langle \Psi(t) | \hat{O} | \Psi(t) \rangle$, $\delta \langle \hat{O} \rangle$ is the subject matter of response theory. Naturally, time-dependent perturbation theory [64] is used in this analysis. Here, $\Psi(t)$ is now an eigenfunction of the time-dependent Schrodinger equation:

$$H\Psi(t) = i\frac{\partial \Psi(t)}{\partial t} \tag{3.107}$$

The change in $\langle \hat{O} \rangle$ through first-order in $\hat{O}(t)$ is the linear response and higher order changes are designated as the non-linear response (quadratic, cubic *etc.*). The idea of probing molecules with a time-dependent field is clearly a very physical one, and also highly relevant since all the spectroscopic techniques are based on such processes. With the proper choice of $\hat{O}(t)$, one can describe, or at least idealize such real experiments.

As indicated earlier, the response functions are usually evaluated using time-dependent perturbation theory [64]. The propagator theory incorporates the many-body language to the time-dependent perturbation theory. It was originated in statistical physics [65], solid state [66], nuclear physics [67] and scattering theory [68] and latter borrowed by quantum chemistry [69]. The response functions also can be evaluated as energy derivatives. This is fairly easy to see for perturbations which do not have time dependence, since for such cases we have a Hellmann-Feynman theorem to guide us. Such perturbations are known as static perturbations. For example, dipole moments, static polarizabilities and hyperpolarizabilities are defined as first-, second- and third-derivatives of the energy which are proportional to the zeroth-, first- and second-order response of a molecule to a static electric field.

However, a straightforward extension of energy derivative methods to time-dependent perturbations is not possible since, in the case of time-dependent perturbations, the corresponding energy is not uniquely defined and hence response functions cannot be obtained automatically as energy derivatives [70]. For such cases an extension of the Hellmann-Feynman theorem to time-dependent perturbations is required [71]. For a given approximate wave function $\tilde{\Psi}(t)$, the energy-like expression

$$W(t) = \langle\tilde{\Psi}(t)|H(t) - i\frac{\partial}{\partial t}|\tilde{\Psi}(t)\rangle \tag{3.108}$$

which is referred to as the quasienergy or pseudoenergy, defined so that it would satisfy a Hellmann-Feynman theorem in the same form as the usual time-independent case at any arbitrary value of a static-field strength, one can then derive frequency dependent response functons as pseudoenergy derivatives [72–76]. This is a natural and very attractive extension of energy derivative.

The focus of this study is on NMR chemical shift and indirect nuclear spin-spin coupling constants. The spin-spin coupling constants are external field independent and belong to the second category of our classification. Chemical shifts are dependent on applied static magnetic field and belong to the first category. As seen in chapter 1, there are both first- and second- order contributions to the total spin-spin coupling and chemical shift tensors involving one-particle type operators. To derive appropriate response equations, we are free to start from more general time dependent perturbation theory, or its many-body equivalent, propagator theory or quasienergy derivative theory and use the resulting equations with appropriate limiting conditions for static properties like NMR chemical shifts and spin-spin coupling constants. Alternatively, one can simply use time-independent perturbation theory or energy derivative theory.

In this chapter, we present the response equations for Hartree-Fock (HF) and coupled-cluster singles and doubles (CCSD) method based on energy derivative theory. In the case of HF method, the energy derivative approach to second-order properties is known as the coupled perturbed Hartree-Fock (CPHF) method. The second derivative of the CCSD energy with respect to the perturbations of interest leads to what we call the quadratic equation-of-motion coupled cluster singles and doubles (EOM-CCSD) approach to second-order properties. The CI-like EOM-CCSD approach, which resembles the usual second-order perturbation theory type expression is derived using expressions which define the quadratic EOM-CCSD method by taking the CCSD similarity transformed Hamiltonian as the zeroth-order Hamiltonian. The equations presented here are valid for any first- or second-order static molecular properties with the choice of appropriate operators.

3.2 Some Basic Preliminaries

Fock Space

From the outset we will introduce the algebraic approximation, in which a finite (say M-elements) set of orthonormal spin-orbitals $\{\varphi_p\}$ is used to construct many-particle wave functions. The Fock-space is defined as direct sum of the n-particle states $F^{(n)}$, consisting of all possible $\binom{M}{n}$ Slater determinants and the abstract vacuum state $F^{(o)}$

$$F = F^{(o)} \oplus F^{(1)} \oplus F^{(2)} \oplus \ldots \oplus F^{(M)} \tag{3.109}$$

The linear, Hermitian symmetric scalar product between two ket states $|\Phi_\mu\rangle$ and $|\Phi_\nu\rangle$ denoted by $\langle\Phi_\mu|\Phi_\nu\rangle$ is zero when the two states correspond to different number of particles and otherwise

$$\langle\Phi_\mu|\Phi_\nu\rangle = \int \Phi_\mu^*(\tau_1, \tau_2, \tau_3, \ldots \tau_n)\Phi_\nu(\tau_1, \tau_2, \tau_3, \ldots \tau_n) d\tau_1 d\tau_2 \ldots d\tau_n \tag{3.110}$$

where τ_i denote the spatial and spin coordinates of the particle i. From now on, we will assume that the set of spin-orbitals $\{\varphi_p\}$ forms an orthonormal set.

Then it follows that the kets corresponding to the Slater determinants including the vacuum ket denoted by $|0\rangle$ form a orthonormal basis for the Fock space.

The complementary space $F^\dagger$ consists of bra states $\langle\Phi_\mu|$ defined as the complex conjugate of the ket states. By definition the bra states are related to the scalar product

$$\langle\Phi_\mu|(|\Phi_\nu\rangle) \equiv \langle\Phi_\mu|\Phi_\nu\rangle = \delta_{\mu\nu} \tag{3.111}$$

where we have used the orthonormality of the basis. The resolution of the identity in Fock-space is given by

$$I = \sum_\mu |\Phi_\mu\rangle\langle\Phi_\mu| \tag{3.112}$$

where the sum over all basis states spanning the Fock-space is assumed. Having defined the resolution of the identity, a general linear operator in Fock-space can be written as

$$\hat{O} = \sum_{\mu,\nu} |\Phi_\mu\rangle\langle\Phi_\mu|\hat{O}|\Phi_\nu\rangle\langle\Phi_\nu| \quad = \sum_{\mu,\nu} |\Phi_\mu\rangle\hat{O}_{\mu\nu}\langle\Phi_\nu| \tag{3.113}$$

Development of correlated many-body methods working in configuration space (Slater determinants) formalism is cumbersome. As an alternative, at a later stage, we will introduce the second-quantization or occupation number representation. Prior to that, we will take a look at one of the most commonly used set of spin-orbitals to represent the Fock-space configurations, the HF molecular orbitals.

Hartree-Fock Approximation

The independent particle or Hartree-Fock (HF) self consistent field (SCF) approximation [77] is undoubtedly the most widely used electronic structure method. The HF method usually provides a reference for subsequent correlated electronic structure methods such as configuration interaction (CI) or coupled-cluster (CC) methods. Before proceeding any further, let us consider our working Hamiltonian, which is the non-relativistic zeroth-order molecular Hamiltonian within the Born-Oppenheimer approximation

$$\hat{H}^o = \sum_i \hat{\mathrm{h}}(i) + \frac{1}{2}\sum_{i>j}\frac{1}{r_{ij}} + \sum_{\alpha>\beta}\frac{Z_\alpha Z_\beta}{R_{\alpha\beta}} \tag{3.114}$$

where

$$\hat{\mathrm{h}}(i) = -\frac{\nabla_i^2}{2} - \sum_\alpha \frac{Z_\alpha}{r_{i\alpha}} \tag{3.115}$$

with variables having the same meaning as described in chapter 1. The nuclear repulsion energy is a scalar parameter in the Born-Oppenheimer approximation.

The HF molecular wave function, Φ_o, is an antisymmetrized product (single determinant) of a variationally optimum set of orthonormal one-particle functions (spin-orbitals)

$$\varphi_i(1) \quad i = 1, 2, \ldots, n \tag{3.116}$$

defined by set of one-particle canonical HF equations. The equations which define Φ_o and $\varphi_i(1)$ are

$$\Phi_o = \hat{\mathcal{A}}(\varphi_1(1)\varphi_2(2)......\varphi_n(n)) \tag{3.117}$$

and

$$\hat{\mathcal{F}}(i)\varphi_i(i) = \varepsilon_i\varphi_i(i) \qquad i = 1, 2, \ldots \tag{3.118}$$

with $\hat{\mathcal{A}} = \frac{1}{\sqrt{n!}}\sum_p(-1)^p\hat{\mathcal{P}}$, $\hat{\mathcal{P}}$ is a permutation of electron labels, and the Fock operator $\hat{\mathcal{F}}$ is

$$\hat{\mathcal{F}}(i) = \hat{\mathrm{h}}(i) + \sum_j^n \int \varphi_j^*(2)(1 - \mathcal{P}_{12})\frac{1}{r_{ij}}\varphi_j(2)d\tau_2 \tag{3.119}$$

The derivation of Eqn. 3.119 can be found in any standard quantum chemistry text books and will not be repeated [77].

The entire set of spin-orbitals defined by Eqn. 3.118 is not necessarily required to be occupied in the HF single determinant. For convenience, the spin-orbitals (molecular orbitals) which are occupied in the HF determinant are labeled by $i, j, \ldots$ while the unoccupied or virtual orbitals are labeled as $a, b, \ldots$. The generic orbitals are usually denoted by $p, q, \ldots$. The HF energy of system under consideration is

$$\begin{aligned} \mathrm{E}_o &= \langle\Phi_o|\hat{H}^o|\Phi_o\rangle \\ &= \sum_i\langle i|\hat{\mathrm{h}}|i\rangle + \frac{1}{2}\sum_{i,j}\langle ij||ij\rangle + \frac{1}{2}\sum_{\alpha,\beta}\frac{Z_\alpha Z_\beta}{R_{\alpha\beta}} \end{aligned} \tag{3.120}$$

The generic two-electron integral $\langle pq||rs\rangle$ is defined as

$$\int\int \varphi_p(\tau_1)\varphi_q(\tau_2)\frac{1}{r_{12}}(1 - \hat{\mathcal{P}}_{12})\varphi_r(\tau_1)\varphi_s(\tau_2)d\tau_1 d\tau_2 \tag{3.121}$$

It is common practice in modern quantum chemistry to expand the molecular orbitals (MO) in terms of Gaussian functions centered on atoms, known as atomic orbitals (AO) or atomic basis functions. In mathematical terms this is equivalent to

$$\varphi_p = \sum_{\mu}^{\mathcal{N}} C_{\mu p} \phi_\mu \tag{3.122}$$

where ϕ_μ is a gaussian basis function located on an arbitrary atomic center. Here, $\mathcal{N}$ is the number of basis functions.

Second Quantization and Normal Order

The occupation number or second quantization formalism has a one-to-one correspondence to the configuration state formalism. We define a set of creation operators $\{\hat{a}_p^\dagger\}$ corresponding to the one-particle spin-orbitals $\{\varphi_p\}$ acting on basis states of Fock-space. Their action on a vacuum state $|0\rangle$ is given by $\hat{p}^\dagger|0\rangle = |\varphi_p\rangle$ while they act to annhilate the function $|\varphi_p\rangle$

$$\hat{p}^\dagger|\varphi_p\rangle = 0 \qquad p = 1, 2, \ldots, \mathcal{N} \tag{3.123}$$

(note that we abbreviate $\hat{a}_p^\dagger$ to $\hat{p}^\dagger$). The annihilation operators are defined by Hermitian conjugation $\langle \Phi_\mu | \hat{p}^\dagger | \Phi_\nu \rangle = \langle \Phi_\nu | \hat{p} | \Phi_\mu \rangle^*$. Both creation and annihilation operators are known as construction operators. It can easily be shown that they satisfy anticommutation relations

$$\begin{aligned} [\hat{p}, \hat{q}]_+ &= [\hat{p}^\dagger, \hat{q}^\dagger]_+ = 0 \\ [\hat{p}^\dagger, \hat{q}]_+ &= \delta_{pq} \end{aligned} \tag{3.124}$$

which reflect the antisymmetry of the many-particle states. The creation and annihilation operators can be used to generate basis states in Fock-space and its dual space respectively. For example, an n-particle ket basis state $|\Phi_\mu\rangle$ can be written as

$$|\Phi_\mu^{(n)}\rangle = \hat{p}_1^\dagger \hat{p}_2^\dagger \dots \hat{p}_n^\dagger |0\rangle \tag{3.125}$$

and corresponds to the normalized Slater determinant

$$|\Phi_\mu\rangle = \frac{1}{\sqrt{n!}} det(\varphi_{p_1}(\tau_1)\varphi_{p_2}(\tau_2)\dots\varphi_{p_n}(\tau_n)) \tag{3.126}$$

The vector space of linear operators on Fock-space is spanned by the $\{\hat{X}^\dagger \hat{Y}\}$ where X and Y are ordered products of creation operators, for example $\hat{X} = \hat{p}^\dagger \hat{q}^\dagger, \dots, \quad \hat{p} < \hat{q} < \dots$. A general linear operator may be represented by

$$\hat{O} = \sum_{X,Y} \hat{O}_{XY} \hat{X}^\dagger \hat{Y} \tag{3.127}$$

which compares with Eqn. 3.113. For particle-conserving operators, the two operator strings X and Y have equal lengths and the lengths of the operator strings are directly related to the number of particles of the irreducible part of the operator. A more elaborate discussion of these points can be found in Nooijen [78].

The sequence of construction operators is said to be in *normal* order when all annihilation operators act before any creation operators. The operators we use will always be written in the normal-ordered form, e.g. $\mathsf{N}(\hat{p}^\dagger \hat{r} \hat{s} \hat{q}^\dagger)$ or $\{\hat{p}^\dagger \hat{r} \hat{s} \hat{q}^\dagger\}$ where N or $\{\}$ denotes the normal ordering of the operators. Within the normal-ordered product, the operators anticommute with the overall sign determined by the number of interchanges: postive overall sign for even number of interchanges and negative overall sign for odd number of interchanges. A convenient feature of the normal-ordered operators is that they annihilate the vaccum state.

As mentioned earlier, any arbitrary operator can be writen in normal ordered from and one would like to have a multiplication rule for normal product operators, that expresses the results again in normal order. This is provided by Wick's theorem. The derivation and in depth discussion of various Wick theorems can be find in several excellent texts [64, 79], so here we only present the final result. To this end we first define the notion of contraction

$$\hat{p}\hat{q} = \mathbb{N}(\hat{p}\hat{q}) + \mathbb{C}(\hat{p}\hat{q}) \tag{3.128}$$

where $\mathbb{C}(\hat{p}\hat{q})$ denote the contraction between $\hat{p}$ and $\hat{q}$. Explicitly the contarctions are

$$\begin{aligned} \mathbb{C}(\hat{p}\hat{q}^\dagger) &= \delta_{pq} \\ \mathbb{C}(\hat{p}^\dagger\hat{q}) &= 0 \end{aligned} \tag{3.129}$$

Now we are in a position to state Wick's theorem. Let $\hat{O}_1$ and $\hat{O}_2$ be strings of construction operators, then

$$\mathbb{N}(\hat{O}_1)\mathbb{N}(\hat{O}_2) = \mathbb{N}(\hat{O}_1\hat{O}_2) + \mathbb{N}(\{\hat{O}_1\hat{O}_2\}) + \mathbb{N}(\{\{\hat{O}_1\hat{O}_2\}\}) + \dots \tag{3.130}$$

where each pair of braces surrounding the operator strings denotes a sum over all possible contractions that can be obtained by taking one construction operator from $\hat{O}_1$ and one from $\hat{O}_2$. Hence, the normal-ordered result of two normal-ordered operator strings acting in successive is equivalent to the sum of the normal product

$\mathsf{N}(\hat{O}_1\hat{O}_2)$ with zero, one, two up to all possible contractions formed by taking one construction operator each from $\hat{O}_1$ and from $\hat{O}_2$.

In the algebraic approximation we are working with the Fock-space Hamiltonian. Because of the limitations of our one-particle basis sets, only a few eigenstates and eigenvalues of it can represent the true eigenvalues and eigenstates. These states usually comprise a few low-lying n-particle states as well as certain n + 1 and n - 1 states. It is convenient for book keeping purposes if we represent these states with respect to an n-particle state which lies closer to them. This leads to the so-called quasi-particle or particle-hole formulation. The n-particle state $|\Phi_o\rangle$ serves as our new vacuum and it is called the Fermi vacuum. Usually, $|\Phi_o\rangle$ is the HF single determinant, but other choices are also equally well applicable. The one-particle states are divided into two subsets, the occupied and virtual states. To distinguish them from one another, we use the same notation introduced in the proceeding discussion. The annihilation operator $\hat{\imath}$ creates a hole in the model vacuum, and it is said to be a quasiparticle creation operator (q-creation operator). Similarly, $\hat{\imath}^\dagger|\Phi_o\rangle = 0$, and q-annihilation operator. Likewise $\hat{a}$ and $\hat{a}^\dagger$ are q-annihilation and q-creation operators respectively.

Now we have adequate tools at hand to write down our working Hamiltonian in normal ordered form. The Fock space Hamiltonian in terms of construction operators is given by

$$\hat{H}^o = \sum_{pq} \hat{\mathrm{h}}_{pq}\hat{p}^\dagger\hat{q} + \frac{1}{4}\sum_{\substack{p,q\\r,s}} \langle pq||rs\rangle \hat{p}^\dagger\hat{q}^\dagger\hat{s}\hat{r} \tag{3.131}$$

where $\hat{\mathrm{h}}_{pq} = \int d\tau\varphi_p(\tau)\hat{h}\varphi_q(\tau)$ and $\langle pq||rs\rangle$ are two electron integrals, as defined previously in Eqn. 3.121. We can rewrite $\hat{\mathrm{H}}^o$ in normal ordered form with respect to the model vacuum $|\Phi_o\rangle$ by direct application of Wick's theorem to the two operator strings in Eqn. 3.131. A detailed derivation can be found elsewhere [78] and we merely quote the final results

$$\hat{H}^o_N = \sum_{pq} \hat{\mathcal{F}}_{pq}\hat{p}^\dagger\hat{q} + \frac{1}{4}\sum_{\substack{p,q\\r,s}} \langle pq||rs\rangle \hat{p}^\dagger\hat{q}^\dagger\hat{s}\hat{r} + \mathrm{E}_o \tag{3.132}$$

where $\hat{\mathcal{F}}_{pq} = \hat{\mathrm{h}}_{pq} + \sum_i \langle pi||qi\rangle$.

3.3 Energy Derivatives

Spin Hamiltonian

For a molecule in a homogeneous magentic field **B**, the energy shift through second-order in the vector potential

$$\mathbf{A}(\mathbf{r}) = \frac{1}{2}\mathbf{B}\times(\mathbf{r}-\mathbf{G}) + \sum_N \gamma_N \frac{\mathbf{I}_N \times (\mathbf{r}-\mathbf{R}_N)}{|\mathbf{r}-\mathbf{R}_N|^3} \tag{3.133}$$

can be written as

$$\begin{aligned} \Delta E \;=\; & -\frac{1}{2}\chi\,\mathbf{B}.\mathbf{B} + \sum_N \gamma_N(1-\sigma_N)\,\mathbf{I}_N.\mathbf{B} + \\ & \sum_{N>N'} \mathbf{I}_N.(\mathbf{T}_{NN'} + \mathbf{J}_{NN'})\cdot\mathbf{I}_{N'} \end{aligned} \tag{3.134}$$

Here, $\boldsymbol{\chi}$ is the magnetic susceptibility tensor, $\boldsymbol{\sigma}_N$ denotes the magnetic shielding constant tensor for nucleus N while $\mathbf{T}_{NN'}$ and $\mathbf{J}_{NN'}$ are the direct and the indirect parts of the nuclear spin-spin coupling constant tensor respectively. The gyromagnetic ratio of nucleus N is denoted γ_N while $\mathbf{I}_N$ and $\mathbf{I}_{N'}$ are nuclear spin angular momenta of nuclei N and N' respectively. The position vector of an arbitrary point in space is denoted $\mathbf{r}$ while $\mathbf{R}_N$ and $\mathbf{G}$ are the position vector of nucleus N and the gauge origin of the vector potential respectively. Equation 3.134 defines an effective spin-Hamiltonian, in terms of the nuclear spin operators $\mathbf{I}_N$, the eigenvalues of which relate directly to the spectrum measured in an NMR experiment. In this study, we are only concerned with the indirect part of the nuclear spin-spin coupling tensors, $\mathbf{J}_{NN'}$ and the shielding tensors, $\boldsymbol{\sigma}_N$. For convenience, let us denote these contributions to the total energy shift as $E^{NN'}$

$$E^{NN'} = \mathbf{I}_N.\mathbf{J}_{NN'}.\mathbf{I}_{N'} + \gamma_N(1 - \sigma_N)\mathbf{I}_N.\mathbf{B} \qquad (3.135)$$

Let us note that the energy shift $E^{NN'}$ depends on the nuclear magnetic moments and the external magnetic field. In this work, we will evaluate the spin-spin coupling tensor and the shielding tensor in a non-relativistic framework. To this end the non-relativistic many-electron Hamiltonian including the vector-potential $\mathbf{A}$ is subject to a perturbation expansion and all terms are retained that are at most quadratic in the nuclear magnetic moment and product terms of nuclear magnetic moment and external field.

Consider an isolated molecule in the presence of a collection of two groups of arbitrary one-particle type perturbations. One of which consists of first-order perturbations and the other group consists of second-order perturbations. The first-quantized Hamiltonian for the system under consideration can be written as

$$\begin{aligned} \hat{H} &= \hat{H}^o + \sum_{N=0} \kappa_N \hat{H}_1^N + \sum_{N>N'=0} \kappa_N \kappa_{N'} \hat{H}_2^{NN'} \\ &= \sum_i \hat{\mathrm{h}}(i) + \frac{1}{2} \sum_{i,j} \frac{1}{r_{ij}} + \sum_{\alpha>\beta} \frac{Z_\alpha Z_\beta}{R_{\alpha\beta}} \end{aligned} \tag{3.136}$$

here, κ_N's are ordering parameters and the new $\hat{\mathrm{h}}(i)$

$$\hat{\mathrm{h}}(i) = -\frac{\nabla_i^2}{2} - \sum_{N=0} \frac{Z_N}{r_{iN}} + \sum_{N=0} \kappa_N \hat{H}_1^N + \sum_{N>N'=0} \kappa_N \kappa_{N'} \hat{H}_2^{NN'} \tag{3.137}$$

The summation over N is assumed to include $N = 0$ to incorporate perturbations which do not depend on nuclear parameters. For example, an applied external magnetic field and the corresponding κ_0 is simply designated as κ. The zeroth-order Hamiltonian is the usual non-relativistic many-electron Born-Oppenheimer Hamiltonian. In the present study, the first-order perturbed Hamiltonian is the sum of the Fermi-contact (FC), spin-dipole (SD), paramagnetic spin-orbit (PSO) and the operators pertinent to the paramagnetic contribution to the NMR chemical shift per each nuclei, while the second-order operators are sums of the diamagnetic spin-orbit operators (DSO) and the operators responsible for the diamagnetic contribution to the NMR chemical shift per each distinguishable pairs of nuclei. Explicit expressions for these operators are given in chapter 1. As we have discussed in chapter 1, the indirect nuclear spin-spin coupling tensor is a second-order property with contributions from second-order DSO operators and a selection of second-order properties that each involve a pair of the FC, SD and PSO operators contributing to the first-order perturbed Hamiltonian.

Except for the different operators involved, contributions to the NMR chemical shift tensor has identical characteristics. The indirect nuclear spin-spin coupling tensor $\mathbf{J}_{NN'}$ and the shielding tensor $\boldsymbol{\sigma}_{NN'}$ relates to the energy derivatives as follows

$$\begin{aligned} \mathbf{I}_N.\mathbf{J}_{NN'}.\mathbf{I}_{N'} &= \left(\frac{\partial^2 \mathrm{E}}{\partial \kappa_N \partial \kappa_{N'}}\right)_{\kappa_N,\kappa_{N'}=0} \\ \mathrm{B}.\boldsymbol{\sigma}_N.\mathbf{I}_N &= \left(\frac{\partial^2 \mathrm{E}}{\partial \kappa_N \partial \kappa}\right)_{\kappa_N,\kappa=0} \end{aligned} \tag{3.138}$$

In the following discussion we derive equations required to evaluate these contributions at the HF and correlated level based on analytical energy derivative theory. Analytical derivative methods rely on explicit computation of the field derivatives of the energy, and of expectation values using perturbation theory.

The Hartree-Fock Analytical Energy Derivatives

The analytical HF derivatives were first propounded by Gerratt and Mills [80] as a means of obtaining nuclear coordinate derivatives of the electronic state potential energy surfaces. Since then analytical evaluation of HF derivatives (first, second and higher) has undergone a remarkable progress, both conceptually and technically [81, 82]. We derive compact expressions for analytic HF energy derivatives through second-order in some detail, to compare with previous work, and with the Random Phase Approximation (RPA) in propagator theory.

The perturbed Hartree-Fock energy of the system in terms of the perturbed HF molecular orbitals can be written as

$$\mathrm{E}_o(\kappa_N) = \sum_i \langle i|\hat{\mathrm{h}}|i\rangle + \frac{1}{2}\sum_{i,j}\langle ij||ij\rangle + \frac{1}{2}\sum_{\alpha,\beta}\frac{Z_\alpha Z_\beta}{R_{\alpha\beta}} \tag{3.139}$$

where the perturbed HF molecular orbitals

$$\varphi_p(\kappa_N) = \sum_\mu \phi_\mu(\kappa_N) C_{\mu p}(\kappa_N) \tag{3.140}$$

and the molecular orbital coefficients $C_{\mu p}(\kappa_N)$ satisfy the orthogonality relation

$$\mathbf{C}^\dagger(\kappa_N)\mathbf{S}(\kappa_N)\mathbf{C}(\kappa_N) = \mathbf{1} \tag{3.141}$$

Here, **S** is the overlap matrix.

The first derivative of HF molecular orbitals coefficients may be expanded conveniently in terms of the unperturbed HF molecular orbital coefficients

$$\frac{\partial \mathbf{C}(\kappa_N)}{\partial \kappa_N} = \mathbf{C}(0)\mathbf{U}^{\kappa_N} = \mathbf{C}\mathbf{U}^{\kappa_N} \tag{3.142}$$

where the matrix elements of $\mathbf{U}^{\kappa_N}$, $U_{pq}^{\kappa_N}$ are widely known as the coupled perturbed Hartree-Fock coefficients (CPHF). They are perturbation dependent. Differentiate the orthogonality relation given in Eqn. 3.141 to obtain

$$\frac{\partial \mathbf{C}^\dagger}{\partial \kappa_N}\mathbf{S}\mathbf{C} + \mathbf{C}^\dagger\frac{\partial \mathbf{S}}{\partial \kappa_N}\mathbf{C} + \mathbf{C}^\dagger\mathbf{S}\frac{\partial \mathbf{C}}{\partial \kappa_N} = 0 \tag{3.143}$$

Replace the derivatives of MO coefficients in terms of CPHF coefficients given in Eqn. 3.142 to obtain

$$\mathrm{U}^{\kappa_N\dagger}\mathrm{C}^{\dagger}\mathrm{S}\mathrm{C} + \mathrm{C}^{\dagger}\frac{\partial \mathrm{S}}{\partial \kappa_N}\mathrm{C} + \mathrm{C}^{\dagger}\mathrm{S}\mathrm{C}\mathrm{U}^{\kappa_N} = 0 \tag{3.144}$$

which, using 3.141, leads to the important relationship

$$\mathrm{U}^{\dagger\kappa_N} + \mathrm{U}^{\kappa_N} + \mathrm{S}^{(\kappa_N)} = 0 \tag{3.145}$$

At this point it is convenient to introduce the notation that we will employ in the following discussion. A superscript within parentheses signifies the derivative of the operator evaluated in the AO basis and rotated into the MO basis of the unperturbed orbitals. For example, in Eqn. 3.145, $\mathrm{S}_{pq}^{(\kappa_N)} = \mathrm{C}^{\dagger}{}_{p\mu}\frac{\partial \mathrm{S}_{\mu\nu}}{\partial \kappa_N}\mathrm{C}_{\nu q}$ and $\mathrm{h}_{pq}^{(\kappa_N)} = \mathrm{C}^{\dagger}_{p\mu}\frac{\partial \mathrm{h}_{\mu\nu}}{\partial \kappa_N}\mathrm{C}_{\nu q}$.

Let us rewrite the HF energy expression expanding the MO's using Eqn. 3.140

$$\mathrm{E}_o = \mathrm{C}^{\dagger}_{i\mu}\hat{\mathrm{h}}_{\mu\nu}\mathrm{C}_{\nu i} + \frac{1}{2}\mathrm{C}^{\dagger}_{i\mu}\mathrm{C}^{\dagger}_{\lambda j}\langle\mu\lambda||\nu\sigma\rangle\mathrm{C}_{\nu i}\mathrm{C}_{\sigma j} + \frac{1}{2}\frac{Z_\alpha Z_\beta \partial}{\partial \kappa_N}\left(\frac{1}{R_{\alpha\beta}}\right) \tag{3.146}$$

The first derivative of the HF energy $\left(\frac{\partial \mathrm{E}_o}{\partial \kappa_N}\right)_{\kappa_N=0}$ is given by

$$\begin{aligned}
\mathrm{E}_o^{\kappa_N} = {} & \frac{\partial \mathrm{C}^{\dagger}_{i\mu}}{\partial \kappa_N}\hat{\mathrm{h}}_{\mu\nu}\mathrm{C}_{\nu i} + \mathrm{C}^{\dagger}_{i\mu}\frac{\partial \hat{\mathrm{h}}_{\mu\nu}}{\partial \kappa_N}\mathrm{C}_{\nu i} + \mathrm{C}^{\dagger}_{i\mu}\hat{\mathrm{h}}_{\mu\nu}\frac{\partial \mathrm{C}_{\nu i}}{\partial \kappa_N} \\
& + \frac{1}{2}\frac{\partial \mathrm{C}^{\dagger}_{i\mu}}{\partial \kappa_N}\mathrm{C}^{\dagger}_{j\lambda}\langle\mu\lambda||\nu\sigma\rangle\mathrm{C}_{\nu i}\mathrm{C}_{\sigma j} + \frac{1}{2}\mathrm{C}^{\dagger}_{i\mu}\frac{\partial \mathrm{C}^{\dagger}_{j\lambda}}{\partial \kappa_N}\langle\mu\lambda||\nu\sigma\rangle\mathrm{C}_{\nu i}\mathrm{C}_{\sigma j} \\
& + \frac{1}{2}\mathrm{C}^{\dagger}_{i\mu}\mathrm{C}^{\dagger}_{j\lambda}\langle\mu\lambda||\nu\sigma\rangle\frac{\partial \mathrm{C}_{\nu i}}{\partial \kappa_N}\mathrm{C}_{\sigma j} + \frac{1}{2}\mathrm{C}^{\dagger}_{i\mu}\mathrm{C}^{\dagger}_{j\lambda}\langle\mu\lambda||\nu\sigma\rangle\mathrm{C}_{\nu i}\frac{\partial \mathrm{C}_{\sigma j}}{\partial \kappa_N} \\
& + \frac{1}{2}\mathrm{C}^{\dagger}_{i\mu}\mathrm{C}^{\dagger}_{j\lambda}\frac{\partial\langle\mu\lambda||\nu\sigma\rangle}{\partial \kappa_N}\mathrm{C}_{\nu i}\mathrm{C}_{\sigma j} + \frac{1}{2}\frac{Z_\alpha Z_\beta \partial}{\partial \kappa_N}\left(\frac{1}{R_{\alpha\beta}}\right)
\end{aligned} \tag{3.147}$$

It is implied in the right-hand side of Eqn. 3.147 that the derivatives are evaluated at $\kappa_N = 0$ and the Einstein convention of implicit summation over repeated indices also is employed. Eqn. 3.147 can be simplified using Eqn. 3.142 to substitute for the derivatives of MO coefficients followed by collecting identical terms to get

$$\begin{aligned} \mathrm{E}_o^{\kappa_N} &= \mathrm{U}_{ir}^{\dagger\kappa_N}\hat{\mathrm{h}}_{ri} + \hat{\mathrm{h}}_{ir}\mathrm{U}_{ri}^{\kappa_N} + \mathrm{U}_{ir}^{\dagger\kappa_N}\langle ri||ij\rangle + \langle ij||rj\rangle\mathrm{U}_{ri}^{\kappa_N} \\ &+ \hat{\mathrm{h}}_{ii}^{(\kappa_N)} + \frac{1}{2}\langle ij||ij\rangle^{(\kappa_N)} + \frac{1}{2}\frac{\mathrm{Z}_\alpha \mathrm{Z}_\beta \partial}{\partial\kappa_\mathrm{N}}\left(\frac{1}{\mathrm{R}_{\alpha\beta}}\right) \end{aligned} \tag{3.148}$$

This expression can be rewritten as

$$\mathrm{E}_o^{\kappa_N} = \mathrm{U}_{ir}^{\dagger\kappa_N}\hat{\mathcal{F}}_{ri} + \hat{\mathcal{F}}_{ir}\mathrm{U}_{ri}^{\kappa_N} + \hat{\mathrm{h}}_{ii}^{(\kappa_N)} + \frac{1}{2}\langle ij||ij\rangle^{(\kappa_N)} + \frac{1}{2}\frac{\mathrm{Z}_\alpha \mathrm{Z}_\beta \partial}{\partial\kappa_\mathrm{N}}\left(\frac{1}{\mathrm{R}_{\alpha\beta}}\right) \tag{3.149}$$

where $\hat{\mathcal{F}}_{ri} = \hat{\mathrm{h}}_{ri} + \sum_j \langle rj||ij\rangle$. The generic orbital index *r* in Eqn. 3.150 can run over both occupied and virtual orbital indices. However, there is no contribution from virtual orbitals since $\langle a|\hat{\mathcal{F}}|i\rangle = \langle i|\hat{\mathcal{F}}|a\rangle = 0$ due to Brillouin's condition, hence the remaining contributions to the energy derivative are

$$\mathrm{E}_o^{\kappa_N} = \mathrm{U}_{ij}^{\dagger\kappa_N}\hat{\mathcal{F}}_{ji} + \hat{\mathcal{F}}_{ij}\mathrm{U}_{ji}^{\kappa_N} + \hat{\mathrm{h}}_{ii}^{(\kappa_N)} + \frac{1}{2}\langle ij||ij\rangle^{(\kappa_N)} + \frac{1}{2}\frac{\mathrm{Z}_\alpha \mathrm{Z}_\beta \partial}{\partial\kappa_\mathrm{N}}\left(\frac{1}{\mathrm{R}_{\alpha\beta}}\right) \tag{3.150}$$

Since $\hat{\mathcal{F}}$ is symmetric, we can rewrite Eqn. 3.150 to obtain

$$\mathrm{E}_o^{\kappa_N} = (\mathrm{U}_{ji}^{\dagger\kappa_N} + \mathrm{U}_{ji}^{\kappa_N})\hat{\mathcal{F}}_{ij} + \hat{\mathrm{h}}_{ii}^{(\kappa_N)} + \frac{1}{2}\langle ij||ij\rangle^{(\kappa_N)} + \frac{1}{2}\frac{\mathrm{Z}_\alpha \mathrm{Z}_\beta \partial}{\partial\kappa_\mathrm{N}}\left(\frac{1}{\mathrm{R}_{\alpha\beta}}\right) \tag{3.151}$$

Finally, the expression for the HF energy derivative in terms of MOs can be written by replacing the term $\left(\mathrm{U}_{ji}^{\dagger\kappa_N} + \mathrm{U}_{ji}^{\kappa_N}\right)$ in Eqn. 3.151 by using the relation given in Eqn. 3.145

$$\mathrm{E}_o^{\kappa_N} = -S_{ji}^{(\kappa_N)}\hat{\mathcal{F}}_{ij} + \hat{\mathrm{h}}_{ii}^{(\kappa_N)} + \frac{1}{2}\langle ij||ij\rangle^{(\kappa_N)} + \frac{1}{2}\frac{Z_\alpha Z_\beta \partial}{\partial\kappa_N}\left(\frac{1}{R_{\alpha\beta}}\right) \tag{3.152}$$

In the case of canonical HF MOs the energy derivative in the AO basis can be written

$$\begin{aligned} \mathrm{E}_o^{\kappa_N} &= D_{\mu\nu}\hat{\mathrm{h}}_{\mu\nu}^{\kappa_N} + \frac{1}{2}\Gamma_{\mu\nu\lambda\sigma}\langle\mu\lambda||\nu\sigma\rangle^{\kappa_N} + D_{\mu\nu}S_{\mu\nu}^{\kappa_N}D_{\mu\nu}\hat{\mathcal{F}}_{\mu\nu} \\ &\quad + \frac{1}{2}\frac{Z_\alpha Z_\beta \partial}{\partial\kappa_N}\Big(\frac{1}{R_{\alpha\beta}}\Big) \end{aligned} \tag{3.153}$$

where the HF one-particle density matrix $D_{\mu\nu} = C_{\mu i}^* C_{\nu i}$ and the HF two-particle density matrix $\Gamma_{\mu\nu\lambda\sigma} = D_{\mu\nu}D_{\lambda\sigma}$. The nuclear repulsion term contributes only when the perturbation under consideration is geometry dependent.

Before we move on to discuss the second derivative of the HF energy, several important observations can be made based on the first-derivative expressions given in Eqns. 3.152 and 3.153. In the case that the perturbation does not influence the AO basis functions, for example an electric field, the derivative expression in Eqn. 3.153 can be simplified to obtain

$$\begin{aligned} \Big(\frac{\partial \mathrm{E}_o}{\partial\kappa_N}\Big)_{\kappa=0} &= \sum_{\mu,\nu} D_{\mu\nu}\ \langle\mu|\Big(\frac{\partial\hat{\mathrm{h}}}{\partial\kappa_N}\Big)_{\kappa_N=0}|\nu\rangle \\ &= \sum_i \langle i|\Big(\frac{\partial\hat{\mathrm{h}}}{\partial\kappa_N}\Big)_{\kappa_N=0}|i\rangle = \sum_i \langle i|\hat{H}_1^N|i\rangle \end{aligned} \tag{3.154}$$

where the molecular geometry was assumed to be fixed. This is clearly a representation of the Hellmann-Feynman theorem introduced earlier. Another important observation is that first derivatives of the HF MOs are not required to evaluate the first derivative of the HF energy. As we can see from Eqn. 3.153, the zeroth-order HF density is perturbation independent and hence various types of first-order properties can be evaluated as a direct product of the perturbation independent density and property integrals.

However, there are instances in which the perturbation influences AO basis functions, for example geometric perturbations. Another such perturbation which is pertinent to this study is an externally applied magnetic field. As discussed in the first chapter, finite basis set NMR chemical shift calculations are gauge dependent: dependent on the origin chosen to represent the vector potential. Exact gauge invariance can be ensured by using "gauge-including atomic orbitals" (GIAO), in which each atomic orbital has its own local gauge origin placed on its center. The idea originated in London's study of molecular diamagnetism some 50 years ago [83] and was first adapted by Ditchfield [84] within quantum chemical NMR chemical shift calculations. The GIAO method for calculating NMR chemical shifts utilizes the following explicitly field-dependent basis functions

$$\chi_\mu(\mathbf{B}) = exp\Big[-\frac{i}{2c}(\mathbf{B}\times\mathbf{R}_\mu).\mathbf{r}\Big]\chi_\mu(\mathbf{0}) \tag{3.155}$$

where $\chi_\mu(\mathbf{0})$ denotes the usual field-independent Gaussian AO basis functions and $\mathbf{R}_\mu$ their center. The derivative of the GIAO basis functions with respect to a magnetic field perturbation is non-zero, and as a consequence, the AO relaxations terms have non-zero contributions to the final derivative. Energies and energy derivatives calculated by using GIAO finite basis sets are gauge-origin independent [85].

The derivation of an expression for the second derivative of the HF energy essentially involves similar manipulations as required by the first derivative. Consequently, we only present the essential steps in the derivation. We start from the MO representation of the first derivative, carry out straightforward differentiation and then follow similar techniques as in the case of the first derivative to obtain

$$\begin{aligned} \mathrm{E}_o^{\kappa_N\kappa_{N'}} = {} & \mathrm{U}_{ir}^{\dagger\kappa_{N'}}\hat{\mathrm{h}}_{ri}^{(\kappa_N)} + \hat{\mathrm{h}}_{ir}^{(\kappa_N)}\mathrm{U}_{ri}^{\kappa_{N'}} + \mathrm{U}_{ir}^{\dagger\kappa_{N'}}\langle rj||ij\rangle^{(\kappa_N)} \\ & + \langle ij||rj\rangle^{(\kappa_N)}\mathrm{U}_{ri}^{\kappa_{N'}} + \hat{\mathrm{h}}_{ii}^{(\kappa_N\kappa_{N'})} + \frac{1}{2}\langle ij||ij\rangle^{(\kappa_N\kappa_{N'})} \\ & -\hat{\mathcal{F}}_{ij}\mathrm{S}_{ji}^{(\kappa_N\kappa_{N'})} - \hat{\mathcal{F}}_{ij}^{\kappa_{N'}}\mathrm{S}_{ji}^{(\kappa_N)} + \frac{1}{2}\frac{Z_\alpha Z_\beta}{\partial\kappa_{N'}\partial\kappa_N}\left(\frac{1}{R_{\alpha\beta}}\right) \end{aligned} \qquad (3.156)$$

This can be rewritten

$$\begin{aligned} \mathrm{E}_o^{\kappa_N\kappa_{N'}} = {} & \mathrm{U}_{ir}^{\dagger\kappa_{N'}}\hat{\mathcal{F}}_{ri}^{(\kappa_N)} + \hat{\mathcal{F}}_{ir}^{(\kappa_N)}\mathrm{U}_{ri}^{\kappa_{N'}} + \hat{\mathrm{h}}_{ii}^{(\kappa_N\kappa_{N'})} + \frac{1}{2}\langle ij||ij\rangle^{(\kappa_N\kappa_{N'})} \\ & -\hat{\mathcal{F}}_{ij}\,\mathrm{S}_{ji}^{(\kappa_N\kappa_{N'})} - \hat{\mathcal{F}}_{ij}^{\kappa_{N'}}\mathrm{S}_{ji}^{(\kappa_N)} + \frac{1}{2}\frac{Z_\alpha Z_\beta\partial^2}{\partial\kappa_{N'}\partial\kappa_N}\left(\frac{1}{R_{\alpha\beta}}\right) \end{aligned} \qquad (3.157)$$

where $\hat{\mathcal{F}}_{ri}^{(\kappa_{N'})} = \hat{\mathrm{h}}_{ri}^{(\kappa_{N'})} + \langle rj||ij\rangle^{(\kappa_{N'})}$.

Clearly, further evaluation requires a knowledge of $\hat{\mathcal{F}}_{ij}^{\kappa_{N'}}$. The Fock matrix represented in the MO basis, $\hat{\mathcal{F}}_{pq}$ has the folowing form

$$\hat{\mathcal{F}}_{pq} = \hat{\mathrm{h}}_{pq} + \sum_m \langle pm||qm\rangle \qquad (3.158)$$

Following similar arguments as in the case of first and second derivatives, the derivative of the Fock matrix can be written as

$$\hat{\mathcal{F}}_{pq}^{\kappa_{N'}} = \mathrm{U}_{pr}^{\dagger\kappa_{N'}}\hat{\mathcal{F}}_{rq} + \hat{\mathcal{F}}_{pr}\mathrm{U}_{rq}^{\kappa_N} + \hat{\mathcal{F}}_{pq}^{(\kappa_{N'})} + \mathrm{U}_{mr}^{\dagger\kappa_{N'}}\langle pr||qm\rangle + \langle pm||qr\rangle\mathrm{U}_{rm}^{\kappa_N} \tag{3.159}$$

Substitute for $\hat{\mathcal{F}}_{ij}^{\kappa_{N'}}$ in Eqn. 3.157 and simplify to obtain

$$\begin{aligned}\mathrm{E}_o^{\kappa_N\kappa_{N'}} = {} & \mathrm{U}_{ir}^{\dagger\kappa_{N'}}\{\hat{\mathcal{F}}_{ri}^{(\kappa_N)} - \hat{\mathcal{F}}_{rj}\mathrm{S}_{ji}^{(\kappa_N)} - \langle mr||ji\rangle\mathrm{S}_{jm}^{(\kappa_N)}\} \\ & + \{\hat{\mathcal{F}}_{ir}^{(\kappa_N)} - \mathrm{S}_{ij}^{(\kappa_N)}\hat{\mathcal{F}}_{jr} - \mathrm{S}_{mj}^{(\kappa_N)}\langle ji||mr\rangle\}\mathrm{U}_{ri}^{\kappa_{N'}} \\ & + \hat{\mathrm{h}}_{ii}^{(\kappa_N\kappa_{N'})} + \frac{1}{2}\langle ij||ij\rangle^{(\kappa_N\kappa_{N'})} - \hat{\mathcal{F}}_{ij}\mathrm{S}_{ji}^{(\kappa_N\kappa_{N'})} \\ & - \mathcal{F}_{ij}^{(\kappa_{N'})}\mathrm{S}_{ji}^{(\kappa_N)} + \frac{1}{2}\frac{Z_\alpha Z_\beta}{\partial\kappa_{N'}\partial\kappa_N}\left(\frac{1}{R_{\alpha\beta}}\right)\end{aligned} \tag{3.160}$$

Let us collect terms and define the operator Ô such that

$$\begin{aligned}\hat{\mathrm{O}}_{ri}^{(\kappa_N)} &= \{\hat{\mathcal{F}}_{ri}^{(\kappa_N)} - \hat{\mathcal{F}}_{rj}\mathrm{S}_{ji}^{(\kappa_N)} - \langle mr||ji\rangle\mathrm{S}_{jm}^{(\kappa_N)}\} \\ \hat{\mathrm{O}}_{ir}^{(\kappa_N)} &= \{\hat{\mathcal{F}}_{ir}^{(\kappa_N)} - \mathrm{S}_{ij}^{(\kappa_N)}\hat{\mathcal{F}}_{jr} - \mathrm{S}_{mj}^{(\kappa_N)}\langle ji||mr\rangle\}\end{aligned} \tag{3.161}$$

and rewrite Eqn. 3.160 in terms of the operator Ô

$$\begin{aligned}\mathrm{E}_o^{\kappa_N\kappa_{N'}} = {} & \mathrm{U}_{ir}^{\dagger\kappa_{N'}}\hat{\mathrm{O}}_{ri}^{(\kappa_N)} + \hat{\mathrm{O}}_{ir}^{(\kappa_N)}\mathrm{U}_{ri}^{\kappa_{N'}} + \hat{\mathrm{h}}_{ii}^{(\kappa_N\kappa_{N'})} + \frac{1}{2}\langle ij||ij\rangle^{(\kappa_N\kappa_{N'})} \\ & - \hat{\mathcal{F}}_{ij}\mathrm{S}_{ji}^{(\kappa_N\kappa_{N'})} - \hat{\mathcal{F}}_{ij}^{(\kappa_{N'})}\mathrm{S}_{ji}^{(\kappa_N)} + \frac{1}{2}\frac{Z_\alpha Z_\beta}{\partial\kappa_N\partial\kappa_{N'}}\left(\frac{1}{R_{\alpha\beta}}\right)\end{aligned} \tag{3.162}$$

Here, the generic orbital index *r* in Eqn. 3.162 can run over both occupied and virtual orbital indices, hence

$$\begin{aligned}\mathrm{E}_o^{\kappa_N\kappa_{N'}} = {} & \mathrm{U}_{ik}^{\dagger\kappa_{N'}}\hat{\mathrm{O}}_{ki}^{(\kappa_N)} + \hat{\mathrm{O}}_{ik}^{(\kappa_N)}\mathrm{U}_{ki}^{\kappa_{N'}} + \mathrm{U}_{ia}^{\dagger\kappa_{N'}}\hat{\mathrm{O}}_{ai}^{(\kappa_N)} + \hat{\mathrm{O}}_{ia}^{(\kappa_N)}\mathrm{U}_{ai}^{\kappa_{N'}} \\ & + \hat{\mathrm{h}}_{ii}^{(\kappa_N\kappa_{N'})} + \frac{1}{2}\langle ij||ij\rangle^{(\kappa_N\kappa_{N'})} - \hat{\mathcal{F}}_{ij}\mathrm{S}_{ji}^{(\kappa_N\kappa_{N'})} - \hat{\mathcal{F}}_{ij}^{(\kappa_{N'})}\mathrm{S}_{ji}^{(\kappa_N)} \\ & + \frac{1}{2}\frac{Z_\alpha Z_\beta}{\partial\kappa_N\partial\kappa_{N'}}\left(\frac{1}{R_{\alpha\beta}}\right)\end{aligned} \tag{3.163}$$

We can group first two terms by exchanging dummy summation indices i and j in the first term which runs over occupied orbitals only, to get

$$\begin{aligned}\mathrm{E}_o^{\kappa_N\kappa_{N'}} = {} & (\mathrm{U}_{ki}^{\dagger\kappa_{N'}} + \mathrm{U}_{ki}^{\kappa_{N'}})\hat{\mathrm{O}}_{ik}^{(\kappa_N)} + \mathrm{U}_{ia}^{\dagger\kappa_{N'}}\hat{\mathrm{O}}_{ai}^{(\kappa_N)} + \hat{\mathrm{O}}_{ia}^{(\kappa_N)}\mathrm{U}_{ai}^{\kappa_{N'}} \\ & + \hat{\mathrm{h}}_{ii}^{(\kappa_N\kappa_{\mathbf{N'}})} + \frac{1}{2}\langle ij||ij\rangle^{(\kappa_N\kappa_{N'})} - \hat{\mathcal{F}}_{ij}\mathrm{S}_{ji}^{(\kappa_N\kappa_{N'})} - \hat{\mathcal{F}}_{ij}^{(\kappa_{N'})}\mathrm{S}_{ji}^{(\kappa_N)} \\ & + \frac{1}{2}\frac{Z_\alpha Z_\beta}{\partial\kappa_N\partial\kappa_{N'}}\left(\frac{1}{R_{\alpha\beta}}\right)\end{aligned} \tag{3.164}$$

Substitute from Eqn. 3.145 for $\left(\mathrm{U}_{ki}^{\kappa_{N'}\dagger} + \mathrm{U}_{ki}^{\kappa_{N'}}\right)$ in Eqn. 3.164 to get

$$\begin{aligned}\mathrm{E}_o^{\kappa_N\kappa_{N'}} = {} & \mathrm{U}_{ia}^{\dagger\kappa_{N'}}\hat{\mathrm{O}}_{ai}^{(\kappa_N)} + \hat{\mathrm{O}}_{ia}^{(\kappa_N)}\mathrm{U}_{ai}^{\kappa_{N'}} + \hat{\mathrm{h}}_{ii}^{(\kappa_N\kappa_{N'})} + \frac{1}{2}\langle ij||ij\rangle^{(\kappa_N\kappa_{N'})} \\ & -\hat{\mathcal{F}}_{ij}\mathrm{S}_{ji}^{(\kappa_N\kappa_{N'})} - \hat{\mathcal{F}}_{ij}^{(\kappa_{N'})}\mathrm{S}_{ji}^{(\kappa_N)} - \mathrm{S}_{ki}^{(\kappa_{N'})}\hat{\mathcal{F}}_{ik}^{(\kappa_N)} \\ & +\mathrm{S}_{ki}^{(\kappa_{N'})}\mathrm{S}_{ij}^{(\kappa_N)}\mathcal{F}_{ik} + \mathrm{S}_{km}^{(\kappa_{N'})}\mathrm{S}_{ij}^{(\kappa_N)}\mathrm{G}_{(jm,ik)} \\ & + \frac{1}{2}\frac{Z_\alpha Z_\beta}{\partial\kappa_N\partial\kappa_{N'}}\left(\frac{1}{R_{\alpha\beta}}\right)\end{aligned} \tag{3.165}$$

Note that we cannot follow a similar strategy to combine the third and forth terms in Eqn. 3.164 since the dummy summation indices run over both occupied and virtuals orbitals and cannot be interchanged.

The expression given in Eqn. 3.165 for the second derivative of the HF energy is compact and, also shows the symmetry with respect to exchange of κ_N and $\kappa_{N'}$ elegantly. As we can see, to evaluate Eqn. 3.165, we need expressions for the virtual-occupied block of the CPHF coefficients. They are obtained by exploiting the Brillouin condition $\hat{\mathcal{F}}_{ai} = 0$ as this implies that $\frac{\partial\hat{\mathcal{F}}_{ai}}{\partial\kappa_{N'}} = 0$ as well.

Therefore from Eqn. 3.159

$$\mathrm{U}^{\dagger\kappa_{N'}}_{ar}\hat{\mathcal{F}}_{ri} + \hat{\mathcal{F}}_{ar}\mathrm{U}^{\kappa_{N'}}_{ri} + \mathrm{U}^{\dagger\kappa_{N'}}_{mr}\langle ar||im\rangle + \hat{\mathcal{F}}^{(\kappa_N)}_{ai} + \langle am||ir\rangle\mathrm{U}^{\kappa_{N'}}_{rm} = 0 \quad (3.166)$$

We can simplify this expression by considering the contributions from occupied and virtual orbitals corresponding to the generic orbital *r* separately, by use employing the Brillouin condition to obtain

$$\begin{aligned} &\mathrm{U}^{\dagger\kappa_{N'}}_{aj}\hat{\mathcal{F}}_{ji} + \hat{\mathcal{F}}_{ab}\mathrm{U}^{\kappa_{N'}}_{bi} + \hat{\mathcal{F}}^{(\kappa_{N'})}_{ai} + \left(\mathrm{U}^{\dagger\kappa_{N'}}_{mn} + \mathrm{U}^{\kappa_{N'}}_{mn}\right)\langle an||im\rangle \\ &+ \mathrm{U}^{\dagger\kappa_{N'}}_{me}\langle ae||im\rangle + \langle am||ie\rangle\mathrm{U}^{\kappa_{N'}}_{em} = 0 \end{aligned} \quad (3.167)$$

Simplify using the relation given in Eqn. 3.145 to get

$$\begin{aligned} &\hat{\mathcal{F}}_{ab}\mathrm{U}^{\kappa_{N'}}_{bi} - \mathrm{U}^{\kappa_{N'}}_{aj}\hat{\mathcal{F}}_{ji} + \hat{\mathcal{F}}^{(\kappa_{N'})}_{ai} - \mathrm{S}^{(\kappa_{N'})}_{mn}\langle an||im\rangle - \mathrm{S}^{(\kappa_{N'})}_{aj}\hat{\mathcal{F}}_{ji} \\ &+ \mathrm{U}^{\dagger\kappa_{N'}}_{me}\langle ae||im\rangle + \langle am||ie\rangle\mathrm{U}^{\kappa_{N'}}_{em} = 0 \end{aligned} \quad (3.168)$$

To simplify Eqn. 3.168 further, let us constrain the zeroth-order MOs to be real. Some of the perturbations considered in this work are pure imaginary and for such situations the first-order changes in MOs can be pure imaginary even though the zeroth-order orbitals are real. Add and subtract the complex conjugate of Eqn. 3.168 to itself and multiply by one-half to obtain equations for the real and imaginary part of the virtual-occupied block of the CPHF coefficients. It follows that the real part of the virtual-occupied block of CPHF coefficients $\mathrm{U}^{\kappa_{N'}}_{em}(\mathrm{R})$ is given by

$$\mathrm{U}^{\kappa_{N'}}_{em}(\mathrm{R})\mathrm{D}_{+(ai,em)} = \mathrm{X}^{\kappa_{N'}}_{ai} \quad (3.169)$$

and similarly, the imaginary part of the virtual-occupied block of CPHF coefficients $\mathrm{U}_{em}^{\kappa_{N'}}(\mathrm{I})$ is given by

$$\mathrm{U}_{em}^{\kappa_{N'}}(\mathrm{I})\mathrm{D}_{-(ai,em)} = \mathrm{Y}_{ai}^{\kappa_{N'}} \tag{3.170}$$

where

$$\mathrm{U}_{em}^{\kappa_{N'}} = \mathrm{U}_{em}^{\kappa_{N'}}(\mathrm{R}) + i\mathrm{U}_{em}^{\kappa_{N'}}(\mathrm{I}) \tag{3.171}$$

$$\begin{aligned} \mathrm{D}_{+(ai,em)} &= \hat{\mathcal{F}}_{ae}\delta_{im} - \hat{\mathcal{F}}_{mi}\delta_{ae} + \langle ae||im\rangle + \langle am||ie\rangle \\ \mathrm{D}_{-(ai,em)} &= \hat{\mathcal{F}}_{ae}\delta_{im} - \hat{\mathcal{F}}_{mi}\delta_{ae} - \langle ae||im\rangle + \langle am||ie\rangle \end{aligned} \tag{3.172}$$

and

$$\begin{aligned} \mathrm{X}_{ai}^{\kappa_{N'}} &= -\{\frac{1}{2}(\hat{\mathcal{F}}_{ai}^{(\kappa_{N'})} + \hat{\mathcal{F}}_{ai}^{(\kappa_{N'})*}) - \mathrm{S}_{aj}^{(\kappa_{N'})}\hat{\mathcal{F}}_{ji} - \mathrm{S}_{mn}^{(\kappa_{N'})}\langle an||im\rangle\} \\ \mathrm{Y}_{ai}^{\kappa_{N'}} &= -\frac{1}{2i}(\hat{\mathcal{F}}_{ai}^{(\kappa_{N'})} - \hat{\mathcal{F}}_{ai}^{(\kappa_{N'})*}) \end{aligned} \tag{3.173}$$

Eqns. 3.161, 3.165, 3.169, 3.170, 3.172 and 3.173 combined give the final expression for the second derivative of the HF energy.

To gain more insight into the second-derivative expression, first let us consider a simpler case that in which the AO basis functions are peturbation independent and the molecular geometry is fixed. The derivative expression then simplifies to give

$$\mathrm{E}_{o}^{\kappa_N\kappa_{N'}} = \mathrm{U}_{me}^{\dagger\kappa_{N'}}\hat{\mathrm{O}}_{em}^{(\kappa_N)} + \hat{\mathrm{O}}_{me}^{(\kappa_N)}\mathrm{U}_{em}^{\kappa_{N'}} + \hat{\mathrm{h}}_{ii}^{(\kappa_N\kappa_{N'})} \tag{3.174}$$

and similarly, the operator $\hat{\mathrm{O}}$

$$\begin{aligned} \hat{\mathrm{O}}_{em}^{(\kappa_N)} &= \hat{\mathcal{F}}_{em}^{(\kappa_N)} = \hat{\mathrm{h}}_{em}^{(\kappa_N)} \\ \hat{\mathrm{O}}_{me}^{(\kappa_N)} &= \hat{\mathcal{F}}_{me}^{(\kappa_N)} = \hat{\mathrm{h}}_{me}^{(\kappa_N)} \end{aligned} \tag{3.175}$$

and the coupled HF coefficients are given by Eqn. 3.169 and 3.170 with simplified expressions for $\mathrm{X}_{ai}^{\kappa_{N'}}$ and $\mathrm{Y}_{ai}^{\kappa_{N'}}$ when the perturbation under consideration is pure real or imaginary

$$\begin{aligned} \mathrm{X}_{ai}^{\kappa_{N'}} &= -\frac{1}{2}(\hat{\mathrm{h}}_{ai}^{(\kappa_{N'})} + \hat{\mathrm{h}}_{ai}^{(\kappa_{N'})*}) \\ \mathrm{Y}_{ai}^{\kappa_{N'}} &= -\frac{1}{2i}(\hat{\mathrm{h}}_{ai}^{(\kappa_{N'})} - \hat{\mathrm{h}}_{ai}^{(\kappa_{N'})*}) \end{aligned} \tag{3.176}$$

The third term in Eqn. 3.174 originates from the second-order terms in the Hamiltonian. Similarly to first-order properties, such contributions can be evaluated as an expectation value with respect to the zeroth-order wave function. The DSO contribution to the NMR spin-spin coupling constant and diamagnetic contribution to the NMR chemical shift tensor belongs to this category and they are calculated as expectation values of their respective operators. Insert the expressions given in Eqn. 3.175 and 3.169 in Eqn. 3.174 and use the Hermiticity of $\hat{\mathrm{h}}$ to rewrite the first two terms to obtain

$$\begin{aligned} \langle\langle \hat{\mathrm{O}}_1; \hat{\mathrm{O}}_2 \rangle\rangle &= (\mathrm{U}_{em}^{\kappa_{N'}}(\mathrm{R}) - i\mathrm{U}_{em}^{\kappa_{N'}}(\mathrm{I}))\hat{\mathrm{h}}^{(\kappa_N)} + \hat{\mathrm{h}}^{(\kappa_N)}(\mathrm{U}_{em}^{\kappa_{N'}}(\mathrm{R}) + i\mathrm{U}_{em}^{\kappa_{N'}}(\mathrm{I})) \\ &= (\hat{\mathrm{h}}_{em}^{(\kappa_N)} + \hat{\mathrm{h}}_{me}^{(\kappa_N)})\mathrm{U}_{em}^{\kappa_{N'}}(\mathrm{R}) + i(\hat{\mathrm{h}}_{me}^{(\kappa_N)} - \hat{\mathrm{h}}_{em}^{(\kappa_N)})\mathrm{U}_{em}^{\kappa_{N'}}(\mathrm{I}) \\ &= -\frac{1}{2}[(\hat{\mathrm{h}}_{em}^{(\kappa_N)} + \hat{\mathrm{h}}_{em}^{(\kappa_N)*})\mathrm{D}_{+(ai,em)}^{-1}(\hat{\mathrm{h}}_{ai}^{(\kappa_{N'})} + \hat{\mathrm{h}}_{ai}^{(\kappa_{N'})*})] + \\ &\quad -\frac{1}{2}[(\hat{\mathrm{h}}_{em}^{(\kappa_N)} - \hat{\mathrm{h}}_{em}^{(\kappa_N)*})\mathrm{D}_{-(ai,em)}^{-1}(\hat{\mathrm{h}}_{ai}^{(\kappa_{N'})} - \hat{\mathrm{h}}_{ai}^{(\kappa_{N'})*})] \\ &= -\frac{1}{2}[(\hat{H}_{1(em)}^{N} + \hat{H}_{1(me)}^{N\dagger})\mathrm{D}_{+(ai,em)}^{-1}(\hat{H}_{1(ai)}^{N'} + \hat{H}_{1(ia)}^{N'\dagger})] + \\ &\quad -\frac{1}{2}[(\hat{H}_{1(em)}^{N} - \hat{H}_{1(me)}^{N\dagger})\mathrm{D}_{-(ai,em)}^{-1}(\hat{H}_{1(ai)}^{N'} - \hat{H}_{1(ia)}^{N'\dagger})] \end{aligned} \tag{3.177}$$

where the $\langle\langle \hat{\mathrm{O}}_1; \hat{\mathrm{O}}_2 \rangle\rangle$ notation is borrowed from propagator theory and the definitions of $\hat{\mathrm{O}}_1$ and $\hat{\mathrm{O}}_2$ are given below.

It will be shown, that the first two terms in Eqn. 3.174 combined amounts to the RPA expression for frequency-independent second-order properties derived alternatively from polarization propagator theory or time-dependent perturbation theory. To show this equivalence, it is convenient to start from the general RPA expression for second-order properties given by

$$\langle\langle \hat{\mathrm{O}}_1; \hat{\mathrm{O}}_2 \rangle\rangle = \begin{bmatrix} (\hat{\mathrm{O}}_1|\hat{\mathrm{Q}}^\dagger) & (\hat{\mathrm{O}}_1|\mathrm{Q}) \end{bmatrix} \mathbf{R} \begin{bmatrix} (\hat{\mathrm{Q}}^\dagger|\hat{\mathrm{O}}_2) \\ (\hat{\mathrm{Q}}|\hat{\mathrm{O}}_2) \end{bmatrix} \tag{3.178}$$

where

$$\mathbf{R} = \begin{bmatrix} \mathbf{S}\mathrm{E}_o + \mathbf{A} & \mathbf{B} \\ \mathbf{B} & -\mathbf{S}\mathrm{E}_o + \mathbf{A} \end{bmatrix}^{-1} \tag{3.179}$$

The operators $\hat{\mathrm{O}}_1 = \sum\limits_{p,q} \hat{H}^N_{1(pq)} \hat{p}^\dagger \hat{q}$, $\hat{\mathrm{O}}_2 = \sum\limits_{p,q} \hat{H}^N_{1(pq)} \hat{p}^\dagger \hat{q}$ and $\{\hat{\mathrm{Q}}^\dagger, \hat{\mathrm{Q}}\} = \{\hat{e}^\dagger \hat{m}, \hat{m}^\dagger \hat{e}\}$ and the matrices $\mathbf{S} = (\hat{\mathrm{Q}}^\dagger|\hat{\mathrm{Q}}^\dagger)$, $\mathbf{A} = -(\hat{\mathrm{Q}}^\dagger|\hat{\mathcal{H}}\hat{\mathrm{Q}}^\dagger)$ and $\mathbf{B} = -(\hat{\mathrm{Q}}^\dagger|\hat{\mathcal{H}}\hat{\mathrm{Q}})$. The superoperator $\hat{\mathcal{H}}$ and the superoperator binary product $(\hat{\mathrm{O}}_1|\hat{\mathrm{O}}_2)$ for two arbitrary operators $\hat{\mathrm{O}}_1$ and $\hat{\mathrm{O}}_2$ are defined as

$$\hat{\mathcal{H}}\hat{\mathrm{O}}_1 = [H^o, \hat{\mathrm{O}}_1] \tag{3.180}$$

and

$$(\hat{\mathrm{O}}_1|\hat{\mathrm{O}}_2) = \langle 0|[\hat{\mathrm{O}}_1^\dagger, \hat{\mathrm{O}}_2]|0\rangle \tag{3.181}$$

A detailed account of the derivation of Eqn. 3.178 and superoperator algebra can be found in several excellent textbooks [69, 86] and will not be repeated here. The matrix elements required in Eqn. 3.178 can be evaluated by using the anti-commutation rules for second quantized-operators introduced in section 1.2 to obtain

$$
\begin{aligned}
&\mathrm{S} = \delta_{ae}\delta_{im} \\
&\mathrm{A}_{(ai,em)} = -\{\hat{\mathcal{F}}_{ae}\delta_{mi} - \hat{\mathcal{F}}_{mi}\delta_{ae} + \langle am||ie\rangle\} \\
&\mathrm{B}_{(ai,em)} = -\langle ae||im\rangle \\
&(\hat{\mathrm{O}}_1|\hat{\mathrm{Q}}^\dagger) = \hat{H}^N_{1(em)} \\
&(\hat{\mathrm{O}}_2|\hat{\mathrm{Q}}) = \hat{H}^{N'}_{1(ia)} \\
&(\hat{\mathrm{Q}}^\dagger|\hat{\mathrm{O}}_1) = \hat{H}^N_{1(ai)} \\
&(\hat{\mathrm{Q}}|\hat{\mathrm{O}}_2) = \hat{H}^{N'}_{1(me)}
\end{aligned}
\tag{3.182}
$$

As mentioned earlier, the energy derivative approach presented here is valid only for the frequency (or time) independent perturbations, while the RPA expression given in Eqn. 3.178 is general in the sense that it is valid for both frequency-dependent or independent perturbations. Consequently, to show the equivalence of RPA to energy derivative method, we only consider the frequency-independent RPA by requiring that the unperturbed ground state energy is identically zero ($\mathrm{E}_o = 0$) in Eqn. 3.178.

Subject to this constraint, we can rewrite the RPA matrix **R** such that

$$
\mathbf{R} = \mathbf{U}\begin{bmatrix} \mathrm{A}+\mathrm{B} & 0 \\ 0 & \mathrm{A}-\mathrm{B} \end{bmatrix}^{-1}\mathbf{U}^\dagger \tag{3.183}
$$

where $\mathbf{U} = \frac{1}{\sqrt{2}}\begin{pmatrix}\mathbf{I} & -\mathbf{I}\\ \mathbf{I} & \mathbf{I}\end{pmatrix}$ and **I** is the unit matrix. Note that the unitary transformation **U** converts the RPA matrix into block-diagonal form and hence, decoupls the **A** and **B** blocks of the RPA matrix. Substitute for the matrix elements and the matrix **R** in Eqn. 3.178 from Eqns. 3.182 and 3.183 and then simplify to obtain

$$\begin{aligned}
\langle\langle \hat{O}_1;\hat{O}_2\rangle\rangle &= \frac{1}{2}\begin{pmatrix}\mathbf{H}_1^N & \mathbf{H}_1^{N\dagger}\end{pmatrix}\mathbf{U}\begin{pmatrix}\mathbf{A+B} & \mathbf{0}\\ \mathbf{0} & \mathbf{A-B}\end{pmatrix}^{-1}\mathbf{U}^\dagger\begin{pmatrix}\mathbf{H}_1^{N'}\\ \\ \mathbf{H}_1^{N'\dagger}\end{pmatrix}\\
&= \frac{1}{2}\begin{pmatrix}\mathbf{H}_1^N + \mathbf{H}_1^{N\dagger} & \mathbf{H}_1^{N\dagger} - \mathbf{H}_1^N\end{pmatrix}\begin{pmatrix}\mathbf{A+B} & \mathbf{0}\\ \mathbf{0} & \mathbf{A-B}\end{pmatrix}^{-1}\begin{pmatrix}\mathbf{H}_1^{N'} + \mathbf{H}_1^{N'\dagger}\\ \\ \mathbf{H}_1^{N'} - \mathbf{H}_1^{N'\dagger}\end{pmatrix}\\
&= \frac{1}{2}\Big\{(\mathbf{H}_1^N + \mathbf{H}_1^{N\dagger})\ (\mathbf{A}+\mathbf{B})^{-1}\ (\mathbf{H}_1^{N'} + \mathbf{H}_1^{N'\dagger}) +\\
&\qquad (\mathbf{H}_1^{N\dagger} - \mathbf{H}_1^N)\ (\mathbf{A}-\mathbf{B})^{-1}\ (\mathbf{H}_1^{N'} - \mathbf{H}_1^{N'\dagger})\Big\}\\
&= -\frac{1}{2}[(\hat{H}_{1(em)}^N + \hat{H}_{1(me)}^{N\dagger})\mathrm{D}_{+(ai,em)}^{-1}(\hat{H}_{1(ai)}^{N'} + \hat{H}_{1(ia)}^{N'\dagger})]\\
&\quad -\frac{1}{2}[(\hat{H}_{1(em)}^N - \hat{H}_{1(me)}^{N\dagger})\mathrm{D}_{-(ai,em)}^{-1}(\hat{H}_{1(ai)}^{N'} - \hat{H}_{1(ia)}^{N'\dagger})]
\end{aligned} \tag{3.184}$$

As we can see, Eqn. 3.184 is identical with the expression given in Eqn. 3.177 derived from the energy derivative theory. This result shows the equivalence of the CPHF and RPA approaches to second-order properties subject to the constraints imposed in the derivation of Eqns. 3.177 and 3.184. As we have seen, the decoupling of **A** and **B** blocks of the RPA matrix is a critical element of our proof. In the case of frequency-dependent RPA matrices, these two blocks cannot be decoupled. Consequently, further analysis is required to investigate the equivalence of frequency-dependent RPA and frequency-dependent HF energy derivative methods. Another important thing to note is that the equivalence of frequency-independent RPA and energy derivative methods shown here is limited to perturbation-independent AO basis functions. However, for perturbation-dependent AO basis functions, this equivalence can still be maintained by redefining the RPA to incorporate the perturbation dependence of AO basis functions, for example, as in the case of RPA GIAO NMR chemical shift calculations.

Coupled Cluster Energy Derivatives and EOM-CCSD Models for Second-Order Properties

The CC energy functional is given by

$$E = \langle 0|(1+\Lambda)e^{-T}\hat{H}e^{T}|0\rangle = \langle 0|(1+\Lambda)\hat{\bar{H}}|0\rangle \tag{3.185}$$

where H denotes the second-quantized form of the many-body Hamiltonian in the presence of perturbations

$$\begin{gathered}\hat{H} = \sum_{pq} \hat{\mathrm{h}}_{pq}\hat{p}^{\dagger}\hat{q} + \frac{1}{4}\sum_{\substack{p,q\\r,s}} \langle pq||rs\rangle \hat{p}^{\dagger}\hat{q}^{\dagger}\hat{s}\hat{r} + \sum_{p,q,N} \kappa_N \hat{H}^{N}_{1pq}\hat{p}^{\dagger}\hat{q} + \\ \sum_{\substack{p,q\\N>N'}} \kappa_N \kappa_{N'} \hat{H}^{NN'}_{2pq}\hat{p}^{\dagger}\hat{q}\end{gathered} \tag{3.186}$$

while $|0\rangle$ is a single determinant reference function, which is assumed to provide an adequate zeroth-order description of the ground state. In the following derivation we assume that the molecular geometry is fixed and consequently, the nuclear repulsion energy is a constant. Hence, for convenience, the nuclear repulsion contributions are not explicitly considered. The cluster operator T is partitioned into n-tuple excitation operators

$$T = T_1 + T_2 + \cdots + \ T_n \ + \cdots = \sum_{\mu} t_{\mu} \hat{q}_{\mu} \tag{3.187}$$

where

$$T_n = \frac{1}{n!} \sum_{\substack{i,j\ldots \\ a,b\ldots}} t_{ij.....}^{ab....} \{a^{\dagger} i b^{\dagger} j....\} \tag{3.188}$$

Similarly the operator Λ is expanded as

$$\Lambda = \Lambda_1 + \Lambda_2 + \cdots + \ \Lambda_n \ + \cdots = \sum_{\mu} \lambda_{\mu} \hat{q}_{\mu}^{\dagger} \tag{3.189}$$

where Λ_n denotes a n-tuple de-excitation operator

$$\Lambda_n = \frac{1}{n!} \sum_{\substack{i,j\ldots \\ a,b\ldots}} \lambda_{ab....}^{ij....} \{i^{\dagger} a j^{\dagger} b.....\} \tag{3.190}$$

Finally in Eqn. 3.185, we have introduced the non-hermitian similarity transformed Hamiltonian

$$\hat{\hat{H}} = e^{-T} \hat{H} e^{T} \tag{3.191}$$

that will be used extensively in the derivation below.

The coefficients parameterizing the T and Λ operators in CC theory are obtained by requiring stationarity of the CC energy functional, a choice which leads to the generic CC and lambda equations

$$\langle q_{\mu} | e^{-T} \hat{H} e^{T} | 0 \rangle = \langle q_{\mu} | \hat{\hat{H}} | 0 \rangle = 0 \tag{3.192}$$

and

$$\langle 0|(1+\Lambda)\left[\hat{\bar{H}}, \hat{q}_\mu\right]|0\rangle = 0 \tag{3.193}$$

This latter equation also can be written as

$$\langle 0|(1+\Lambda)\left(\hat{\bar{H}} - E\right)|q\rangle = 0 \tag{3.194}$$

Because of the stationarity of the CC energy functional, the first derivative with respect to the perturbation order parameter $\kappa_{N'}$ takes the form

$$E^{\kappa_{N'}} = \frac{\partial E}{\partial \kappa_{N'}} = \langle 0|(1+\Lambda)e^{-T}\hat{H}^{\kappa_{N'}}e^{T}|0\rangle = \langle 0|(1+\Lambda)\hat{\bar{H}}^{\kappa_{N'}}|0\rangle \tag{3.195}$$

where we have defined

$$\hat{\bar{H}}^{\kappa_{N'}} = e^{-T}\left(\frac{\partial H}{\partial \kappa_{N'}}\right)_{\kappa_{N'}=0} e^{T} = e^{-T}\hat{H}^{\kappa_{N'}}e^{T} \tag{3.196}$$

In deriving Eqn. 3.195, we have neglected MO relaxation effects and also assumed that the AO basis functions are independent of the external perturbation. As shown by Salter *et al.* [87] Eqn. 3.195 is a representation of the generalized Hellmann-Feynman theorem. Consequently, the first-order properties are given by

$$\begin{aligned}\left(\frac{\partial E}{\partial \kappa_{N'}}\right)_{\kappa_{N'}=0} &= \langle 0|(1+\Lambda)\hat{\bar{H}}^{\kappa_{N'}}|0\rangle \\ &= \sum_{p,q} \hat{H}_{1pq}^{\kappa_{N'}} \langle 0|(1+\Lambda)e^{-T}\{\hat{p}^\dagger \hat{q}\}e^{T}|0\rangle \\ &= \sum_{p,q} \hat{H}_{1pq}^{\kappa_{N'}} D_{pq}\end{aligned} \tag{3.197}$$

where the "response density" D_{pq} is

$$D_{pq} = \langle 0|(1+\Lambda)e^{-T}\mathbb{N}\{\hat{p}^\dagger \hat{q}\}e^{T}|0\rangle \tag{3.198}$$

The "response density" is independent of the perturbation and hence, any first-order response property can be calculated as a direct product of the same "response density" and property integrals corresponding to the property of interest. Identical expressions for the first-order properties can also be derived from CC response theory [88].

It is important to note that the MO relaxation effects are not incoporated in the "response density". When MO relaxation effects are incorporated, we can identify a similar quantity known as the "relaxed density" and first-order properties once again can be calculated as a direct product of the perturbation independent "relaxed density" and repective property integrals [3]. The effects of orbital relaxation on first-order properties have been shown to be negligibly small [3].

Taking the second derivative with respect to the order parameter κ_N subject to the same constraints as the first derivative, we get

$$\begin{aligned} E^{\kappa_{N'}\kappa_N} = {} & \langle 0|\Lambda^{\kappa_N}\hat{\bar{H}}^{\kappa_{N'}}|0\rangle \; + \; \langle 0|(1+\Lambda)\left[\hat{\bar{H}}^{\kappa_{N'}}, T^{\kappa_N}\right]|0\rangle \; + \\ & \langle 0|(1+\Lambda)\hat{\bar{H}}^{\kappa_{N'}\kappa_N}|0\rangle \end{aligned} \tag{3.199}$$

where

$$T^{\kappa_N} = \left(\frac{\partial T}{\partial \kappa_N}\right)_{\kappa_N = 0} \tag{3.200}$$

$$\Lambda^{\kappa_N} = \left(\frac{\partial \Lambda}{\partial \kappa_N}\right)_{\kappa_N = 0} \tag{3.201}$$

and

$$\hat{\bar{H}}^{\kappa_{N'}\kappa_N} = e^{-T}\left(\frac{\partial \hat{H}}{\partial \kappa_{N'}\kappa_N}\right)_{\kappa_N,\kappa_{N'} = 0} e^{T} \tag{3.202}$$

The equations that determine the first order operators T^{κ_N} and Λ^{κ_N} are obtained by differentiation of the CC and lambda equations with respect to κ_N, which yields

$$\langle q_\mu | \hat{\bar{H}}^{\kappa_N} + \left[\hat{\bar{H}}, T^{\kappa_N}\right] |0\rangle = 0 \tag{3.203}$$

$$\langle 0|\Lambda^{\kappa_N}\left[\hat{\bar{H}}, \hat{q}_\mu\right]|0\rangle + \langle 0|(1+\Lambda)\left[\left(\hat{\bar{H}}^{\kappa_N} + \left[\hat{\bar{H}}, T^{\kappa_N}\right]\right), \hat{q}_\mu\right]|0\rangle = 0 \tag{3.204}$$

It is possible to eliminate the derivative Λ^{κ_N}, which depends on the solution for T^{κ_N}, from the expression for the second derivative of the energy. Multiplying Eqn. 3.203 (in which we replace κ_N by $\kappa_{N'}$) by the coefficients $\Lambda_\mu^{\kappa_N}$ and summing over μ gives

$$\langle 0|\Lambda^{\kappa_N}\hat{\bar{H}}^{\kappa_{N'}}|0\rangle = -\langle 0|\Lambda^{\kappa_N}\left[\hat{\bar{H}}, T^{\kappa_{N'}}\right]|0\rangle \tag{3.205}$$

The right-hand side of this equation subsequently can be rewritten by multiplying Eqn. 3.204 by $T_\mu^{\kappa_{N'}}$ and summing over μ. This procedure yields

$$\begin{aligned} \langle 0|\Lambda^{\kappa_N}\hat{\bar{H}}^{\kappa_{N'}}|0\rangle &= -\langle 0|\Lambda^{\kappa_N}\left[\hat{\bar{H}}, T^{\kappa_{N'}}\right]|0\rangle \\ &= \langle 0|(1+\Lambda)\left[\left(\hat{\bar{H}}^{\kappa_N} + \left[\hat{\bar{H}}, T^{\kappa_N}\right]\right), T^{\kappa_{N'}}\right]|0\rangle \end{aligned} \tag{3.206}$$

In this latter expression we have eliminated Λ^{κ_N} at the expense of introducing a second commutator. If we substitute this expression into Eqn. 3.199, the total second-order energy derivative takes the form

$$\begin{aligned} E^{\kappa_N\kappa_{N'}} =& \langle 0|(1+\Lambda)[\hat{\bar{H}}^{\kappa_{N'}}, T^{\kappa_N}]|0\rangle + \langle 0|(1+\Lambda)[\hat{\bar{H}}^{\kappa_N}, T^{\kappa_{N'}}]|0\rangle \\ &+ \langle 0|(1+\Lambda)[[\hat{\bar{H}}, T^{\kappa_N}], T^{\kappa_{N'}}]|0\rangle + \langle 0|(1+\Lambda)\hat{\bar{H}}^{\kappa_N\kappa_{N'}}|0\rangle \end{aligned} \tag{3.207}$$

which is symmetric in κ_N and $\kappa_{N'}$, as required by elementary considerations. The first three terms in Eqn. 3.207 define the quadratic EOM-CCSD model when the T and Λ operators are restricted to single- and double-substitution operators. The third term originates from the second-order terms in the Hamiltonian, and similarly to the situation with correlated first-order properties, these contributions are evaluated simply as a direct product of "response density" and property integrals corresponding to the property of interest. Note that, here, the derivation of Eqn. 3.207 has been carried out specifically for NMR spin-spin coupling constants. However, it is equally applicable to any other second-order property when substituted with appropriate operators for $\hat{\bar{H}}^{\kappa_N}$ and $\hat{\bar{H}}^{\kappa_{N'}}$ [89]. It is also important to note that the quadratic EOM-CCSD model scales correctly with the size of the system and is identical to the CC linear response function [88]. However, Eqn. 3.207 in general cannot be written as a sum-over-states expression and therefore will differ from the second-order perturbation theory expression which defines the CI-like EOM-CCSD model.

In order to make the connection with second-order perturbation theory we expand the commutators in Eqn. 3.207, and regroup the terms as

$$\begin{aligned} E^{\kappa_N \kappa_{N'}} = {} & \langle 0|(1+\Lambda)\left(\hat{\bar{H}}^{\kappa_{N'}} T^{\kappa_N} + \hat{\bar{H}}^{\kappa_N} T^{\kappa_{N'}}\right)|0\rangle - \\ & \langle 0|(1+\Lambda) T^{\kappa_N}\left(\hat{\bar{H}}^{\kappa_{N'}} + \left[\hat{\bar{H}}, T^{\kappa_{N'}}\right]\right)|0\rangle - \end{aligned} \tag{3.208}$$

$$\begin{gathered}\langle 0|(1+\Lambda)T^{\kappa_{N'}}\left(\hat{\bar{H}}^{\kappa_N}+\left[\hat{\bar{H}},T^{\kappa_N}\right]\right)|0\rangle + \\ \langle 0|(1+\Lambda)\left[\hat{\bar{H}},T^{\kappa_{N'}}T^{\kappa_N}\right]|0\rangle + \langle 0|(1+\Lambda)\hat{\bar{H}}^{\kappa_N\kappa_{N'}}|0\rangle\end{gathered}$$

The second (and similarly the third term) can be simplified greatly. First we use the fact that Eqn. 3.203 for the perturbed T–amplitudes is satisfied, and by inserting a resolution of the identity in the second term, after T^{κ_N}, it is seen that only the contribution from the reference state remains

$$\langle 0|(1+\Lambda)T^{\kappa_N}|0\rangle\langle 0|\hat{\bar{H}}^{\kappa_{N'}}+\left[\hat{\bar{H}},T^{\kappa_{N'}}\right]|0\rangle \tag{3.209}$$

The second term in the product above can be rewritten

$$\begin{aligned}\langle 0|\hat{\bar{H}}^{\kappa_{N'}}+\left[\hat{\bar{H}},T^{\kappa_{N'}}\right]|0\rangle &= \langle 0|(1+\Lambda)\left(\hat{\bar{H}}^{\kappa_{N'}}+\left[\hat{\bar{H}},T^{\kappa_{N'}}\right]\right)|0\rangle \\ &= \langle 0|(1+\Lambda)\hat{\bar{H}}^{\kappa_{N'}}|0\rangle = E^{\kappa_{N'}}\end{aligned} \tag{3.210}$$

where in deriving the first equality we used once more the equation for the perturbed amplitudes T^{κ_N}, Eqn. 3.203, while in going from the second to the third expression we invoked the lambda equations 3.193. Combining these results we rewrite equation 3.208

$$\begin{aligned}E^{\kappa_N\kappa_{N'}} =& \langle 0|(1+\Lambda)\left(\hat{\bar{H}}^{\kappa_{N'}}-E^{\kappa_{N'}}\right)T^{\kappa_N}|0\rangle + \\ & \langle 0|(1+\Lambda)\left(\hat{\bar{H}}^{\kappa_N}-E^{\kappa_N}\right)T^{\kappa_{N'}}|0\rangle + \\ & \langle 0|(1+\Lambda)\left[\hat{\bar{H}},T^{\kappa_N}T^{\kappa_{N'}}\right]|0\rangle + \\ & \langle 0|(1+\Lambda)\hat{\bar{H}}^{\kappa_N\kappa_{N'}}|0\rangle\end{aligned} \tag{3.211}$$

As we will show below, the first two terms constitute precisely the second-order perturbation theory expression for second-order properties within the equation of motion coupled cluster framework, which we refer to as the CI-like approximation to EOMCC. The last term constitutes the quadratic correction term that is added to the CI-like approximation to yield the quadratic EOMCC model. Let us note that all these manipulations are strictly valid, in particular, if the excitation space is restricted to single- and double-substitution operators. Therefore Eqns. 3.211 and 3.207 are completely equivalent, and in practice we use Eqn. 3.207 to evaluate the complete-second order energy within the quadratic approximation.

The quadratic correction term can be rewritten as

$$\begin{gathered}
\langle 0|(1+\Lambda)\left[\hat{\bar{H}}, T^{\kappa_{N'}}T^{\kappa_N}\right]|0\rangle = \\
\langle 0|(1+\Lambda)\left[\left(\hat{\bar{H}}-E\right), T^{\kappa_{N'}}T^{\kappa_N}\right]|0\rangle = \\
\langle 0|(1+\Lambda)\left(\hat{\bar{H}}-E\right)|Q\rangle\langle Q|T^{\kappa_{N'}}T^{\kappa_N}|0\rangle
\end{gathered} \tag{3.212}$$

where the projection operator $|Q\rangle\langle Q|$ refers to the higher excitations that are not explicitly considered in the CC model under consideration. In the last step we used the alternative from of the lambda equations, Eqn. 3.194. It is seen that the quadratic and CI-like models in EOM-CC theory are completely equivalent if and only if the cluster expansion is complete. Otherwise they differ by the amount given in Eqn. 3.212. The quadratic model is size-extensive, which follows from the commutator form of the second-order energy. The CI-like model contains disconnected terms and therefore does not fully satisfy the size-extensivity criterion. Previous discussion of this topic has been given by Kobayashi *et al.* [90] and Sekino and Bartlett [91].

In order to establish the connection between the CI-like EOM-CCSD model and the sum-over-states expression, let us analyze the first-order amplitude equations

$$\langle q_\mu| \left[\hat{\bar{H}}, T^{\kappa N}\right] |0\rangle = -\langle q_\mu| \hat{\bar{H}}^{\kappa N} |0\rangle \tag{3.213}$$

Expanding the operator $T^{\kappa N}$ we find that the coefficients $t_\mu^{\kappa N}$ can be obtained from a linear system of equations

$$\sum_\nu \langle q_\mu| \left[\hat{\bar{H}}, \hat{q}_\nu\right] |0\rangle t_\nu^{\kappa N} \equiv \sum_\nu A_{\mu\nu} t_\nu^{\kappa N} = -\langle q_\mu| \hat{\bar{H}}^{\kappa N} |0\rangle \tag{3.214}$$

The matrix **A** is the matrix-representation of $\left(\bar{H} - E\right)$, within the space of singly and doubly substituted determinants. In order to obtain the desired sum-over-states expression, we diagonalize the CC Jacobian **A** to obtain its spectral representation.

$$\mathbf{A} = \sum_\lambda \mathbf{f}_\lambda (E_\lambda - E) \tilde{\mathbf{f}}_\lambda \tag{3.215}$$

Here **f** and $\tilde{\mathbf{f}}$ denote the right and left hand eigenvectors of the matrix **A**, whose eigenvalues correspond to approximate excitation energies of the system. Let us note that the matrix **A** is non-singular if the ground state is non-degenerate, and in terms of the eigenstates of **A** the perturbed amplitudes can then immediately be written

$$T^{\kappa N}|0\rangle = \sum_\lambda -\frac{|f_\lambda\rangle\langle\tilde{f}_\lambda| \hat{\bar{H}}^{\kappa N} |0\rangle}{(E_\lambda - E)} = \sum_\lambda \frac{|f_\lambda\rangle\langle\tilde{f}_\lambda| \hat{\bar{H}}^{\kappa N} |0\rangle}{(E - E_\lambda)} \tag{3.216}$$

and the second-order energy expression becomes

$$E^{NN'} = \sum_{\lambda} \frac{\langle 0|(1+\Lambda)(\hat{\bar{H}}^{\kappa_N} - E^{\kappa_N})|f_\lambda\rangle\langle\tilde{f}_\lambda|\hat{\bar{H}}^{\kappa_{N'}}|0\rangle}{(E - E_\lambda)} + \\ \sum_{\lambda} \frac{\langle 0|(1+\Lambda)(\bar{H}^{\kappa_{N'}} - E^{\kappa_{N'}})|f_\lambda\rangle\langle\tilde{f}_\lambda|\hat{\bar{H}}^{\kappa_N}|0\rangle}{(E - E_\lambda)} \tag{3.217}$$

Further note that the states $|f\rangle$ and $\langle\tilde{f}|$ are obtained by diagonalizing $\bar{H} - E$ over a restricted subspace. In particular, the reference state is missing from the expansion manifold. Alternatively, we can diagonalize $\bar{H} - E$ over the space of singles, doubles, *and* the reference determinant $|0\rangle$. Due to the special structure of the matrix, i.e. $\langle q|\big(\bar{H} - E\big)|0\rangle = 0$, there exists a trivial relationship between the full eigenvectors $|\Psi_\lambda\rangle$ and the eigenvectors in the restricted subspace, $|f_\lambda\rangle$, while the eigenvalues are completely identical [5]. The full space, of course, yields one additional eigenvalue equal to zero, and the corresponding left- and right-eigenvectors describe the CC ground state. In summary

$$\begin{gathered} |\Psi_k\rangle = |f_k\rangle + c_k|0\rangle \\ |\Psi_0\rangle = |0\rangle \\ \langle\tilde{\Psi}_k| = \langle\tilde{f}_k| \\ \langle\tilde{\Psi}_0| = \langle 0|(1+\Lambda) \end{gathered} \tag{3.218}$$

Therefore, since

$$\langle\tilde{\Psi}_0|\Big(\hat{\bar{H}}^{\kappa_N} - E^{\kappa_N}\Big)|0\rangle = 0 \tag{3.219}$$

one can replace the states $|f_\lambda\rangle$ by $|\Psi_\lambda\rangle$ in Eqn. 3.217, and the CI-like EOM-CCSD expression for second-order properties is equivalent to the second-order perturbation expression based upon $\bar{H}$ as the zeroth-order Hamiltonian, and where all configurations are restricted to be at most doubly excited

$$E^{\kappa_N \kappa_{N'}} = \sum_{k \neq 0} \frac{\langle \tilde{\Psi}_0 | \left(\hat{\bar{H}}^{\kappa_N} - E^{\kappa_N} \right) | \Psi_k \rangle \langle \tilde{\Psi}_k | \hat{\bar{H}}^{\kappa_{N'}} | 0 \rangle}{(E - E_k)} + \sum_{k \neq 0} \frac{\langle \tilde{\Psi}_0 | \left(\hat{\bar{H}}^{\kappa_{N'}} - E^{\kappa_{N'}} \right) | \Psi_k \rangle \langle \tilde{\Psi}_k | \hat{\bar{H}}^{\kappa_N} | 0 \rangle}{(E - E_k)} \tag{3.220}$$

This expression may be directly compared to the generic sum-over-states expression based on second-order perturbation theory expression. We might add here, that once the substitution $|f_\lambda\rangle \longrightarrow |\Psi_\lambda\rangle$ is made, the first-order energy contribution is redundant, because of the orthogonality of the states involved.

As mentioned earlier, the derivation presented here was specifically for NMR spin-spin coupling constants, but Eqn. 3.220 is more general and can be used with any other second-order property when substituted with the appropriate $\hat{\bar{H}}^{\kappa_N}$ and $\hat{\bar{H}}^{\kappa_{N'}}$. The EOM-CCSD CI-like approximation has already been used to calculate dynamic molecular polarizabilities [92, 89] and NMR spin-spin coupling constants [91, 93].

To summarize, the CI-like EOMCC expression given in Eqn. 3.220 is identical with the quadratic EOMCC or CC energy derivative expression (without orbital relaxation effects), only when the operators T and Λ are untruncated (e.g. two electron systems in the CCSD case). When the excitation operators are truncated, the coupled cluster second-order energy derivative can be recovered from the

CI-like approximation by adding the so-called quadratic term (see the third term in Eqn. 3.211). Alternatively, and more practically, the CC energy derivative is evaluated from equation 3.207. A consequence of neglecting the quadratic term, as in the case of EOM-CCSD CI-like method, is that the approximation is not rigorously size extensive. The numerical accuracy of the EOM-CCSD CI-like method has been tested on calculating dipole polarizabilities and it has shown to be accurate for small isolated molecules although there are exceptions [89]. However, as Kobayashi*et al.* [90] demonstrated the size-extensivity error may become excessive if the the first-order property contribution in the CI-like expression for the second-order property becomes dominant. For NMR spin-spin coupling constants this is an unlikely occurence as most first-order contributions vanish by symmetry. Only the PSO contribution can suffer from this source of error, but the first-order PSO contribution is usually small.

CHAPTER 4
THEORETICAL CALCULATION OF INDIRECT NUCLEAR SPIN-SPIN COUPLING CONSTANTS: AN HISTORICAL PERSPECTIVE

4.1 Introduction

In this chapter, we will present a brief literature survey of the theoretical calculation of indirect nuclear spin-spin coupling constants. This will help us to assess the current state of the problem, identify both conceptual and theoretical problems associated with indirect nuclear spin-spin coupling constant calculations, and also to identify interesting practical applications. In the conclusion, we present an assessment of the current state of the problem and also a discussion of the problems associated with the theoretical calculation of NMR spin-spin coupling constants.

4.2 Theoretical Indirect Nuclear Spin-Spin Coupling Constants

Original molecular orbital calculations of nuclear spin-spin coupling were reported by Pople and Santry in 1964 [94, 95]. These early studies were based on the semi-empirical uncoupled Hartree-Fock method and were limited only to the FC contribution. Theoretical developments prior to 1965 have been reviewed by Barfield and Grant [96]. Pople and coworkers [97, 97] adapted the finite perturbation (FP) method as a means of applying the coupled

Hartree-Fock (CPHF) method to the nuclear spin-spin coupling problem. The semi-empirical finite perturbation Hartree-Fock method, limited only to the FC contribution has been tested thoroughly on simple organic molecules and shown to predict qualitative trends [98–100]. Blizzard and Santry [101] incorporated the analytical Hartree-Fock energy derivative method, thus increasing the accuracy and the efficiency of indirect nuclear spin-spin coupling constant calculations by CPHF. They reported both the PSO and SD contributions in addition to the FC contribution, all based on the semi-empirical analytical CPHF method. Shortly after that, Ditchfield and Snyder [102] reported the first *ab initio* CPHF NMR spin-spin coupling constants. These and several other authors demonstrated the importance of the PSO and SD contributions in certain couplings, such as $^1J(^{13}C^{19}F)$ of CH_3F based on *ab initio* CPHF results. The DSO contribution has also been shown to be significant in certain cases, for example the $^1J(^1H^1H)$ of first-row hydrides [103, 104].

The performance of the *ab initio* CPHF method had been tested thoroughly on a wide variety of systems and the reported results are summarized in Kowalewski's review [105]. The *ab initio* CPHF method usually predicts qualitative trends correctly, but it tends to overestimate the indirect nuclear spin-spin coupling constants by a factor of two in certain cases. It also suffers from the well-known triplet instability problem [106]. However, the CPHF method itself and various semi-empirical approximations to it are in fact routinely used in qualitative calculations of NMR spin-spin coupling constants of larger molecules [107, 108]. It is also evident from these studies that for carbon hydrogen coupling constants in organic molecules, the FC is dominant and all the other non-contact contributions can be neglected. However, this is not often the case for coupling constants involving other nuclei. Another general picture that arises is that the basis set requirements vary for different types of coupling and for different chemical situations. From the experience with CPHF calculations one concludes that, for quantitatively accurate results, all the non-contact contributions and electron correlation effects need to be considered.

Various theoretical methods which go beyond the CPHF approximation have been used to include electron correlation effects. Methods derived from energy derivatives can be applied to any level of theory when combined with numerical evaluation of derivatives, and many examples of such finite perturbation calculations are reported in the literature. A brief list include finite-perturbation configuration-interaction (FP-CI) [109, 110], finite perturbation multi-configurational self-consistent field (FP-MCSCF), density functional methods [111], finite-perturbation second-order many-body perturbation theory (FP-MBPT(2)) [112–114], finite perturbation higher-order many-body perturbation theories (FP-MBPT(3), FP-MBPT(4)) and finite perturbation coupled-cluster methods (FP-CC) [115, 116] which have all been used to calculate NMR spin-spin coupling constants. Since each component of the coupling tensor requires at least two separate energy calculations, finite field calculations become very cumbersome for all couplings, except for the FC contribution. As a result, these finite perturbation calculations were limited to smaller molecules and most often the non-contact contributions were ignored or estimated by the CPHF method. Recently, FP-MBPT(2) methods have been used to calculate the nuclear spin-spin coupling tensors including all four contributions [117]. Finite perturbation methods have been very useful to calibrate various correlated theoretical models with respect to nuclear spin-spin coupling constant calculations.

Analytical methods do not suffer from any of the complications listed above and the full spin-spin coupling tensor can be directly obtained by a single calculation. However, due to technical difficulties in implementing analytical derivatives for high-level correlated methods, their wide spread application to indirect nuclear spin-spin coupling constants has been limited mainly to the CPHF approximation [118]. Other analytical correlated approaches for nuclear spin-spin coupling constants are based upon the polarization propagator (PP) [69, 119] or equation-of-motion formalism [120, 121]. The EOM or PP calculations have been performed at various levels of approximation, in most cases starting with the RPA level, the first-order approximation to the EOM or PP, which is indentical to the CPHF method derived from Hartree-Fock energy derivative theory as shown in chapter 2. The second-order polarization propagator approach (SOPPA) [122] is a consistent second-order approximation to the PP. If the second-order reference state, used in

SOPPA, is replaced by a coupled-cluster approximation for the ground state (CCD or CCSD are commonly used) one obtains the coupled-cluster polarization propagator approach (CCDPPA or CCSDPPA) . Other analytical correlated methods include, for example, uncoupled perturbation-CI [127, 128], valence-bond theory [129, 130], multi-configuration coupled Hartree-Fock (MCCHF) [131], equation-of-motion/higher-order random phase approximation (EOM/HRPA) [121, 132, 133], multi-configuration linear response theory (MCLRT) [134]. These analytical methods should be in principle, widely applicable and convenient for the calculation of non-contact interactions. In some instances, a combination of both energy derivatives and analytical sum-over-state type expressions have been used. As an example, in recent density functional work of Malkin and coworkers [135], the FC contribution is calculated as an energy derivative and the PSO contribution is calculated analytically using a sum-over-state's-type expression.

It is evident from the correlated calculations that the FC term usually requires larger basis sets and correlations effects beyond second-order. However, the other contributions are less sensitive to the basis set and correlation effects. In general, C and H coupling constants of organic molecules in usual bonding situations are pretty well described by most of the correlated methods, such as HRPA, SOPPA, CCSDPA, MCLRT and density functional methods and in addition the non-contact contributions to such coupling constants are negligibly small. The difficult cases like F and H coupling in HF, N and N coupling in N_2 and C and O coupling in CO, not only have large non-contact contributions but also require highly correlated methods. The CCSDPPA and MCLRT combined with appropriate basis sets seems to give quantitative results for such cases as evident from the limited results available in the literature based on such methods.

4.3 Conclusions

With the use of modern high resolution NMR spectrophotometers, nuclear spin-spin couplings can be measured more and more accurately on a wide variety of systems. Their applications in structure elucidations [136] and conformational analysis also have seen a large growth, in particular, in the areas of conformational analysis of proteins, nucleic acids and polysaccharides. In some instances totally new nuclear spin-spin coupling phenomena have been observed. For example, very large and strongly temperature-dependent one-bond hydrogen-hydrogen coupling constants, $^{1}J(^{1}H^{1}H)$, between metal-bonded hydride protons are observed in the ^{1}H NMR of transition-metal trihydrides, with extremely large one bond boron and tin coupling constants $^{1}J(^{11}B^{119}Sn)$ occur in boranes with tin bonded to the apical position (these types of couplings are the largest that have been measured so far). A compilation of recent measurements of indirect nuclear spin-spin coupling constants can be found in an excellent review by Kamien′ska-trela [1]. Accurate theoretical calculations are required, for instance to verify these measurements, or in some cases, the coupling constants of interest cannot be directly measured and one has to resort to theoretical calculations. The spin-spin coupling mechanisms are subtle and correlating them to the charge distribution, bonding and dynamic exchange processes in molecules is not straightforward and requires theoretical support.

The problems associated with the theoretical calculation of indirect nuclear spin-spin couplings are two-fold. First, the indirect nuclear spin-spin coupling constants formally are second-order properties. Usually, second-order properties are much more sensitive to electron correlation and basis set effects than their first-order counterparts. The indirect nuclear spin-spin coupling constants often require large basis sets and electron correlation effects beyond second-order perturbation theory. The second problem is that in nonrelativistic theory the full spin-spin coupling tensor is the sum of four contributions: Fermi-contact (FC), spin-dipole (SD), paramagnetic spin-orbit (PSO) and diamagnetic spin-orbit (DSO). It is well known that for quantitative accuracy all four of these terms need to be calculated. As a general rule, the FC term is much more sensitive to the correlation and basis effects compared to the other three terms. Fortunately, in the case of the FC contribution there is only one perturbation for each one of the coupled nuclei, while there are three and six perturbations in case of the PSO and SD terms respectively. Consequently, the PSO and SD contribution are roughly nine and thirty-six times more expensive than the FC contribution. The DSO term is evaluated as a relatively cheap expectation value, but the algorithm to evaluate atomic orbital integrals over Gaussian basis functions has not been available until recently [137]. Moreover, the current algorithm requires a numerical step and, altogether, the DSO integral evaluation is time consuming.

In spite of these formal and technical difficulties, as noted earlier, recent theoretical models such as CCSDPPA and MCLR with appropriate basis sets are able to provide accurate nuclear spin-spin coupling constants. However, these methods are severely demanding of computer resource and their applications are often limited to smaller systems. As indicated earlier, however, there will be a lot of interesting new applications for methods which would give quantitative nuclear spin-spin coupling constants for medium size molecules (8–10 non-hydrogen atoms).

CHAPTER 5

A CRITICAL ASSESSMENT OF THE EOM-CCSD METHOD FOR INDIRECT NUCLEAR SPIN-SPIN COUPLING CONSTANT CALCULATIONS

5.1 Introduction

Before applying a new theoretical method to a hitherto unknown molecular property, it is important to asses the strengths, weaknesses and overall quality of the method by comparing the results obtained with the new method to other theoretical and experimental data for similar types of problems. This "calibration" is a dynamic and continuous process. Each time the method is applied to a new problem, new information about the performance is gained, thus modifying the assessment of the method both its accuracy and strength.

The selection of an appropriate standard to compare a new theoretical method is not a simple task. An obvious choice would be experimental results, but there are some potential problems. For instance, what we can compute directly may not be easily accessible experimentally. For example, computed indirect nuclear spin-spin coupling constants correspond to isolated molecules at absolute zero degree temperature. Experimental data for such an ideal situation is of course not available and we have to resort to the experiments which are closest to our ideal model, in this case gas-phase experiments. In other instances, computed results agree with the experiment due to fortuitous error cancellations. If such problems are given due attention, experimental results can be very useful to calibrate a theoretical method, but it is worth considering other standards as well.

For a given Hamiltonian and basis set, the full configuration interaction (Full-CI) is exact, and hence, is an ideal standard to assess a new method. Unfortunately, full-CI calculations are nearly impossible except for the simplest systems and the results available for comparison are severely limited. Another option is to compare with methods that are better than the method in question from well-defined theoretical standpoints. A example would be comparison of the EOM-CCSD CI-like approximation to the EOM-CCSD quadratic model which, from theoretical stand-points, is superior. However, quite often, the implementation of full models, due to additional complications, follows after the approximate models, forcing such comparisons to wait. A final option is to compare with methods which cannot really be designated as "better", but which are very well tested on the problem at hand. Although, these comparisons are the least definitive, they are the most common in the calibration of any new method.

In this chapter, a systematic study of the performance of the EOM-CCSD method applied to indirect nuclear spin-spin coupling constant calculations is presented. The overall performance of the EOM-CCSD method is assessed by comparison with experiment and other well-established methods. The basis set dependence and the electron correlation effects on the nuclear spin-spin coupling constant calculations within the EOM-CCSD model, considered separately for the individual contributions (FC, SD, PSO and DSO) is reported. The molecules were choosen to cover a wide variety of coupling constants, and often have couplings which were identified as difficult cases for quantitative theoretical estimation by previous calculations. Certain systems, known to have large non-contact couplings, were taken into consideration too.

5.2 Basis Set Dependence and Electron Correlation Effects on Nuclear Spin-Spin Coupling Constants Within the EOM-CCSD Method.

In order to assess the magnitude of non-contact (SD, PSO, and DSO) contributions, basis set and electron correlation effects, calculations have been carried out on a number of molecules using different basis sets. The selection of molecules includes B_2H_6, CH_3CN, CH_3F, C_2H_4 and CH_3NH_2 and covers a wide range of coupling situations. All the geometries of our selection of molecules have been optimized at the CCSD level using a triple-zeta double polarization (TZ2P) basis set; results are presented in Table 5.1. The TZ2P basis consists of (11s,6p,2d)/[5s,3p,2d] contraction for B, C, N and F and a (5s,2p)/[3s,2p] contraction for hydrogen. The sp set has been taken from Dunning [138]. Polarization exponents have been optimized locally for several prototype molecules at the MBPT(4) level of correlation and are contracted following a recipe by Dunning [139]. Spherical harmonic gaussian basis functions have been used in all the geom-

Table 5.1. The CCSD/TZ2P optimized geometries for all the molecules considered. Bond distances are given in Angstroms and bond angles as well as dihedral angles are in degrees.

Molecule	Optimized geometrical parameters
CH_3CN	r(CC) = 1.468751, r(CN) = 1.151726, r(CH) = 1.085622, α(HCC) = 109.895971
CH_3F	r(CF) = 1.385657, r(CH) = 1.085519, α(FCH) = 108.711488
C_2H_4	r(CC) = 1.330651, r(CH) = 1.079306, α(HCC) = 121.536974
B_2H_6	r(BH_b) = 1.330651, r(BH_t) = 1.182268, α(H_bBH_t) = 121.536974, r(BB) = 1.757107
CH_3NH_2	r(NH) = 1.008905, r(CN) = 1.469082, r(CH_1) = 1.092148, r(CH_2) = 1.086809, α(H_2NC) = 109.090497, α(H_1NC) = 114.649346, τ(H_2CNH_1) = 121. 458330, τ(HNX_1X_2) = 52.912409[a]

[a] X_1 and X_2 are two dummy atoms perpendicular to each other and also attached to the nitrogen atom.

etry optimizations. We have chosen to use CCSD/TZ2P optimized geometries instead of experimental geometries to avoid any ambiguities arising from uncertainties in the reported experimental structures and also to have a consistent set of geometrical parameters for the selected set of molecules.

We have chosen the double-zeta plus polarization (DZP), triple-zeta plus polarization (TZP), a basis set due to Chipman [140], which is of triple-zeta plus polarization quality but especially optimized for properties which depend only on the quality of the wave function at the nuclei and, finally a quadruple-zeta plus polarization (QZP) basis set. These basis sets are widely used in correlated electronic structure calculations, hence it is useful to calibrate the EOM-CCSD models with respect to these basis sets when applied to NMR spin-spin coupling constant calculations. The detailed structure of each basis set is as follows:

1. The DZP basis consists of a [9s,5p,1d]/(4s,2p,1d) contraction for B, C, N, O, F and a [4s,1p]/(2s,1p) contraction for H. The sp set has been taken from Dunning [138] and the polarization exponents have been optimized locally at a correlated level [141].
2. The TZP basis consists of [10s,6p,1d]/(5s,3p,1d) contraction for B, C, N, O, F and a [5s,1p]/(3s,1p) contraction for H [139]. The polarization exponents are identical to those of the DZP basis sets described above.

3. Chipman's basis consists of a [10s,6p,1d]/(6s,3p,1d) contraction for B, C, N, O, F and a [6s,1p]/(4s,1p) contraction for H [142].
4. The QZP basis consists of a [11s,7p,1d]/(6s,4p,1d) contraction for C, N, O, F and a [7s,2p]/(4s,2p) contraction for H [143]. The exponents of the polarization functions have been chosen for the QZP basis sets as follows: 0.8 for C, 1.0 for N, 1.2 for O, 1.4 for F and 1.39 and 0.46 for H.

In our calculation on C_2H_4 we used in addition basis sets consisting of a [15s,7p,4d]/(10s,5p,4d) contraction for C and a [9s,2p]/(6s,2p) contraction for H [125].

For each molecule there are several coupling constants and each of the coupling constants has four contributions. Since we consider several molecules with several different basis sets there is an enormous amount of data to present and analyse. We have chosen, therefore, to present detailed results for one representative molecule and to limit the discussion to a statistical analysis for the other molecules. The statistical analysis mainly concerns the study of basis set effects and the effects of the quadratic contribution. To analyse the effect of electron correlation and to compare with experiment and other theoretical methods, we present all the couplings obtained with the most extensive QZP basis set.

The CH_3CN molecule has been chosen as our representative example to discuss the basis set effects and the effects of the quadratic contribution. Tables 5.2–5.5, present the FC, SD, PSO, and DSO contributions to each of the coupling constants of CH_3CN obtained using four different basis sets (DZP, TZP, Chipman, and QZP). Both EOM-CCSD CI-like and the quadratic results are presented for FC, SD and PSO contributions. The DSO contributions given in Table 5.5 are evaluated using the CCSD response density (no orbital relaxation effects).

Along with those, we have also presented the difference of the DZP, TZP and Chipman basis set absolute results for the FC, SD, PSO, and DSO contributions and the corresponding results in the QZP basis. This difference is multiplied by the sign of the contribution at the QZP level, such that the difference provides a direct measure of the difference in magnitude or absolute value of the contribution. If the difference is positive the magnitude of the QZP value is larger than the magnitude of the respective basis set value, and conversely. This convention will allow us to observe a trend towards more pronounced values for the couplings, with increasing size of the basis set, if such a trend exists.

As a statistical measure of basis set dependence of the FC contribution, we use both the mean absolute deviation and the mean absolute percentage from the QZP results. For the other three contributions, we report only the mean absolute deviation as the contributions are often so small that the percentage error is not very meaningful. For similar reasons the FC contributions less than 1 Hz

Table 5.2. The Fermi-contact contribution to the NMR spin-spin coupling constants CH_3CN (in Hz) obtained using different basis sets[a]

					Deviations[b]		
	DZP	TZP	Chipman	QZP	DZP	TZP	Chipman
$^1J(^{13}C^{15}N)$	-12.30	-12.71	-14.39	-13.15	0.85	0.44	-1.24
	-12.32	-12.71	-14.48	-13.17	0.85	0.46	-1.31
Quad. Con.	0.02	0.00	0.09	0.02			
$^1J(^{13}C^1H)$	118.17	122.37	125.03	123.29	5.12	0.92	-1.74
	118.86	123.08	125.72	124.06	5.20	0.98	-0.08
Quad. Con.	0.69	0.71	0.69	0.77			
$^2J(^{13}C^{15}N)$	2.36	2.37	2.53	2.46	0.10	0.09	-0.07
	2.41	2.42	2.60	2.52	0.11	0.10	-0.08
Quad. Con.	0.05	0.05	0.07	0.07			
$^2J(^{13}C^1H)$	-9.81	-9.63	-10.07	-9.91	0.10	0.28	-0.16
	-10.21	-10.07	-10.51	-10.39	0.18	0.32	-0.12
Quad. Con.	0.40	0.44	0.44	0.48			
$^3J(^{15}N^1H)$	-1.00	-1.06	-1.28	-1.16	0.16	0.10	-0.12
	-1.07	-1.14	-1.38	-1.25	0.18	0.11	-0.13
Quad. Con.	0.07	0.08	0.1	0.09			
$^3J(^1H^1H)$	-14.98	-15.54	-15.94	-15.59	0.61	0.05	-0.35
	-15.26	-15.88	-16.28	-15.97	0.71	0.09	-0.31
Quad. Con.	0.28	0.34	0.34	0.38			
Mean abs. deviation					1.16	0.31	0.61
					1.21	0.35	0.60
Mean abs. percent deviation					5.67	3.25	4.65
					5.93	3.45	4.66

[a] For each coupling, the first-row of data corresponds to CI-like EOM-CCSD results and the second-row corresponds to quadratic EOM-CCSD results.

[b] The deviations are evaluated by taking the difference of DZP, TZP and Chipman basis results from the QZP basis results. The FC contributions less than 1 Hz is neglected in the averaging.

Table 5.3. The spin-dipole contribution to the NMR spin-spin coupling constants CH_3CN (in Hz) obtained using different basis sets[a].

					Deviations[b]		
	DZP	TZP	Chipman	QZP	DZP	TZP	Chipman
$^1J(^{13}C^{15}N)$	-4.19	-4.18	-4.13	-4.39	0.20	0.21	0.26
	-4.34	-4.37	-4.29	-4.60	0.26	0.23	0.31
Quad. Con.	0.15	0.19	0.16	0.21			
$^1J(^{13}C^1H)$	0.05	-0.21	0.03	0.03	-0.02	0.24	0.00
	0.05	-0.20	0.03	0.03	-0.02	0.23	0.00
Quad. Con.	0.00	-0.01	0.00	0.00			
$^2J(^{13}C^{15}N)$	-0.09	-0.11	-0.09	-0.10	0.01	-0.01	0.01
	-0.10	-0.11	-0.09	-0.10	0.00	-0.01	0.01
Quad. Con.	0.01	0.00	0.00	0.00			
$^2J(^{13}C^1H)$	0.13	0.12	0.14	0.13	0.00	0.01	-0.01
	0.13	0.13	0.14	0.13	0.00	0.00	-0.01
Quad. Con.	0.00	0.01	0.00	0.00			
$^3J(^{15}N^1H)$	0.03	0.03	0.04	0.03	0.00	0.00	-0.01
	0.04	0.04	0.04	0.03	-0.01	-0.01	-0.01
Quad. Con.	0.01	0.01	0.00	0.00			
$^3J(^1H^1H)$	0.26	0.30	0.33	0.31	0.05	0.01	-0.02
	0.26	0.30	0.33	0.31	0.05	0.01	-0.02
Quad. Con.	0.00	0.00	0.00	0.00			
Mean abs. deviation					0.06	0.08	0.06
					0.07	0.08	0.07

[a] For each coupling, the first-row of data corresponds to the CI-like EOM-CCSD results and the second-row corresponds to the quadratic EOM-CCSD results.

[b] The deviations are evaluated by taking the differences of absolute of DZP, TZP and Chipman basis results from the QZP basis results, and multiplication by the sign of the QZP results (see text). The SD contributions less than 0.05 Hz is neglected in the averaging.

Table 5.4. The paramagnetic spin-orbit contribution to the NMR spin-spin coupling constants CH_3CN (in Hz) obtained using different basis sets.

					Deviations[a]		
	DZP	TZP	Chipman	QZP	DZP	TZP	Chipman
$^1J(^{13}C^{15}N)$	1.48	0.50	1.54	0.33	-1.15	-0.17	-1.21
	1.38	0.37	1.44	0.30	-1.08	-0.07	-1.14
Quad. Con.	-0.10	-0.13	-0.10	-0.03			
$^1J(^{13}C^1H)$	0.48	1.14	0.61	1.07	0.59	-0.07	0.46
	0.48	1.15	0.62	1.08	0.60	-0.07	0.46
Quad. Con.	0.00	0.01	0.01	0.01			
$^2J(^{13}C^{15}N)$	0.45	0.40	0.48	0.40	-0.05	0.00	-0.08
	0.46	0.41	0.49	0.42	-0.04	0.01	-0.07
Quad. Con.	0.01	0.01	0.01	0.02			
$^2J(^{13}C^1H)$	0.09	0.09	0.09	0.16	0.08	0.08	0.08
	0.08	0.08	0.09	0.16	0.08	0.08	0.07
Quad. Con.	-0.01	-0.01	0.00	0.00			
$^3J(^{15}N^1H)$	-0.21	-0.30	-0.21	-0.36	0.15	0.06	0.15
	-0.21	-0.30	-0.21	-0.36	0.15	0.06	0.15
Quad. Con.	0.00	0.00	0.00	0.00			
$^3J(^1H^1H)$	2.28	2.37	2.34	2.81	0.53	0.44	0.47
	2.28	2.37	2.34	2.82	0.54	0.45	0.48
Quad. Con.	0.00	0.00	0.00	0.01			
Mean abs. deviation					0.43	0.14	0.41
					0.42	0.12	0.40

[a] For each coupling, the first-row of data corresponds to the CI-like EOM-CCSD results and the second-row corresponds to the quadratic EOM-CCSD results.

[b] The deviations are evaluated by taking the differences of DZP, TZP and Chipman basis results from the absolute QZP basis results, and multiplication by the sign of the (QZP) results (see text). The PSO contributions less than 0.05 Hz is neglected in the averaging.

Table 5.5. The diamagnetic spin-orbit contribution to the NMR spin-spin coupling constants CH_3CN (in Hz) obtained using different basis sets.

					Deviation [a]		
	DZP	TZP	Chipman	QZP	DZP	TZP	Chipman
$^1J(^{13}C^{15}N)$	-0.01	0.00	-0.01	0.00	0.01	0.00	-0.01
$^1J(^{13}C^1H)$	0.55	0.54	0.53	0.52	-0.03	-0.02	-0.01
$^2J(^{13}C^{15}N)$	0.08	0.08	0.08	0.08	0.00	0.00	0.00
$^2J(^{13}C^1H)$	-0.15	-0.16	-0.16	-0.17	0.02	0.01	0.01
$^3J(^{15}N^1H)$	0.22	0.22	0.22	0.23	0.01	-0.07	0.01
$^3J(^1H^1H)$	-2.98	-3.00	-3.02	-3.06	0.08	0.06	0.04
Mean abs. deviation[b]					0.03	0.03	0.01

[a] The deviations are evaluated by taking the difference of DZP, TZP and Chipman basis results from the QZP basis set results, and multiplication by the sign of the QZP results (see text).

[b] The DSO contributions less than 0.05 Hz are neglected in the averaging.

and the PSO, SD and DSO contributions less than 0.05 Hz have been discarded in the averaging. The averages for each molecule are presented in Table 5.6. The difference between absolute quadratic EOM-CCSD results and CI-like EOM-CCSD results are reported in Tables 5.2–5.5 (abbreviated as Quad. con.) as a measure of the magnitude of the quadratic contribution. As we can see, the quadratic contribution to the FC, SD, and PSO contributions are small in all the couplings of CH_3CN. This is usually the case for all molecules considered in this study. The largest quadratic contribution is about 3 Hz and occurs in

Table 5.6. The mean absolute deviation of DZP, TZP and Chipman basis set results for the FC, SD, PSO and DSO contributions from the corresponding QZP basis set results[a].

		Δ(QZP - DZP)	Δ(QZP - TZP)	Δ(QZP-Chipman)
B_2H_6	FC	12.27 (12.51)	2.02 (2.06)	3.38 (3.50)
		1.31 (1.34)	0.37 (0.37)	0.40 (0.39)
	SD	0.13 (0.14)	0.20 (0.19)	0.15 (0.15)
	PSO	0.24 (0.24)	0.16 (0.16)	0.21 (0.21)
	DSO	0.10	0.02	0.13
CH_3CN	FC	5.57 (5.99)	3.25 (3.51)	4.65 (4.59)
		1.16 (1.20)	0.31 (0.35)	0.61 (0.60)
	SD	0.08 (0.07)	0.06 (0.08)	0.04 (0.07)
	PSO	0.43 (0.42)	0.13 (0.12)	0.41 (0.40)
	DSO	0.03	0.02	0.01
C_2H_4	FC	13.46 (10.09)	5.77 (3.79)	12.71 (8.64)
		1.66 (1.70)	0.46 (0.49)	0.48 (0.45)
	SD	0.02 (0.02)	0.06 (0.06)	0.03 (0.03)
	PSO	0.48 (0.48)	0.29 (0.29)	0.48 (0.47)
	DSO	0.05	0.03	0.02
CH_3F	FC	4.86 (5.08)	2.15 (2.18)	2.63 (2.55)
		6.49 (6.64)	2.30 (2.34)	1.19 (1.28)
	SD	0.40 (0.42)	0.11 (0.10)	0.42 (0.45)
	PSO	1.43 (1.44)	0.26 (0.26)	1.38 (1.48)
	DSO	0.07	0.05	0.06

Table 5.6. (Continued) The mean absolute deviation of DZP, TZP and Chipman basis set results for the FC, SD, PSO and DSO contributions from the corresponding QZP basis set results[a].

		Δ(QZP-DZP)	Δ(QZP-TZP)	Δ(QZP-Chipman)
CH_3NH_2	FC	7.22 (7.07)	4.30 (5.07)	3.61 (4.49)
		1.49 (1.60)	0.38 (0.48)	0.40 (0.35)
	SD	0.04 (0.04)	0.04 (0.04)	0.03 (0.03)
	PSO	0.38 (0.38)	0.18 (0.17)	0.34 (0.33)
	DSO	0.04	0.03	0.02

[a] In the case of FC contribution the mean absolute percent deviation from the QZP basis set results are also given. The corresponding quadratic results are given in parenthesis.

the $^1J(^{13}C^{19}F)$ coupling of the CH_3F molecule. Another important observation from Tables 5.2–5.5, is that the magnitude of the quadratic contribution shows a very small variation among basis sets for all three coupling contributions. As mentioned in Chapter 2, the evaluation of the quadratic contribution is an additional non-iterative N^6 (N is the number of basis functions) procedure for each pair of perturbations on top of CI-like EOM-CCSD calculation. As a result, the evaluation of the quadratic contributions is costly for large molecules, in particular for the PSO and SD contributions since these two contribution have three and six different perturbations per nucleus respectively. On the other hand, even though the effect of the quadratic contribution seems to be insignificant for the molecules considered in this study, that effect is expected to become more important for larger molecules because it corrects for the size-extensitivity error in the EOM-CCSD CI-like approximation. In this case we can take advantage of the fact that the quadratic effects more or less remain constant with different basis sets. A reliable estimate of the quadratic contribution can be obtained from a smaller basis set such as DZP.

As we can see from the mean absolute deviations presented in Table 5.6, the FC contribution shows the largest variation among basis sets compared to the other three contributions. The absolute DZP basis results for the FC contribution are consistently lower than their QZP counterparts for all the couplings of CH_3CN molecule. This trend pretty much remains true for the rest of the molecules considered in this study. However, there are occasional exceptions, for example the absolute DZP results of $^1J(^{13}C^{19}F)$ of CH_3F are about 18 Hz larger than the corresponding QZP results. There is quite an improvement in the FC contribution going from the double zeta to triple zeta level of accuracy. Moreover the Chipman and TZP basis sets, which have approximately the same size, yield results of comparable quality. Overall, convergence of the FC contribution with the basis set looks fairly smooth.

As regards the other contributions, the DSO contribution shows the least variation among the basis sets and in fact even a smaller basis set such as DZP provides a pretty good estimate of this contribution. As discussed earlier, the evaluation of DSO integrals is costly and for larger molecules a reliable estimate of the DSO contribution can be obtained using smaller basis set, which is very useful. For all systems, except possibly CH_3F the SD contribution is also reasonably well converged at the DZP level. This is very fortunate as there are six perturbations per nucleus for this contribution, and the total number of perturbations therefore increases very rapidly with the size of the system. The PSO contributions show somewhat larger variations, and in particular the TZP basis provides better comparisons with the QZP basis than the Chipman basis.

Table 5.7 present CI-like and quadratic EOM-CCSD results of several selected coupling constants from each molecule, calculated using DZP, TZP, Chipman and QZP basis sets. Experimental results are also given in order to assess how well different basis sets results compare with experiment. The coupling constants less than 5 Hz are not included since the absolute percent errors from the experiment for such couplings are not very meaningful. There is little agreement in the literature on the experimental coupling constants of B_2H_6 and therefore they are not included in Table 5.7. A detailed discussion of B_2H_6 coupling constants is given later. In the case of CI-like EOM-CCSD results, the mean absolute percent deviations from experiment are 13.9, 8.4, 7.3 and 7.6 respectively, for DZP, TZP, Chipman and QZP basis sets. The corresponding quadratic EOM-CCSD results are 13.7, 7.7, 7.5 and 7.9 and as we can see, they are quite close to the CI-like results. This information on the expected average error, for a given basis set,

Table 5.7. Comparison of DZP, TZP, Chipman and QZP basis set EOM-CCSD results with experiment[a].

Coupling	Molecule	DZP	TZP	Chipman	QZP	Exp.
$^1J(^{13}C^{15}N)$	CH_3CN	-15.02(-15.29)	-16.39(-16.71)	-16.99(-17.34)	-17.21(-17.41)	±17.05±0.4
$^1J(^{13}C^1H)$		119.25(119.94)	123.84(124.57)	126.20(126.90)	124.85(125.69)	±136.0±0.2
$^3J(^{13}C^1H)$		-9.74(-10.15)	-9.58(-10.02)	-10.00(-10.44)	-9.78(-10.27)	±10.0±0.2
$^1J(^{13}C^{19}F)$	CH_3F	-192.83(-196.22)	-176.20(-179.04)	-174.48(-177.25)	-169.56(-172.37)	-157.5±0.2
$^1J(^{13}C^1H)$		130.45(131.08)	136.70(137.36)	138.39(139.20)	137.15(137.89)	149.1±0.2
$^2J(^1H^{19}F)$		46.85(47.82)	47.17(48.10)	46.78(47.38)	49.00(49.93)	46.36±0.1
$^1J(^{13}C^1H)$	C_2H_4	141.90(142.62)	145.24(145.98)	147.60(148.32)	146.83(147.66)	156.4
$^3J(^1H^1H)_{cis}$		9.31(9.49)	9.83(10.03)	10.00(10.18)	10.20(10.41)	11.6
$^3J(^{13}C^1H)_{trans}$		13.50(13.82)	15.01(15.35)	15.11(15.46)	15.71(16.07)	19.1
$^1J(^{15}N^1H)$	CH_3NH_2	-57.10(-57.30)	-59.75(-59.97)	-61.33(-61.56)	-61.33(-61.72)	-65.0±0.2
$^2J(^{13}C^{15}N)$		-3.60(-3.58)	-4.42(-4.42)	-4.86(-4.87)	-4.93(-5.09)	-4.5±0.5

[a] The quadratic EOM-CCSD results are given in parenthesis.

may prove quite useful in the application of the EOM-CCSD method to spin-spin coupling constants, which are often not known experimentally. For instance, for medium size molecules, it is not always possible to use basis sets as large as QZP and one has to resort to smaller basis sets such as DZP. The percentage deviations from experiment reported here provide us guidence to evaluate the quality of such calculations.

We conclude from our basis set studies that the Chipman basis usually gives a better value for the FC contribution than the TZP basis set, or even the QZP basis set, when compared to experiment. However the PSO contribution is better evaluated using the TZP basis set. The DZP basis set seems sufficiently accurate when evaluating the computationally expensive SD and the DSO contributions to the spin-spin coupling constants, and is still very reasonable for the FC contribution and in particular the PSO contribution. However, for quantitative accuracy it is advisable that a basis set of at least triple zeta quality be used for these latter two contributions to spin-spin coupling constants. Since the different contributions to the overall spin-spin coupling constant show different convergence behavior with the size of the basis set, but are completely independent, it seems perfectly legitimate to evaluate these contributions from different calculations, and in particular, different basis sets. This observation allows for a significant savings when evaluating the non-contact contributions.

Now, we focus on the effect of electron correlation effects on the calculation of NMR spin-spin coupling constants within the EOM-CCSD model. We also consider magnitudes of non-contact contributions and compare our best results with experiment and other well established correlated methods. In Tables 5.8–5.12, we present results from CPHF and CI-like EOM-CCSD calculations, using the QZP basis set, of FC, SD and PSO contributions as well as the Hartree-Fock and CCSD (unrelaxed) DSO contributions to the NMR spin-spin couplings of B_2H_6, CH_3F, CH_3CN, CH_3NH_2 and C_2H_4.

As we can see from Tables 5.8–5.12, electron correlation has a large effect on the FC contribution, but for the SD, PSO and DSO contributions electron correlation is less important. When we consider the correlated results, the FC contribution is dominant in almost all the couplings of B_2H_6, C_2H_4 and CH_3NH_2. The case of $^1J(^1H_t{}^1H_t)$ coupling in B_2H_6 is an exception and the DSO contribution is dominant. For these three molecules, the SD contribution is negligible for all the coupling constants and the PSO contribution is significant only in certain coupling constants. For example, $^2J(H_tH_t)$, $^2J(^{11}B^{11}B)$ and $^2J(H_bH_b)$ in B_2H_6, $^1J(^{15}N^1H)$, $^2J(^1H^1H)$,$^3J(^1H^1H)_{cis}$, $^3J(^1H^1H)_{trans}$ and $^3J(^1H^1H)$ in CH_3NH_2 and $^2J(^1H^1H)$ in C_2H_4. The DSO contribution is significant in proton-proton coupling constants in these molecules. The $^1J(^1H^{19}F)$ and $^1J(^{13}C^{19}F)$ in CH_3F and $^1J(^{13}C^{15}N)$ in CH_3CN are special cases in terms of having large SD and PSO contributions.

Table 5.8. The NMR spin-spin coupling constants of B_2H_6 (in Hz)[a].

		FC	SD	PSO	DSO	Total
$^1J(^{11}B^1H_b)$	CPHF	53.09	-0.18	0.00	0.66	53.57
	EOM-CCSD	42.05	-0.09	0.06	0.67	42.69 (43.08)
$^1J(^{11}B^1H_t)$	CPHF	151.45	0.17	-0.44	0.31	151.49
	EOM-CCSD	122.11	0.24	-0.51	0.33	122.17 (122.86)
$^2J(^1H_t{}^1H_t)$	CPHF	-7.42	0.14	2.07	-1.73	-6.94
	EOM-CCSD	-1.44	0.11	2.01	-2.41	-1.43 (-1.50)
$^3J(^1H_t{}^1H_t)_{cis}$	CPHF	3.20	-0.01	0.35	-0.52	3.02
	EOM-CCSD	3.01	-0.01	0.33	-0.52	2.81 (2.86)
$^3J(^1H_tH_t)_{trans}$	CPHF	13.49	0.01	1.43	-1.80	13.13
	EOM-CCSD	11.37	0.01	1.38	-1.79	10.98 (11.23)
$^1J(^{11}B^{11}B)$	CPHF	-1.72	-0.06	-2.01	0.06	-3.73
	EOM-CCSD	-3.58	-0.04	-2.20	0.06	-5.76 (-5.90)
$^2J(^1B^1H_t)$	CPHF	4.40	-0.07	-0.09	-0.37	3.87
	EOM-CCSD	4.94	-0.05	-0.13	-0.37	4.39 (4.40)
$^2J(^1H_l{}^1H_b)$	CPHF	-12.58	0.01	0.92	-1.03	-12.68
	EOM-CCSD	-7.07	0.01	0.90	-1.02	-7.18 (-7.36)
$^2J(^1H_b{}^1H_b)$	CPHF	14.75	1.01	2.05	-1.39	16.42
	EOM-CCSD	12.50	0.81	2.02	-1.70	13.63 (13.68)

[a] At the CCSD/TZ2P geometry using QZP basis set. The total quadratic EOM-CCSD results are given in parenthesis. Experimental results are unsettled and not given here. A detailed discussion can be found in the text.

Table 5.9. The NMR spin-spin coupling constants of CH_3F (in Hz)[a].

		FC	SD	PSO	DSO	Total	Exp[b].
	CPHF	-191.56	23.62	34.22	0.44	-133.28	
$^1J(^{13}C^{19}F)$	EOM-CCSD	-226.16	19.97	36.19	0.44	-169.56(-172.16)	-157.5±0.2[b]
	CPHF	179.75	-0.25	0.06	0.63	180.19	
$^1J(^{13}C^1H)$	EOM-CCSD	136.44	0.04	0.01	0.66	137.15(137.89)	149.1±0.2[b]
	CPHF	57.45	-4.12	11.39	-1.84	62.88	
$^2J(^1H^{19}F)$	EOM-CCSD	41.70	-2.76	11.88	-1.82	49.00(49.94)	46.36±0.1[b]
	CPHF	-21.28	0.49	2.76	-3.06	-21.09	
$^2J(^1H^1H)$	EOM-CCSD	-9.84	0.36	2.67	-3.01	-9.82(-10.03)	

[a] At the CCSD/TZ2P geometry using a QZP basis set. The total quadratic EOM-CCSD results are given in parenthsis.

[b] S. G. Frankiss, [144].

Table 5.10. The NMR spin-spin coupling constants of CH_3CN (in Hz)[a].

		FC	SD	PSO	DSO	Total	Exp[b].
$^1J(^{13}C^{15}N)$	CPHF	-64.48	-16.24	-4.95	0.01	-85.66	
	EOM-CCSD	-13.15	-4.39	0.33	0.00	-16.99 (-17.20)	±17.5±0.4
$^1J(^{13}C^1H)$	CPHF	171.32	-0.22	1.06	0.49	172.65	
	EOM-CCSD	123.29	0.03	1.07	0.52	124.91 (125.69)	±136.0±0.2
$^2J(^{13}C^{15}N)$	CPHF	12.12	-0.39	0.36	0.08	12.17	
	EOM-CCSD	2.46	-0.10	0.40	0.08	3.01 (3.08)	±3.0±0.4
$^2J(^{13}C^1H)$	CPHF	-50.27	0.57	-0.02	-0.17	-49.89	
	EOM-CCSD	-9.91	0.13	0.16	-0.17	-10.00 (-10.44)	±10.0±0.2
$^3J(^{15}N^1H)$	CPHF	-12.91	0.31	-0.50	0.23	-12.87	
	EOM-CCSD	-1.16	0.03	-0.36	0.23	-1.23 (-1.33)	±1.80±0.1
$^3J(^1H^1H)$	CPHF	-37.56	0.40	2.88	-3.11	-37.39	
	EOM-CCSD	-15.99	0.31	2.81	-3.06	-16.29 (-16.63)	

[a] At CCSD/TZ2P geometry using QZP basis sets. The total quadratic EOM-CCSD results are given in parenthesis.

[b] W. Mcfarlane [145].

Table 5.11. Nuclear spin-spin coupling constant of CH_3NH_2 (in Hz)[a].

		FC	SD	PSO	DSO	Total	Exp[b].
$^1J(^{15}N^1H)$	CPHF	-75.50	-0.03	-2.82	-0.20	-78.55	-65.0±0.2
	EOM-CCSD	-58.24	-0.24	-2.65	-0.20	-61.33 (-61.72)	
$^1J(^{13}C^1H_A)$	CPHF	162.29	-0.31	0.81	0.54	163.33	
	EOM-CCSD	122.59	0.01	0.79	0.56	123.95 (124.97)	
$^1J(^{13}C^1H_B)$	CPHF	158.47	-0.32	0.85	0.55	159.55	132.2±0.2
	EOM-CCSD	119.18	0.01	0.86	0.57	120.62 (121.61)	
$^2J(^1H_A{}^1H_B)$	CPHF	-22.35	0.49	2.66	-2.93	-22.13	
	EOM-CCSD	-10.70	0.36	2.59	-2.89	-10.64 (-10.93)	
$^2J(^1H_A{}^1H_A)$	CPHF	-25.12	0.86	4.84	-4.67	-24.09	
	EOM-CCSD	-11.87	0.60	4.75	-4.60	-11.12 (-11.45)	
$^2J(^{15}N^1H)$	CPHF	0.06	0.00	-0.28	0.14	-0.08	
	EOM-CCSD	-1.62	0.00	-0.29	0.14	-1.77 (-1.83)	
$^2J(^{15}N^1H)$	CPHF	1.96	0.06	-0.26	0.20	1.96	-1.0±0.1
	EOM-CCSD	0.97	0.03	-0.27	0.20	0.93 (0.93)	
$^3J(^1H^1H)_{cis}$	CPHF	3.83	0.10	0.95	-1.23	3.65	
	EOM-CCSD	2.39	0.08	0.93	-1.16	2.24 (2.22)	

Table 5.11. (Continued) Nuclear spin-spin coupling constant of CH_3NH_2 (in Hz)[a].

		FC	SD	PSO	DSO	Total	Exp.
$^3J(^1H^1H)_{trans}$	CPHF	18.66	0.05	3.53	-3.98	18.26	
	EOM-CCSD	13.65	0.01	3.44	-3.96	13.38 (13.56)	
$^3J(^1H^1H)$	CPHF	3.01	0.09	0.96	-1.18	2.88	7.1±0.1
	EOM-CCSD	2.13	0.07	0.93	-1.21	1.92 (1.86)	
$^2J(^{13}C^1H)$	CPHF	-11.07	0.07	0.55	-0.54	-10.99	
	EOM-CCSD	-3.97	0.07	0.58	-0.53	-3.85 (-3.96)	
$^2J(^{13}C^{15}N)$	CPHF	-14.30	-0.81	0.32	-0.05	-14.84	-4.5±0.5
	EOM-CCSD	-3.64	-0.73	-0.51	-0.05	-4.93 (-5.09)	

[a] At the CCSD/TZ2P geometry using a QZP basis set. The total quadratic EOM-CCSD results are given in parenthesis.

[b] Paolillo*et al.*, [146].

Table 5.12. The NMR spin-spin coupling constants (in Hz) of C_2H_4[a].

		FC	SD	PSO	DSO	Total	Exp[b].
$^1J(^{13}C^1H)$	QZP	145.63	0.21	0.53	0.46	146.83 (147.66)	156.4
	Special	151.37	0.12	0.35	0.45	152.29 (153.23)	
$^2J(^1H^1H)$	QZP	0.18	0.22	3.55	-3.84	0.07 (-0.14)	2.5
	Special	0.25	0.28	3.97	-3.85	0.65 (0.44)	
$^3J(^1H^1H)_{cis}$	QZP	10.75	-0.02	0.54	-1.07	10.20 (10.41)	11.6
	Special	11.74	-0.04	0.71	-1.08	11.33 (11.57)	
$^3J(^{13}C^1H)_{trans}$	QZP	16.44	0.23	2.60	-3.56	15.71 (16.07)	19.1
	Special	17.67	0.23	3.05	-3.57	17.38 (17.80)	
$^2J(^{13}C^1H)$	QZP	-0.75	-0.01	-1.08	-0.69	-2.53 (-2.82)	
	Special	-0.90	-0.00	-1.03	-0.69	-2.61 (-2.95)	

[a] At the CCSD/TZ2P geometry using QZP basis set and the [10s,5p,4d/6s,2p] C and H basis set used by Geertsen *et al.*[125] denoted here as special. The total quadratic EOM-CCSD results are given in parenthesis.

[b] Lynden-bell *et al.*, [147].

We also note the unusually large electron correlation effects on FC, SD and PSO contributions to these two particular coupling constants. The other coupling constants in these two molecules show a similar behavior as described above for the rest of the molecules.

Some of the couplings constants in B_2H_6 have been measured experimentally. However, there are disagreements among different measurements of these coupling constants. For example, the$^1J(^{11}B^1H_b)$ was reported to be (in Hz) 46 ± 2 [148], 46 ± 2 [149], 43 [150] 48 [151] 44 [152], 45.3–46.3 [153] and 46.3 [154]. Similarly, the$^1J(^{11}B^1H_t)$ was reported to be (in Hz) 135 ± 2 [148], 135 ± 2 [149], 125 [150], 137 [151], 128 ± 4 [155], 128 [152], 131–137 [153] and 133.5 [154]. Our best calculated values for these two coupling constant are 43 Hz and 122 Hz respectively. As we can see, they are in better agreement with Ogg's 1954 values of 43 Hz and 125 Hz. However, it is important to note that our EOM-CCSD model has an average error of 10% and therefore we are not in a position to rule out the other measurements for $^1J(^{11}B^1H_b)$ since they are within the error bars of our calculated results. But in the case of $^1J(^{11}B^1H_t)$ we can confidently rule out measurements larger than about 134 Hz. The HRPA results reported by Galasso *et al.* [133] are the only previously available correlated B_2H_6 coupling constants. In the case of B_2H_6 coupling constants, the reported HRPA results are quite close to the EOM-CCSD results reported in this study. For example, the HRPA results (in Hz) 121.31, 13.98, 8.74, 1.73, 43.19, and −7.86 of $^1J(^{11}B^1H_t)$,

$^2J(H_bH_b)$, $^3J(H_tH_t)_{trans}$, $^3J(H_tH_t)_{cis}$, $^1J(^{11}B^1H_b)$ and $^2J(H_tH_b)$ respectively, compared to the respective EOM-CCSD results 122.17, 13.63, 10.98, 2.81, 42.69, and −7.81. However, as we will see later, for difficult cases like $^1J(^1H^{19}F)$,$^1J(^{13}C^{17}O)$ and $^1J(^{14}N^{15}N)$ in HF, CO and N_2 respectively, correlation effects beyond HRPA become essential. As we can see from Table 5.8, both $^1J(^{11}B^1H_t)$ and$^2J(^{11}B^1H_t)$ are reproduced fairly well by the EOM-CCSD method. Contrary to Farrar and Quinting [154], who state that $^1J(^{11}B^{11}B)$ on the one hand, and $^3J(^1H_t{}^1H_t)$ (*cis* and *trans*) on the other, should have the same sign, we report opposite absolute signs for these coupling constants.

It is seen from the collected results in Tables 5.9−5.11, that our EOM-CCSD results are in good agreement with experimentally measured NMR spin-spin coupling constants of CH_3F, CH_3CN, and CH_3NH_2. For example, the calculated results for the $^1J(^{13}C^{19}F)$, $^1J(^{13}C^1H)$ and$^1J(^{19}F^1H)$ coupling constants in CH_3F show 8%, 8% and 6% absolute percentage deviations from experimental results respectively. Upon careful inspection of the CH_3NH_2 coupling reported in Table 5.11, one can notice that we report two different values for $^1J(^{13}C^1H)$ and similarly, three different values for $^1J(^1H^1H)$. This is due to the fact that in C_s symmetry (see Table 5.1) we have two different kind of methyl hydrogens. However, at room temperature, due to rapid rotation around the carbon-nitrogen bond, experimently measured coupling constants correspond to an average of all possible conformers and as a result all three methyl hydrogens appear to be identical. Therefore comparison of calculated results with experiment must be done with caution for the coupling constants in question.

In the case of CH_3CN, the absolute signs of the coupling constants are not unambiguously determined from the experiment. The calculated $^1J(^{13}C^{15}N)$, $^1J(^{13}C^1H)$, $^2J(^{13}C^{15}N)$, $^2J(^{13}C^1H)$ and $^3J(^{15}N^1H)$ coupling constants show 3%, 7%, 0.3%, 0% and 31% absolute percent deviations from the experiment. As shown in Table 5.10, the EOM-CCSD results also predicts the absolute signs of these coupling constants. There are no other correlated studies on the spin-spin couplings of CH_3F, CH_3CN and CH_3CN in the literature and the present results are the best calculated results, reported so far, for the spin-spin couplings of these molecules.

The coupling constants of C_2H_4 require special attention. As shown in Table 5.12, with the QZP basis set which has already been shown to work very well in predicting NMR spin-spin coupling constants of several other molecules, the EOM-CCSD quadratic results for the $^2J(^1H^1H)$ coupling has the wrong sign. The EOM-CCSD CI-like approximation results has the correct sign but shows 97% absolute deviation from experiment. We also note that the PSO and DSO contributions are dominant for this coupling constant. But, they have similar magnitudes with opposite signs and effectively cancel each other, leaving the FC and SD contributions as determining contributions of the overall sign and the magnitude of this coupling. Let us also mention that the DZP, TZP, and Chipman basis sets gives negative FC contributions and negative overall sign for the $^2J(^1H^1H)$ contrary to experiment. To further investigate the behavior of EOM-CCSD method with respect to this coupling, we use the [15s,7p,4d]/(10s,5p,4d) and [9s,2p]/(6s,2p) carbon and hydrogen basis sets which are specifically optimized to calculate the FC contact contributions [125] accurately. As we can see, with this basis set both EOM-CCSD models now have the correct sign and the absolute percent error from the experiment of the EOM-CCSD CI-like approximation has now dropped to 78%. The HRPA results reported by Galasso [121] are the only other correlated results available in the literature. The reported HRPA results for $^1J(^{13}C^1H)$,$^2J(^{13}C^1H)$,$^2J(^1H^1H)$,$^3J(^1H^1H)_{cis}$ and$^3J(^1H^1H)_{trans}$ coupling constants are 142.87, −5.07, −4.04, 9.10 and 14.27 Hz, respectively. These can be compared with the EOM-CCSD results presented in Table 5.12. However, these comparisons must be done with caution since HRPA results were obtained using a different geometry and relatively smaller basis set. We note a significantly better agreement of EOM-CCSD results with experiment, compared to HRPA. This is not surprising, since C_2H_4 is triplet unstable and consequently, CPHF will fail, requiring that a higher level of correlation be added than in HRPA.

5.3 Direct Comparison of the EOM-CCSD Method with Other Theoretical Methods and Experiment

In this section, a direct comparison of the EOM-CCSD method with other widely used correlated methods, in particular the polarization propagator methods is presented. Such a direct comparison, in fact requires EOM-CCSD results for a set of molecules at identical geometries, using the same basis set sets as used in the prior calculations. Since we are mainly interested in comparison with the polarization propagator results, a set of molecules were choosen for which well defined (known geometries and basis sets) propagator results are available in the literature. This includes molecules, such as H_2, HF, CO, N_2, H_2O and CH_4. Some of the molecules in this selection have recently been studied by multi-configuration linear response theory (MCLRT) under identical condition and these results are also reported for comparison.

Calculated EOM-CCSD indirect nuclear spin-spin coupling constants of these molecules are presented in Tables 5.14–5.18 along with the polarization propagator and experimental results. Whenever they are available the MCLRT results are also given.

Prior to a quantitative comparison of results obtained from different methods, we focus on the effects of the electron correlation and non-contact contributions. In this selection of molecules, as reported in Tables 5.13–5.17, non-contact contributions are significant for HF, CO, N_2 and H_2O. Indeed, the PSO contribution is the largest in the case of $^1J(^{14}N^{15}N)$ and $^1J(^{13}C^{17}O)$ in N_2 and CO respectively. Also note the large SD contributions in CO and N_2 coupling constants. The DSO contribution is negligible for all the coupling constants considered in this selection of molecules with the exception of $^2J(^1H^1H)$ in H_2O and CH_4.

Table 5.13. Nuclear spin-spin coupling constant of HD, $^1J(^1H^2H)$, in Hz[a].

Method	FC	SD	PSO	DSO	Total
CPHF[b]	53.11	0.57	0.83	-0.33	54.18
HRPA[c]	42.62	0.52	0.82	-0.33	43.63
MCLRT[d]	40.24	0.48	0.81	-0.31	41.22
SOPPA[e]	42.60	0.51	0.83	-0.33	43.61
CCSDPPA[e]	39.93	0.49	0.82	-0.33	40.91
EOM-CCSD (CI-like)[b]	39.11	0.48	0.81	-0.31	40.09
EOM-CCSD (Quadratic)[b]	39.11	0.48	0.81	-0.31	40.09
Experiment[e]					42.94±0.04

[a] At the equilibrium internuclear separation r = 1.40 a.u. [156], using and [14s,6p,2d] uncontracted basis set [124].

[b] The present work.

[d] V. J. Galasso, [121]

[d] Vahtras *et al.*, [134].

[e] Oddershede *et al.*, [124]

[e] J. R. Beckett, [157].

For the entire collection of molecules the FC contribution shows the largest variation with the inclusion of electron correlation effects using various levels of theory. The electron correlation effects are significant for SD and PSO contributions of HF, CO and N_2 couplings and less important for CH_4 and H_2O couplings.

Table 5.14. Nuclear spin-spin coupling constant of $H^{19}F$, $^1J(H^{19}F)$, in Hz[a].

Method	FC	SD	PSO	DSO	Total
CPHF [b]	467.5	-12.4	119.4	-0.1	654.1
HRPA [c]	419.9	-6.4	164.9	***	578.4
MBPT(2)[d]	390.7	-17.5	195.1	1.7	570.0
SOPPA[c]	338.3	-1.0	195.7	***	532.9
CCSDPPA[c]	329.4	-0.6	195.7	***	524.4
EOM-CCSD (CI-like)[b]	338.3	-1.0	189.1	0.0	526.4
EOM-CCSD (Quadratic)[b]	337.0	-1.0	189.5	0.0	525.5
Experiment[e]					529±23

[a] At the equilibrium internuclear separation r = 1.7328 a.u.[156], using [8s,3p,1d]/(6s,3p,1d) and [13s,8p,4d]/(9s,6p,4d) basis sets for hydrogen and Fluorine respectively [125].

[b] The present work.

[c] Geertsen *et al.*, [125].

[d] Finite field second-order perturbation theory (MBPT(2)) results. A [7s,4p,2d]/(5s2p) basis set has been used to calculate the FC contact contribution. The SD results were obtained by using the 6–31G* basis set, and the PSO and DSO results were obtained by using the 6–31G** basis set. Fukui *et al.* [117].

[e] Muenter *et al.*, [158].

There is no significant change in the DSO contribution with correlation effects. It is seen from the collection of Tables 5.13−5.18, for a given basis set the FC, SD and PSO contributions are more or less converged with respect to correlation effects for methods which go beyond second-order.

Table 5.15. Nuclear spin-spin coupling constant of CO, $^1J(^{13}C^{17}O)$, in Hz[a].

Method	FC	SD	PSO	DSO	Total
CPHF[b]	-8.1	-9.3	12.3	0.1	-5.1
HRPA[c]	1.5	-2.9	11.9	***	10.6
SOPPA[c]	7.3	-4.0	14.8	***	18.1
MCLRT[d]	6.7	-4.3	13.7	0.09	16.1
EOM-CCSD (CI-like)[b]	7.0	-4.5	13.0	0.1	15.6
EOM-CCSD (Quadratic)[b]	6.9	-4.8	13.0	0.1	15.2
Experiment[e]					16.4±0.1

[a] At the equilibrium internuclear separation r = 2.132 a.u. [156], using [12s,7p,3d]/(8s,4p,3d) basis set [123].
[b] The present work.
[c] Geertsen *et al.*, [123].
[d] Vahtras *et al.*, [134].
[e] Wasylishen *et al.*, [159].

Consistent with the previous observations using several other molecules, the quadratic effects are small for this selection of molecules as well and we only consider the CI-like approximation results to compare with the experiment. However, there are occasional exceptions, for example $^1J(^{13}C^{17}O)$ in CO and $^1J(^{13}C^{19}F)$ in CH_3F (Table 5.9). As we can see the absolute CPHF results tend to overestimate the corresponding experimental coupling constants.

Table 5.16. Nuclear spin-spin coupling constant of N_2, $^1J(^{14}N^{15}N)$, in Hz[a].

Method	FC	SD	PSO	DSO	Total
CPHF[b]	-7.7	-8.1	0.5	0.03	-15.3
HRPA[c]	-0.6	-1.4	2.5	***	0.5
SOPPA[c]	0.5	-1.6	3.3	***	2.2
MCLRT[d]	-0.2	-1.9	2.8	0.07	0.8
EOM-CCSD (CI-like)[b]	0.3	-1.7	2.7	0.02	1.3
EOM-CCSD (CI-like)[b]	0.3	-1.8	2.7	0.02	1.2
Experiment[e]					1.8±0.1

[a] At the equilibrium internuclear separation r = 2.068 a.u. [156], using [12s,7p,3d]/(8s,4p,3d) basis set [123].
[b] The present work.
[c] Geertsen *et al.*, [123].
[d] Vahtras *et al.*, [134].
[e] Friedrich *et al.*, [160].

At this point it is interesting to compare the HRPA results of B_2H_6 (Table 5.10), HF and CO with respective experimental results. In contrast to the HRPA results of HF and CO in the case of B_2H_6 the HRPA results are in quantitative agreement with experiment. Inclusion of electron correlation effects by HRPA or MBPT(2) improves the CPHF results but for difficult cases like HF and CO, methods which go beyond HRPA or MBPT(2) are required for quantitative accuracy.

Table 5.17. Nuclear spin-spin coupling constant of H_2O, $^1J(^{17}O^1H)$ and $^1J(^1H^1H)$, in Hz[a].

		FC	SD	PSO	DSO	Total
$^1J(OH)$	CPHF[b]	-84.81	0.39	-12.25	-0.07	-96.74
	MBPT(2)[c]	-64.61	0.52	-10.51	-0.17	-76.53
	SOPPA[d]	-65.24	-0.07	-11.15	-0.07	-76.53
	EOM-CCSD (CI-like)[b]	-65.34	-0.18	-11.26	-0.08	-76.88
	EOM-CCSD (quadratic)[b]	-65.40	-0.18	-11.28	-0.08	-76.94
	Experiment[e]					-73.5
$^1J(HH)$	CPHF[b]	-24.99	1.46	8.12	-7.17	-22.58
	MBPT(2)[c]	-19.69	1.41	7.09	-7.09	-18.28
	SOPPA[d]	-13.53	1.05	7.85	-7.17	-11.80
	EOM-CCSD (CI-like)[b]	-12.72	1.07	8.05	-7.02	-10.61
	EOM-CCSD (Quadratic)[b]	-12.96	1.07	8.06	-7.02	-10.85
	Experiment[e]					-7.2

[a] At the geometry r(O-H) = 1.811095 a.u. and HÔH = 104.45° [122], using [5s,1p]/(3s,1p) and [11s,5p,1d]/(4s,3p,1d) basis sets for hydrogen and oxygen respectively [122].

[b] The present work.

[c] The FC results were obtained by the 6–311G** basis set. The SD results were obtained by using the 6–31G basis set and the PSO and DSO results were obtained by using the 6–31G** basis set. Reference 117.

[d] Geertsen *et al.*, [122].

[e] Holems *et al.*, [161] and Florin *et al.*, [162].

Table 5.18. Nuclear spin-spin coupling constant of CH_4, $J(^1H^{13}C)$ and $^2J(^1H^1H)$, in Hz[a].

		FC	SD	PSO	DSO	Total
	CPHF[b]	155.58	-0.23	1.39	0.25	156.99
	SOPPA[c]	126.62	-0.02	1.48	0.25	128.32
	CCSDPPA[c]	122.12	-0.01	1.50	0.25	123.87
$^1J(CH)$	MCLRT[d]	123.53	0.02	1.48	0.27	125.30
	EOM-CCSD (CI-like)[b]	119.39	0.04	1.47	-0.08	120.82
	EOM-CCSD (quadratic)[b]	120.05	0.04	1.47	-0.08	121.48
	Experiment[e]					120.78±0.05
	CPHF[b]	-27.63	0.43	3.63	-3.54	-27.11
	SOPPA[c]	-16.04	0.34	3.62	-3.54	-15.67
	CCSDPPA[c]	-14.70	0.33	3.60	-3.54	-14.31
$^2J(HH)$	MCLRT[d]	-15.73	0.35	3.59	-3.51	-15.30
	EOM-CCSD (CI-like)[b]	-13.95	0.33	3.56	-3.50	-13.56
	EOM-CCSD (Quadratic)[b]	-14.23	0.33	3.57	-3.50	-13.83
	Experiment[e]					12.564±0.004

[a] At the experimental equilibrium geometry r(C-H) = 2.051864 a.u. [163], using [15s,7p,4d]/(10s,5p,4d) and [9s,2p]/(6s,2p) basis sets for carbon and hydrogen respectively [125].

[b] The present work.

[c] Geertsen *et al.*, [125].

[d] Vahtras *et al.*, [134]

[e] Bennett *et al.*, [164] and Anet *et al.*, [165].

It can be seen from Tables 5.13, 5.14 and 5.18 that the CCSDPPA results are quite close to the EOM-CCSD results and the largest variation in $^1J(^{13}C^1H)$ of CH_4 is about 3 Hz. In some cases the total EOM-CCSD and CCSDPPA results are close but the individual contributions shows larger differences, for example the FC and PSO contribution to $^1J(^1H^{19}F)$ of HF. In Table 5.19, we have given the absolute percent deviation of EOM-CCSD CI-like, CCSDPPA, MCLRT and SOPPA results from experiment. The average percent deviations are also given and the coupling constants less than 10 Hz are neglected in the averaging. Within the limited results available for direct comparison, the EOM-CCSD results on the average show better agreement with experiment when compared with CCSDPPA and MCLRT and SOPPA results. The CCSDPPA and MCLRT results have average percent errors of 5% and 8% respectively and are competitive with the EOM-CCSD results which has average percent error of 4%. However, these assertions are based on a very limited set of data and must be used with caution.

Table 5.20 shows a direct comparison of the EOM-CCSD results with experiment. Mean absolute and absolute per cent errors are presented as measures of the accuracy of the EOM-CCSD results compared to experiment. For this purpose a selection of coupling constants for which unambiguous experimental results are available was chosen. Some of the experimental results are gas phase measurements and the others are measurements taken from a neat sample or sample dissolved in inert organic solvents.

Table 5.19. Absolute percent deviation of the EOM-CCSD, CCSDPPA, MCLRT and SOPPA results from experiment.

Coupling	EOM-CCSD	CCSDPPA	MCLRT	SOPPA
$^1J(^1H^1H)$	6.6	4.7	4.0	1.6
$^1J(^{19}F^1H)$	0.5	0.9	***	0.7
$^1J(^{17}O^{13}C)$	4.9	***	1.8	10.3
$^1J(^{15}N^{14}N)$	27.8	***	55.6	22.2
$^1J(^1H^{17}O)$	4.6	***	***	4.1
$^2J(^1H^1H)$	47.4	***	***	63.9
$^1J(^1H^{13}C)$	0.0	2.6	3.7	6.2
$^2J(^1H^1H)$	7.9	13.9	21.8	24.7
Average[a]	4.1	5.5	7.8	7.9

[a] Coupling constants less than 10 Hz are discarded in the averaging.

The QZP basis set results are selected for CH_3F, CH_3CN, C_2H_4 and CH_3NH_2 molecules. The basis sets used in HD, HF, CO, N_2, H_2O and CH_4 calculations have been optimized previously and we can assume that the EOM-CCSD results obtained from them are converged with respect to basis sets. In the mean absolute percent deviation, the spin-spin coupling constants less than 5 Hz are not included since for such small coupling constants the percent averages are meaningless.

5.4 Conclusions

The main purpose of the present investigation is to calibrate some routinely used basis sets when applied to NMR spin-spin coupling constant calculations within the EOM-CCSD model. We also focus on the effects of the quadratic contribution, and large non-contact contributions to certain coupling constants. Ultimately, the overall accuracy of the EOM-CCSD results in comparison to experiment and other well estabished correlated metods is considered.

In this respect, we report that the mean absolute percent deviations from experiment are 13.9, 8.4, 7.3 and 7.6 respectively, for DZP, TZP, Chipman and QZP basis sets. The corresponding quadratic EOM-CCSD deviations are 13.7, 7.7, 7.5 and 7.9 which shows that the quadratic results are usually very close to the CI-like results. We also notice that for the systems considered in this study, the magnitude of the quadratic contribution is quite stable as the basis set changes from DZP to larger and better quality basis sets. This is very useful information since for molecules where the quadratic contribution is significant, a reliable estimate may be obtained economically by using a smaller basis set such as DZP.

The FC contribution shows the largest variation with the change of basis sets, well-recognized trend in the literature. However, the overall convergence of the FC contribution as the basis set improves looks fairly smooth.

Table 5.20. Comparison of EOM-CCSD indirect nuclear spin-spin coupling constants with experiment, (in Hz)†.

Molecule	Coupling	EOM-CCSD	Exp.	Abs. Error	Abs. % Error
H_2	$^1J(^1H^2H)$	40.09	42.94±0.04	2.85	7
HF	$^1J(^{19}F^1H)$	526.4	529±23	2.6	1
CO	$^1J(^{13}C^{17}O)$	15.6	16.4±0.1	0.8	5
N_2	$^1J(^{14}N^{15}N)$	1.3	1.8±0.6	0.5	28
H_2O	$^1J(^1H^{17}O)$	-76.88	-73.5	3.38	5
	$^2J(^1H^1H)$	-10.61	-7.2	3.41	47
CH_4	$^1J(^{13}C^1H)$	120.82	120.78	0.04	0
	$^2J(^1H^1H)$	-13.56	±12.564±0.004	1.00	8
C_2H_4	$^1J(^{13}C^1H)$	146.83	156.4	9.57	6
	$^3J(^1H^1H)_{trans}$	15.71	19.1	3.39	18
	$^3J(^1H^1H)_{cis}$	10.20	11.6	1.40	14
	$^2J(^1H^1H)$	0.65	2.5	1.85	74
CH_3CN	$^1J(^{13}C^{15}N)$	-16.99	±17.5±0.4	0.51	3
	$^1J(^{13}C^1H)$	126.20	±136.0±0.2	9.8	7
	$^2J(^{13}C^{15}N)$	3.01	±3.0±0.4	0.01	0
	$^2J(^{13}C^1H)$	10.00	±10.0±0.2	0.00	0
	$^3J(^{15}N^1H)$	-1.23	±1.80±0.1	0.59	32
CH_3F	$^1J(^{13}C^{19}F)$	-169.56	-157.5±0.2	12.56	8
	$^2J(^1H^{19}F)$	46.8	46.36±0.1	0.44	1
CH_3NH_2	$^1J(^{13}C^1H)$	137.15	149.1±0.2	11.95	8
	$^1J(^{15}N^1H)$	-61.33	-65.0±0.2	3.67	6
	$^1J(^{13}C^1H)$	120.62	132.2±0.2	11.58	9
	$^2J(^{15}N^1H)$	0.93	-1.0±0.1	0.07	7

Chipman's basis set is especially designed to evaluate point properties at the nucleus, like the Fermi contact term, and it is seen that, indeed, our Chipman results compare best to experiment. Except for very few cases, the FC contribution is the largest in all the couplings in the selected set of molecules and is most sensitive to electron correlation. The other contributions are affected only slightly by electron correlation. We also found that the DSO term, and, to a slightly smaller extent, the SD contribution, show very little variation with the size of the basis set. The DZP basis set seems to do the job. This is very fortunate, because the integrals for the DSO contribution are very costly to evaluate, while on the other hand there are six perturbations per nucleus for the SD term and this term is costly for this reason. The PSO contributions shows moderate variations with the basis set. We note that a TZP basis set is more suitable for the PSO contribution than the Chipman basis set. Let us mention here, that, in general, solving for the perturbed amplitudes is the rate determining step in the calculation of spin-spin coupling constants, and therefore it is advantageous to tailor the basis set to the particular property of interest, since the evaluation and transformation of integrals as well as the ground state CCSD calculation are only minor steps in the calculation. In our opinion there are no objections to using different basis sets for different contributions to the overall spin-spin coupling constants, since each of the components converges smoothly.

There are no well established criteria to identify coupling constants having large non-contact contributions beforehand. We have observed several qualitative trends, some of which are well known in the literature. The hydrogen-hydrogen spin-spin coupling constants have consistently large DSO contributions. A simple explanation for this behavior can be given based on the form of the DSO operator derived in chapter 1. The DSO contribution is proportional to the product of two gyromagnetic ratios of the coupled nuclei. Lighter atoms such as H have large gyromagnetic ratios and, as a consequence of that, also have larger DSO contributions. Coupling constants which involve multiply bonded atoms usually have large non-contact contributions. Fluorine is a special case and one-bond coupling constants of Fluorine to other atoms often seem to have large non-contact contributions, in particular large PSO contributions. The FC contribution is usually the largest contribution to the carbon-hydrogen coupling constants in organic molecules and the other contributions are less important. This behavior is well-known in the literature and extremely useful in the practical applications of high-level correlated methods such as EOM-CCSD since the FC is the least expensive term to evaluate. However, these qualitative assertions must always be used with extreme caution and further research is required to identify the mechanisms governing the coupling interactions.

The ${}^{1}J({}^{13}C{}^{19}F)$ and ${}^{1}J({}^{13}C{}^{15}N)$, ${}^{1}J({}^{1}H{}^{19}F)$, ${}^{1}J({}^{13}C{}^{17}O)$ and ${}^{1}J({}^{14}N{}^{15}N)$ coupling constants of CH_3F and CH_3CN, HF, CO, and N_2 molecules have been identified before as difficult cases in the literature [105]. The EOM-CCSD results for the respective coupling constants, −169.56, −16.99, 525.5, 15.2 and 1.2 are in remarkable agreement with the experimental results, −157.5±0.2, ±17.5±0.4, 529±23, 16.4±0.1 and 1.8±0.1 respectively. These coupling constants are special cases in terms of having large non-contact contributions.

In conclusion, we consider the overall quality of the EOM-CCSD results compared to experiment; refer to Table 5.20. The mean absolute and mean absolute percent error of the EOM–CCSD results compared to experiment are 3.5 Hz and 7% respectively. The maximum absolute error of the EOM-CCSD results is about 12 Hz. The mean absolute percent error exaggerates the error in small coupling constants and is not a suitable measure of the quality of the EOM-CCSD results for such coupling constants. It seems that the mean absolute error gives a better representation of the accuracy of the EOM-CCSD results for small coupling constants.

CHAPTER 6
NMR SPECTRA OF ALKYL CARBOCATIONS

6.1 Introduction

Carbocations are the positive ions of carbon compounds. They are intermediates of organic reactions that start from non-ionic reactants and lead to nonionic products. The existence and role of carbocations in organic chemistry is now firmly established and well reviewed [166–168].

Carbocations can be "classical", having a trivalent sp^2 hybridized electron deficient carbon atom, or "non-classical", having pentacoordinated (or higher coordinated) carbon atoms. In condensed media, carbocations can exist as an equilibrium mixture of rapidly interconverting classical and non-classical forms. Kinetic and stereochemical evidence predominated in the early studies of carbocations. In the absence of direct evidence to support one form or the other, the stable form of the carbocations in condensed media often led to controversies [169, 170], for example, that concerning the structure of 2–norbornyl cation.

Direct observation of stable long-lived carbocations such as alkyl carbocations in solution remained as an elusive goal until 1962, when Olah [171] reported the first direct observation of carbocations in highly non-nucleophilic media, commonly known as "superacids". Olah's "superacids" scheme provides a means of isolating carbocations in condensed media at low temperatures as long-lived species and this facilitated the study of their structure and chemistry directly by physical and chemical methods. Various spectroscopic methods, such as ^1H and ^{13}C NMR, Raman, IR and X-ray photoelectron spectroscopy [172] have been used in the study of carbocations while NMR spectroscopy provide the most direct evidence for the existence of carbocations and, information about their structures. For example, Olah *et al.* [172] concluded from ^1H and ^{13}C NMR, Raman and X-ray photoelectron spectroscopic studies that the actual structure of 2–norbornyl cation is indeed non-classical.

However, application of NMR spectroscopy to resolve such controversies is not always problem free-either. Since NMR spectroscopy is a relatively slow physical method with a limited time scale, the differentiation of the non-classical form from a rapidly equilibrating mixture of classical forms based on NMR spectroscopy alone is a difficult task. As Olah pointed out in his Noble lecture [168], in such instances accurate theoretically calculated NMR chemical shifts and spin-spin coupling constants become invaluable.

In this chapter, we illustrate the application of the EOM-CCSD method to the calculation of NMR spin-spin coupling constants of alkyl carbocations. In this regard we have chosen two representative alkyl carbocations; ethyl cation and 2–norbornyl cation.

Even though our focus is on NMR spin-spin coupling constants, for completeness, we also consider NMR chemical shifts, energetics, and vibrational spectra of the two selected cations.

6.2 The Ethyl Carbocation ($C_2H_5^+$)

The ethyl carbocation ($C_2\ H_5^+$) is the prototypical primary alkyl carbocation. It is not stable enough to be observed directly in superacid media [173–176]. The ground state of the ethyl cation may take the non-classical form (Fig. 5.1, (I)) or the classical form (Fig. 5.1, (II)). Experimental results, alone, cannot support the existence of either of the two forms since the CD_3CH_2F-SbF_5 complex undergoes rapid intramolecular hydrogen (as well as carbon and fluorine) scrambling. However, the lower adiabatic than vertical ionization energy of the ethyl radical indicates the bridged form to be ~5–9.5 kcal/mol lower in energy in the gas phase [177, 178]. Numerous theoretical investigations at increasingly more sophisticated *ab initio* levels [178–180] predict the bridged isomer to be ~6–8 kcal/mol more stable than the "classical form". The latter serves as the transition structure (one imaginary frequency at correlated levels of theory) for hydrogen scrambling [178, 177, 179, 180].

Here, we employ the equation-of-motion coupled cluster singles and doubles (EOM-CCSD) method to present an initial prediction of the NMR spin-spin coupling constants for I and II. For the completeness, we also present GIAO-

MBPT(2) (gauge including atomic orbitals, second-order many body perturbation theory) NMR chemical shifts and vibrational frequencies for both forms. This calculation fills a void in the data for hydrogen bridged carbocations of the protonated ethylene type, and should assist experimental characterization of such species. For example, while the IR spectrum of the H-bridged-2–butyl cation has been observed in a low temperature SbF_5 matrix [181], rapid hydrogen scrambling precludes resolution of the NMR spectra.

Geometries of both the classical and the non-classical forms are determined at the coupled-cluster singles and doubles (CCSD) level using a triple-zeta plus double polarization (TZ2P) basis set comprised of (11s,6p,2d)/[5s,3p,2d] contraction for C and (5s,2p)/[3s,2p] contraction for H. The sp set has been taken from Dunning [138]. Polarization exponents have been optimized locally for several prototype molecules at the MBPT(4) level of correlation and are contracted following a recipe by Dunning [139]. Harmonic vibrational frequencies are calculated by finite differences of analytically computed gardients at CCSD/TZ2P level. We obtain CCSD(T) single point energies at the critical geometries of the "classical" transition structure and bridged form, using an augmented polarized valence triple-zeta (cc-pVTZ) basis set which comprised (10s,5p,2d,1f)/[4s,3p,2d,1f] contraction for C and (5s,2p,1d)/[3s,2p,1d] contraction for H [182]. Spherical harmonic gaussian basis functions have been used in all the geometry optimizations, vibrational frequency and single point energy calculations. The NMR chemical shift calculations use gauge-including atomic orbitals (GIAO) at the MBPT(2) level [183, 184], and QZ2P basis set for C [11s,7p,2d]/(6s,3p,2d) and for a H [7s,2p]/(4s,2p) (polarization exponents are 1.39 and 0.46) [143].

Table 6.21. Ground state equilibrium geometries of the "classical" transition structure and bridged forms of the $C_2H_5^+$ cation.[a]

	C_{2v} (I)	C_s(II)
C_1C_2	1.38023	1.41818
C_1H_b	1.30942	......
C_2H_1	......	1.07999
C_1H_2	1.08187	......
C_2H_2	......	1.10813
C_1H_3	......	1.08564
C_1H_4	......	1.08590
$H_2C_1H_2$	119.05099	......
$H_2C_2H_2$	......	98.61009
$H_2C_1H_b$	105.66690	......
$H_2C_2H_1$	......	113.33686
$H_1C_2C_1$	......	116.74616
$H_4C_1C_2$	......	122.96805
$H_3C_1C_2$	......	120.05834

[a] Bond lengths are in Angstroms and bond angles are in degrees.

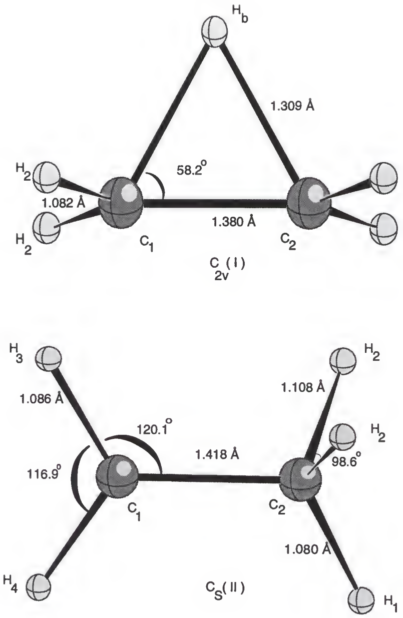
H_b
1.309 Å
58.2°
H_2
1.082 Å
H_2
C_1
1.380 Å
C_2
C_2v (I)
H_3
1.086 Å
120.1°
116.9°
1.418 Å
C_1
H_2
1.108 Å
H_2
98.6°
C_2
1.080 Å
H_4
C_S(II)
H_1

Figure 5.1

The NMR spin-spin coupling constants are calculated at EOM-CCSD level using two different Cartesian Gaussian basis sets to assess convergence. One of the basis set (basis-I) consists of (6s,1p)/[4s,1p] contraction for H and (10s,6p,1d)/[6s,3p,1d] contraction for C [140] and the other (basis-II) consist of (8s,3p)[5s,3p] contraction for H (polarization exponents are 2.292, 0.838 and 0.292) and (13s,8p,2d)/[8s,5p,2d] contraction for C (polarization exponents are 2.292 and 0.46) [143].

The CCSD/TZ2P bridged (Fig. 5.1, (I)) and "classical" (Fig. 5.1, (II)) geometries are given in Table 6.21, and depicted in Figure 5.1. The $H_2C_2H_2$ angle of only 98 degrees, the relatively long (1.108 Å) C_2H_2 and short $H_2...H_2$ (1.68 Å) separation might be said to characterize the three center-two electron bonding arising from the hyperconjugative interaction of the "vacant" C1(p) orbital with both hydrogens [185], as being somewhat similar to an H_2 complex of the classical vinyl cation, $H_2CCH^+...H_2$. Yet the $H_2..H_2$ distance has a much longer bond length than usual for H_2 (0.746 Å). A consequence of the structure is the unusually small $^1J(C_2H_2)$ coupling constant (109 Hz) computed for II (see Table 6.25).

These extremum points, I and II, on the $C_2H_5^+$ potential energy surface are characterized by the CCSD/TZ2P finite difference vibrational frequencies (Table 6.22). The perpendicular stretching vibration ($\omega_5(A_1)$) involving the bridging hydrogen in I is predicted to give rise to an intense signal at 2186 cm^{-1} in an unusual region of the IR spectrum.

Table 6.22. The CCSD/TZ2P vibrational frequencies (in cm^{-1}). Intensities are given in parenthesis (in km/mol)[a].

	C_{2v}(I)		C_s(II)
A_1	3170.8 (0.1)	A'	3253.7 (38.5)
	2186.2 (41.9)		3235.7 (2.6)
	1601.2 (6.8)		3140.0 (4.2)
	1153.1 (40.2)		2941.2 (15.2)
	1601.2 (6.8)		1569.6 (1.8)
A_2	3278.9 (0.0)		1483.5 (12.6)
	1278.2 (0.0)		1280.7 (67.2)
	1097.5 (0.0)		1215.3 (32.8)
B_1	3165.5 (29.4)		1095.7 (134.7)
	1507.5 (20.5)		813.6 (19.4)
	1307.5 (7.0)	A"	2944.4 (62.9)
	697.1 (148.7)		1425.3 (26.1)
B_2	3293.9 (59.3)		1289.4 (1.0)
	1499.3 (19.6)		759.6 (3.9)
	852.3 (0.0)		368.6i (39.0)

[a] At the CCSD/TZ2P optimized geometries.

A similar feature (at 2175 cm^{-1} has been observed for the 2–butyl cation [186, 187]. The transition structure for H-scrambling, II, $(\omega_{15}(A''))$ has a rather large imaginary frequency (369*i*), corresponding to a complex twisting motion [178–180]. Our $\Delta^{\ddagger}H_o$ (including zero-point vibration at 0 K) barrier predictions, 6.9 and 8.1 kcal/mol at CCSD and CCSD(T) respectively, at the CCSD/TZ2P geometries, are at the highest levels which have been reported to date.

As shown in Table 6.23, the computed chemical shifts of H_2 (7.89) and C_1 (163.97) of bridged $C_2H_5^+$, relative to TMS, may be compared with the ^1H and ^{13}C chemical shifts computed for ethylene, 5.21 and 133.60, respectively (the gas phase experimental C_2H_4 values are 5.08 and 133.88 [188]). The positive charge is responsible for the downfield shift of H_2 and C_1 of bridged $C_2H_5^+$ compared to those of C_2H_4. The chemical shift (-0.02) of bridging hydrogen, H_b in I, is unexceptional and the charges on such bridging H's are similar to those of the other hydrogens [189]. However, this behavior can be rationalized by the fact that the induced magnetic field produced at the bridged proton by a slightly deformed π electron cloud is opposed to the external magnetic field. Hence, the resultant magnetic field felt by the bridged proton is lowered resulting an upfield shift for the bridged proton in the NMR spectrum. This is not an uncommon situation as it occurs in the NMR spectrum of annulenes [190]. Table 6.23 also summarizes the average ^1H and ^{13}C chemical shifts, which might result from complete scrambling, assuming I or II were the only populated forms. These quite different values demonstrate how easily they could be distinguished, in principle. Of course, the individual H and C chemical shifts computed for II vary considerably.

Table 6.23. The GIAO-MBPT(2)/QZ2P NMR chemical shifts (δ, in ppm) of the "classical" transition structure and bridged form of the $C_2H_5{}^+$ cation[a].

	C_{2v} (I)	Average (I)	C_s(II)[b]	Average (II)
C_1	163.97	163.97	361.17	217.57
C_2	……		73.96	
H_b (H_1)	-0.02	6.31	5.16	8.54
H_2	7.89		5.26	
H_3	……		13.56	
H_4	……		13.47	

[a] The reported chemical shifts are relative to TMS as the reference. The ^{13}C and ^{1}H shielding for ethylene is 133.60 ppm (MBPT(2)/QZ2P) and 5.21 ppm (MBPT(2)/QZ2P), respectively.

The chemical shifts computed for C_1 (the carbenium carbon) as well as the attached hydrogens, H_3 and H_4 of the "classical" ethyl cation (Table II), are all highly deshielded, consistent with experimental observations, e.g. for the 2–propyl cation [173].

Tables 6.24 and 6.25 shows the EOM-CCSD NMR spin-spin coupling constants of bridged and "classical" form obtained by using basis-I and basis-II. In the following discussion, we use basis-II results since they appear to be converged.

Table 6.24. The NMR spin-spin coupling constants of $C_2H_5^+$ for the bridged form (in Hz)[a].

Coupling	Basis	FC	SD	PSO	DSO	Total
$^1J(C_1H_b)$	basis-I	10.19	-0.05	2.07	0.58	12.79
	basis-II	10.23	-0.08	2.30	0.56	13.01
$^2J(H_BH_2)$	basis-I	-8.78	0.06	1.45	-1.67	-.8.56
	basis-II	-8.58	0.10	1.83	-1.70	-8.52
$^1J(C_1H_2)$	basis-I	168.20	0.43	-0.92	0.35	168.06
	basis-II	166.64	0.45	-0.75	0.32	166.66
$^3J(H_2H_2)_{cis}$	basis-I	8.10	-0.02	0.57	-1.05	7.60
	basis-II	8.31	0.00	0.77	-1.06	8.02
$^3J(H_2H_2)_{trans}$	basis-I	17.58	0.05	1.85	-3.50	15.98
	basis-II	17.72	0.05	3.04	-3.53	17.28

[a] EOM-CCSD NMR spin-spin coupling constants at CCSD/TZ2P optimized geometries.

The EOM-CCSD spin-spin coupling constants show that $^1J(C_1H_b) = 13$ Hz for bridged form. This is an unusually small value as ($^1J(CH)$'s in hydrocarbons generally range between 125 and 250 Hz, with the ethylene value being 156 Hz [147]; the 13 Hz coupling constant should provide a fingerprint for such 1,2–hydrogen bridged non-classical cations.

Table 6.25. The NMR spin-spin coupling constants of $C_2H_5^+$ for the "classical" transition structure (in Hz[a]).

Coupling	Basis	FC	SD	PSO	DSO	Total
$^1J(C_1H_3)$	basis-I	163.57	1.05	-3.26	0.14	161.50
	basis-II	162.87	1.04	-3.17	0.10	160.84
$^1J(C_1H_4)$	basis-I	162.30	1.14	-3.20	0.13	160.37
	basis-II	161.49	1.15	-3.09	0.09	159.64
$^1J(C_2H_1)$	basis-I	153.14	0.14	0.11	0.47	153.86
	basis-II	151.43	0.18	0.38	0.45	152.44
$^1J(C_2H_2)$	basis-I	108.26	0.04	0.78	0.54	109.62
	basis-II	107.19	0.05	1.17	0.51	108.92
$^3J(H_1H_4)$	basis-I	9.42	0.09	0.60	-0.95	9.16
	basis-II	9.65	0.12	0.76	-0.97	9.56
$^3J(H_1H_3)$	basis-I	15.87	0.01	1.73	-3.37	14.24
	basis-II	15.89	0.00	2.85	-3.40	15.34
$^3J(H_2H_3)$	basis-I	-1.86	0.14	0.73	-1.03	-2.02
	basis-II	-1.85	0.14	0.92	-1.05	-1.84
$^3J(H_2H_4)$	basis-I	-0.09	0.08	1.60	-2.82	-1.23
	basis-II	-0.02	0.09	2.51	-2.85	-0.27

[a] EOM-CCSD NMR spin-spin coupling constants at CCSD/TZ2P optimized geometries.

Unsupported μ-H-bridged (C-H-C) carbocations are known that have consistent $^1J(CH)$'s, in the 35–40 Hz range [186, 187, 191, 192], although lower values have been measured in more weakly bonded unsymmetrical systems [193]. The $^1J(CH)$ = 166.7 Hz computed for non-bridging H's of I, is 10.7 Hz larger than the ethylene value. As the FC component dominates the coupling, the bond polarization which increases $^1J(CH)$ exceeds the lowering effect caused by the hybridization change from sp^2 to sp^3. Olah *et al.* [175] observed that SbF_5 complexation of CH_3CH_2F led to a about 12 Hzincrease in the alpha $^1J(CH)$ to 162 Hz, but only to slight deshielding of the alpha ^{13}C and ^1H chemical shifts. Comparing these results with our predictions of the "classical" ethyl cation (II) magnetic properties (Tables 6.23 and 6.25), the chemical shifts computed for C_1 (the carbenium carbon) as well as the attached hydrogens, H_3 and H_4, are all highly deshielded, consistent with experimental observations, e.g. for the 2–propyl cation [173]. Also, the computed $^1J(C_1H_3)$ and $^1J(C_1H_4)$ values are both near 160 Hz. It is apparent, though, that the CH_3CH_2F-SbF_5 complex has little bridged carbocation ion character.

6.3 2–Nobornyl Cation ($C_7H_{11}^+$)

The structure of the 2–norbornyl cation (Fig. 5.2) has been the focal point of one of the longest lasting controversies in physical organic chemistry [194, 195]. A vast amount of experimental effort over the last 40 years has attempted to establish clearly whether the non-classical structure (Fig. 5.2, (IV)) or the classical structure (Fig. 5.2, (III)) is more stable (or exists?) and whether one or the other form can be rationalized best by existing experimental data. The structure of the 2–norbornyl cation has been studied by a variety of spectroscopic techniques such as ^{1}H and ^{13}C NMR [196, 172, 6], Raman [197], and X-ray photoelectron spectroscopy [172], while NMR spectroscopy has been the more prominent technique. The isotopic perturbation of resonance technique developed by Saunders and co-workers have been applied to 2–norbornyl cation [198, 199]. Yannoni and Myher have studied the 2–norbornyl cation by solid-state ^{13}C NMR spectroscopy using cross polarization magic angle spinning techniques at very low temperatures [200]. The experimental evidence favors the symmetric bridged structure (non-classical) for the 2–norbornyl cation in non-nucleophlic media, where direct spectroscopic measurements can be made. Recently, Schleyer and Chandrasekhar concluded that the 2–norbornyl cation has an extra stabilization of 6 ± 1 kcal/mol due to bridging in stable ion media [201]. This stabilization might be due to some factors other than bridging, however, as Schleyer and Chandrasekhar pointed out that the experimental evidence favoring the bridged structure of the 2–norbornyl cation is now overwhelming. A number of theoretical studies of the energetics of various structures of the 2–norbornyl cation has been carried out. The MINDO/3 calculations [202] with full geometry optimizations predicted the classical structure to be 1.9 kcal/mol more stable than the non-classical structure. Acoording to MINDO/3 results, the non-classical structure is not a local minimum but rather a transition state for the degenerate rearrangement of the two classical structures. Goetz *et al.* [203] empolyed minmal STO-3G and split-valence 4–31G basis sets in Hartree-Fock (HF) calculations of 2–norbornyl structures.

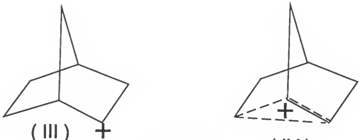

(III) (IV)

Figure 5.2

The non-classical ion was 5.2 kcal/mol higher in energy for the STO-3G basis and partially optimized geometries, while in the 4–31G basis the difference is 0.2 kcal/mol. However, these authors argue that in the gas phase, the non-classical form is more stable after approximate corrections for basis set extension and electron correlation effects. Wenke and Lenoir [204] predicted the non-classical ion to be 5.9 kcal/mol higher in energy based on minimal basis set HF calculations at the MINDO/3 geometries. Köhler and Lischka [205] considered effects of electron correlation and of having polarization functions on carbon atoms. According to their double zeta (DZ) basis set HF results at the STO-3G geometries, the classical form was predicted to be 0.8 kcal/mol more stable. Inclusion of polarization functions on the carbons near the positions of the formal positive charge preferentially stabilized the non-classical ion, yielding an energy 2 kcal/mol lower than the classical one. Electron correlation effects at the CEPA (coupled-electron-pair approximation) level further stabilize the non-classical cation, placing it 13 kcal/mol lower in energy than the classical structure. Goddard and coworkers [206] have employed near-double-zeta quality basis set in a *full*, rigorous HF geometry optimization of the 2–norbornyl cation. They have concluded that the classical form is 0.2 kcal/mol more stable than the non-classical form at the SCF/4–21G leval while at the SCF/DZ level, the classical form is 1.0 kcal/mol more stable. When the carbon 4–21G basis set is augmented with d polarization functions (4–21G + d), the non-classical form becomes 0.2 kcal/mol more stable than the classical form.

As previous theoretical investigations suggest, for conclusive results electron correlation effects and basis sets of at least double-zeta-plus-polarization quality should be incorporated in geometry optimizations and energy calculations. Here, we employ double-zeta-plus-polarization (DZP) basis sets combined with MBPT(2) level of theory in geometry optimizations and CCSD level of theory in single point energy calculations. Much-needed theoretical support for the experimental NMR assignments of 2–norbornyl cation has not been available as yet.

In this work, we also provide the NMR chemical shifts and spin-spin coupling constants based on the GIAO-MBPT(2) and EOM-CCSD methods for possible structures of the 2–norbornyl cation.

Geometries are determined at the the SCF and MBPT(2) level using a DZP basis set comprised of (9s,5p,1d)/[4s,2p,1d] contraction for C and (4s,1p)/[2s,1p] contraction for H. The sp set has been taken from Dunning [138]. Polarization exponents have been optimized locally at the correlated level [141]. The NMR chemical shifts and spin-spin coupling constants are calculated by employing a DZP basis set on C atoms and a double zeta (DZ) basis set on hydrogens. The DZ basis set on H comprised of the (4s)/[2p] contraction of the Dunning (4s) primitive set [138]. Spherical harmonic Gaussian basis functions have been used in geometry optimizations, vibrational frequency, and single-point energy calculations while Cartesian Gaussian basis functions have been used in NMR chemical shift and spin-spin coupling constant calculations.

The MBPT(2)/DZP geometry of the non-classical form is depicted in Fig. 5.3; it is a true minimum on the potential energy surface with the C_s abelian symmetry as was shown by the SCF/DZP vibrational frequency calculations. Any attempt to obtain the SCF/DZP or MBPT(2)/DZP optimized geometries for the classical form from a starting geometry which resembles the classical form with the

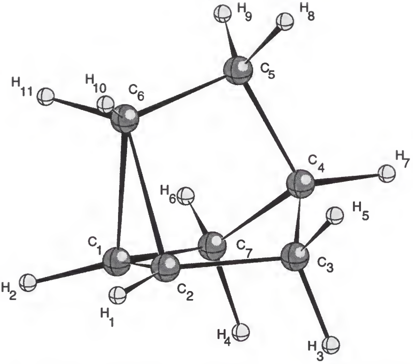

Figure 5.3. $r(C_6C_5)$ = 1.53040 Å, $r(C_5C_4)$ = 1.53942 Å, $r(C_4H_7)$ = 1.09389 Å, $r(C_5H_8)$ = 1.09518 Å, $r(C_1H_{10})$ = 1.09887 Å, $r(C_1C_6)$ = 1.83263 Å, $r(C_1H_2)$ = 1.09035 Å, $r(C_3C_4)$ = 1.54120 Å, $r(C_7H_6)$ = 1.09526 Å, $r(C_7H_4)$ = 1.10058 Å, $\alpha(C_6C_5C_4)$ = 100.83496°, $\alpha(C_5C_4H_7)$ = 115. 72723°, $\alpha(C_4C_5H_8)$ = 112.31048°, $\alpha(C_5C_6H_{10})$ = 117.51181°, $\alpha(C_2C_6H_5)$ = 102.83263°, $\alpha(C_6C_1H_2)$ = 110.16942°, $\alpha(C_7C_4H_7)$ = 115.62391°, $\alpha(C_4C_7H_6)$ = 114.51134°, $\alpha(C_4C_7H_4)$ = 112.43223, $\tau(H_8C_5C_4H_7)$ = 61.74691°, $\tau(H_{10}C_6C_5C_4)$ = 116.12871°, $\tau(C_2C_6C_5C_4)$ = 23.10284°, $\tau(H_2C_1C_6C_5)$ = 145.63273°, $\tau(C_{13}C_4C_3C_2)$ = 120.39001°, $\tau(H_6C_7C_4H_7)$ = 68.57200°, $\tau(H_4C_7C_4H_7)$ = 56.86067°

C_1 abelian symmetry fails since the final optimized geometry corresponds to the non-classical structure. This shows that there is no energy barrier at the SCF/DZP or MBPT(2)/DZP level between the non-classical and the classical forms of the 2–norbornyl cations and hence, at least at this level of theory, the stable structure is exclusively non-classical. This is contrary to what previously has been reported in the literature [206]. However, the existence of the classical form as a stationary point in previous theoretical calculations may be an artifact due to the inadequacy of not having polarization functions in the basis sets employed. Further support for this argument comes from the fact that we have been able to characterize both the classical and non-classical structures by SCF/STO-3G and SCF/DZ geometry optimizations. In the following NMR calculations, we only consider the non-classical structure with the MBPT(2)/DZP optimized geoemtrical parameters.

Tables 6.26 and 6.27 present the GIAO-MBPT(2) NMR chemical shift and EOM-CCSD NMR spin-spin coupling constants of the non–classical 2–norbornyl cation. The calculated NMR chemical shifts of the non-classical form are in good agreement with the experimentally measured NMR chemical shifts of the 2–norbornyl cation at -159 °C temperature in $SbF_5/SO_2ClF/SO_2F_2$ solution [6]. Observation of the C_1 and C_2 carbons ^{13}C chemical shifts about 125 and C_6 chemical shift about 20–30 supports a symmetrical bridged structure for the 2–norbornyl cation since five (or higher coordinate) carbons usually shows sheilded (upfield) ^{13}C chemical shifts [207–209].

Table 6.26. The GIAO-MBPT(2) NMR chemical shifts (δ, in ppm) of the non-classical 2–norbornyl cation[a].

	Chemical shift	Experiment[b]
C_6	22.92	21.2
C_5	24.81	20.4
C_4	40.44	37.7
C_1, C_2	121.79	124.5
C_3, C_7	40.97	36.3
H_7	2.95	2.82
H_8, H_9	1.22	1.37
H_{10}, H_{11}	2.48	3.17
H_1, H_2	6.34	6.75
H_5, H_6	2.07	2.13
H_3, H_4	2.03	2.13

[a] The GIAO-MBPT(2) NMR chemical shifts are calculated at the MBPT(2)/DZP optimized geometry employing a DZP basis on C atoms and a DZ basis on hydrogen atoms. The reported chemical shifts are relative to TMS as the reference.

[b] G. A. Olah *et al.*, [6].

Table 6.27. The EOM-CCSD NMR spin-spin coupling constants of the non-classical 2–norbornyl cation (in Hz)[a].

Coupling	FC	Average	Exp.[b]
$^1J(C_2H_1)$, $^1J(C_1H_2)$	175.4		187.7
$^1J(C_6H_{11})$, $^1J(C_6H_{10})$	138.4		147.1±5
$^1J(C_7H_6)$, $^1J(C_3H_5)$	133.9		131.2
$^1J(C_7H_4)$, ^{1} $J(C_3H_3)$	125.2		
$^1J(C_5H_9)$, $^1J(C_5H_8)$	130.6		153.2±5
$^1J(C_4H_7)$	144.5		150.9
$J(H_1H_7)$, $J(H_2H_7)$	0.4	0.4	0.4
$J(H_{11}H_7)$, $J(H_{10}H_7)$	0.0		
$J(H_6H_7)$, $J(H_5H_7)$	1.0	1.6	1.6
$J(H_4H_7)$, $J(H_3H_7)$	2.2		
$J(H_2H_6)$, $J(H_1H_5)$	1.9	0.9	1.4
$J(H_2H_4)$, $J(H_1H_3)$	0.3		
$J(H_{11}H_6)$, $J(H_{10}H_5)$	-0.3		
$J(H_{11}H_4)$, $J(H_{10}H_3)$	0.9		
$J(H_{11}H_3)$, $J(H_{10}H_4)$	5.4		
$J(H_{11}H_5)$, $J(H_{10}H_6)$	0.2		
$J(H_2H_5)$, $J(H_1H_6)$	-0.1		
$J(H_2H_3)$, $J(H_1H_4)$	-0.8		
$^1J(C_5C_6)$	37.7		
$^1J(C_5C_4)$	28.7		
$^1J(C_4C_7)$, $^1J(C_4C_3)$	30.3		
$^1J(C_1C_7)$, $^1J(C_2C_{C3})$	35.2		

Table 6.27. (Continued) The EOM-CCSD NMR spin-spin coupling constants of the non-classical 2–norbornyl cation (in Hz)[a].

Coupling	FC	Average	Exp.[b]
$^1J(C_1C_2)$,	41.83		
$^1J(C_1C_6)$, $^1J(C_2C_6)$	-5.6		

[a] The EOM-CCSD NMR spin-spin coupling constants at the MBPT(2)/DZP optimized geometries employing a DZP basis on C atoms and a DZ basis on H atoms.

[b] G. A. Olah *et al.*, [6].

The absence of highly deshielded (downfield) carbon atoms, a characteristic of the trivalent sp^2 carbon atoms, for example t-butyl cation, cyclopentyl cation [210] also supports the bridged nature of the 2–norbornyl cation. At higher temperatures, the proton NMR is not well resolved due to the fast 2,3 hydrogen, 6, 1, 2 hydrogen and Wagner-Meerwein ($\sigma-$bond shift) shifts [211]. Yannoni and Myhre have obtained magic angle cross polarization ^{13}C NMR of the ^{13}C-enriched 2–norbornyl cation in SbF_5 solid matrix at -159 °C temperature and their solid state chemical shifts are similar to Olah *et al.* low temperature liquid phase results [6].

As we have seen in chapter 3, the significance of non-contact contributions for the NMR spin-spin coupling constants of hydrocarbons is negligible. We take advantage of this fact and only consider the FC contribution for NMR spin-spin coupling constants of 2–norbornyl cation. Calculation of non-contact contributions for medium-sized molecules such as 2–norbornyl cation demands extensive use of computer resources and is not very practical. As we can see from Table 6.27, for theoretically calculated FC only NMR spin-spin constants of the non-classical 2–norbornyl cation is in good agreement with the experimentally measured NMR spin-spin coupling constants of the 2–norbornyl cation at -159 ^{o}C temperature in $SbF_5/SO_2ClF/SO_2F_2$ [6]. This further supports Olah's claim that the experimentally measured NMR spectrum corresponds to the non-classical form of the 2–norbornyl cation. Consequently, the symmetric bridged form of the 2–norbonyl cation exists as a long lived species in superacid medium at low temperatures. The $^1J(^{13}C^{13}C)$ coupling constants are usually in the range of +10-40 Hz. However, in Table 6.27, the $^1J(^{13}C_6{}^{13}C_1)$ and $^1J(^{13}C_6{}^{13}C_2)$; coupling constants of pentacoordinated bridged carbon atom (C_6) to bridgehead carbon atoms (C_1 and C_2) is negative and have a smaller magnitude compared to a typical value for $^1J(^{13}C^{13}C)$ coupling constants. This can be used as a fingerprint to identify penta (or higher) coordinated bridged carbon structures.

At this point it is important to note that a rapidly interconverting mixture of classical carbocations via the Wagner-Meerwein ($\sigma-$bond shift) shifts can give a NMR spectrum which is indistinguishable from that of the non-classical ion [195]. Spectral line shapes and changes in peak positions with the temperature may be used to establish that a given NMR is responsible for a rapidly equilibrating mixture or single long lived species. Other physical methods such as X-ray photoelectron and Raman spectroscopy can be helpful in this task, too. Broad and temperature dependent NMR spectra indicative of rapidly equilibrating mixtures. For example, as Olah *et al.* [6] noted that ^{1}H NMR of 2–norbornyl cation shows a single peak for all the protons due to rapid 2,3 hydrogen, 6,1,2 hydrogen and Wagner-Meerwein shifts. Cooling the solution to -100 °C results in three peaks at δ 4.92 (4 protons), 2.82 (1 proton) and 1.93 (6 protons), indicating that the 2,3 hydrogen shift is fully frozen, whereas the 6,1,2 and Wagner-Meerwein shifts are still fast on the NMR time scale. Further cooling to -158 °C results in significant changes in the spectrum; and the corresponding chemical shifts and spin-spin coupling constants are given in Tables 6.26 and 6.27. The observation of comparably narrow widths at this temperature led Olah *et al.* [6] to argue that either the 6,1,2 hydrogen and Wagner-Meerwein shifts are completely frozen and the 2–norbornyl cation has a non-classical structure or the 6,1,2 shifts are frozen and the Wagner-Meerwein shifts are still fast on the NMR time scale with a very shallow activation barrier. Yannoni *et al.* [200] have obtained magic angle cross polarization ^{13}C NMR of the ^{13}C enriched 2–norbornyl cation in SbF_5 solid matrix -190 °C and their solid state chemical shifts are similar to Olah *et al.* [6] liquid phase NMR results at -158 °C. Another study by the same authours have obtained the solid state ^{13}C NMR spectrum at -269 °C with no change in the relative peak positions, indicating that the barrier for a rapid Wagner-Meerwein-like shift, if it still exists must be less than 0.2 kcal/mol. As a consequence of that Olah *et al.* [6] suggests that if such a process occurs, it must be exclusively between unsymmetrical non-classical structures equlibrating with the symmetrical non-classical structure and open classical form cannot be involved as populated species.

In the case of theoretical NMR spectroscopy, the structure responsible for the calculated NMR spectrum is prior known. On the other hand, in the case of experimental NMR spectroscopy, the molecular structure responsible for the NMR spectrum has to be inferred from the measured spectrum.

The agreement shown in Tables 6.26 and 6.27 of the calculated NMR parameters of the non-classical 2–norbornyl cation with the experimentally measured NMR parameters at -158 °C unambiguously rule out the possible existence of the classical structure. This is a perfect illustration of employing calculated NMR parameters for conclusive correlations of the measured spectrum with the molecular structure. However, at this point our calculated results cannot confirm or rule out the possible existence of unsymmetrical non-classical structures equilibrating with the symmetrical non-classical structures.

6.4 Conclusions

In this chapter, we have demonstrated the application of theoretically calculated EOM-CCSD NMR spin-spin coupling constants in the study of structures of alkyl carbocations.

The first application we have considered here was the structure and the NMR spectra of the ethyl carbocation. There are two possible structures for the ethyl carbocation, the classical form with a trivalent carbon atom or the non-classical form with three center two electron bonds. Due to the rapid intermolecular hydrogen scrambling, the ethyl cation cannot be isolated in superacid medium for direct observation by physical methods. Consequently, predictive theoretical calculations are required to study the energetics, vibrational and NMR spectra. In the gas phase, the non-classical form was shown to be about 5–6 kcal/mol more stable than the classical form at the CCSD(T)/TZ2P level. The non-classical structure is a true minimum on the potential energy surface and the classical structure is the transition state for proton scrambling. In this research, we have provided theoretically predicted NMR spectra for the classical and non-classical structures. The $^{1}J(CH_b)$ in the non-classical structure is predicted to be 13 Hz and, serves as a fingerprint for the hydrogen bridged structures.

In the second application, we have studied the structure and the NMR spectra of the 2–norbornyl cation. Based on the kinetic and stereochemical evidence, Brown argues [195] that the structure of the 2–norbornyl is an equlibrium mixture of rapidly interconverting classical structures with trivalent carbon atoms. Based on the NMR and X-ray photoelectron results, Olah [197, 194, 6, 168] and several other workers [200, 201] argue that the structure of 2–norbornyl cation is non-classical with a penta-coordinated carbon atom. We only find the non-classical structure at the MBPT(2)/DZP level of theory and it is a true minimum. In other words, there is no barrier between the classical and the non-classical form of the 2–norbornyl cation and the stable equlibrium structure is exclusively non-classical. This is quite contrary to the previously reported theoretical results. We have shown that the presence of a stationary point in the potential surface corresponding to the classical structure in previous theoretical calculations was an artifact resulting from the poor quality basis sets employed, and inadequate amount of electron correlation. The calculated NMR parametres are in good agreement with the experimentally measured NMR parameters for the 2–norbornyl cation at -159 °C in $SbF_5/SO_2ClF/SO_2F_2$ [6]. This will further support the conclusion made by Olah [6] from the NMR and X-ray photoelectron results that the structure of the 2–norbornyl cation exists in solution is non-classical. The negative and smaller magnitude of $^1J(^{13}C_6{}^{13}C_1)$ and $^1J(^{13}C_6{}^{13}C_2)$ in the non-classical structure may serve as a fingerprint for the penta- or higher coordinated carbon bridged structures.

Comparisons between computed and experimental NMR chemical shifts have become a powerful, ever more widely applied tool for structure elucidation [184, 186, 212], Accurate computation of NMR coupling constants [93, 213, 214], as illustrated here, and which can be obtained regardless the atoms involved, will greatly extend the applicability of such theoretical predictions.

CHAPTER 7
APPLICATION OF EOM-CCSD NMR SPIN-SPIN COUPLING CONSTANTS IN CONFORMATIONAL ANALYSIS

7.1 Introduction

The variation of vicinal NMR spin-spin coupling constants with the dihedral angle between coupled nuclei is a well-known phenomenon [215, 216]. Such variations are assumed to be described by *model* mathematical relations between the spin-spin coupling constants and dihedral angle ϕ of the coupled nuclei. Often these realtions have the form

$$^3J = Acos^2\phi + Bcos\phi + C \tag{7.221}$$

commonly known as "Karplus-like relations" [217, 215, 218, 219]. The basic assumption of "Karplus relations" given in Eqn. 7.221 is that the coupling constants depen predominantly dependent on the dihedral angle between the coupled nuclei. The existence of such relations is usually established by employing approximate theoretical methods to calculate NMR spin-spin coupling constants as a function of the dihedral angle [220–222]. More recently, X-ray crystallographic studies coupled with high resolution NMR measurements also support the existence of such qualitative relations [223–225]. In general, the coupling constants are intricate functions of the geometrical (bond lengths, angles) and electronic (electronegativities, formal charges) parameters of the molecule under consideration. As discussed in chapter 4, even at the *ab initio* Hartree-Fock level of theory, there are large error bars in the calculated NMR spin-spin coupling constants and relations similar to Eqn. 7.221 derived from results obtained from qualitative theoretical calculations must be used with caution. Instead, systematic investigations using quantitatively accurate theoretical methods are required to calculate the variation of the coupling constants as a function of molecular parameters to establish much improved correlations and also to understand the intrinsic factors which govern the coupling surface.

In spite of these potential fundamental problems, relations similar to that one given in Eqn. 7.221 have been used extensively in conformational studies; given the experimentaly measured ^3J and prior determined "Karplus-like relation" one can calculate the angle ϕ. For example, variation of $^3J(^1H^1H)$ and $^3J(^1H^1H)$ for H-C-C-H and H-N-C-H moieties with respective dihedral angles [226, 216] have been widely used in conformational analysis. In the latter case, variation of $^3J(^1H^1H)$ for the H-N-C-H moiety is particularly important since it can be used in the conformational studies of polypeptides. At present the most powerful means for studying the structures of polypeptides in solution is NMR spectroscopy, whose potential in static conformational analysis does not lag far behind the X-ray method. An outstanding merit of the NMR method is its ability to provide a deep insight into the dynamical aspects of the three-dimensional molecular structure and intra- and intermolecular interactions in solution. Application of "Karplus-like relations" coupled with high resolution multi-dimensional NMR spectroscopic measurements are begining to complement other types of investigations of polypeptide structures in solution [227–233]. Before we continue any further, there are several important points that need to be discussed on the application of this technique to conformational analysis.

First, one needs to establish values of A, B and C in the Karplus relation given in Eqn. 7.221. This is quite often done by studying model systems which can mimic the structures in question. For example, in the case of peptides, N-methylacetamide and alanine dipeptide are commonly used as model sytems, i.e. readily accessible small molecules. After the selection of the appropriate model system, it requires $^3J(^1H^1H)$ for the model system at different dihedral angles. Except for a few cases, individual conformers corresponding to different dihedral angels are inaccessible to direct measurment by NMR spectroscopy and one has to calculate, theoretically, $^3J(^1H^1H)$ values. This is where the selection of a small molecule as the model system is essential. Semiemperical (INDO) [220] and uncoupled Hartree-Fock methods [223] have been used for this purpose but as we discussed in chapter 4, correlation effects are essential for an accurate calculation of NMR spin-spin coupling constants. The main purpose of this study is to employ the newly developed EOM-CCSD method to calculate spin-spin coupling constants as a function of the dihedral angle and thus improve the existing relations.

The second point we need to consider is the transferability of such "Karplus-like relations". As indicated earlier, the constants *A*, *B* and *C* are derived for a model system and then the same constants are used to determine the conformation of peptide linkages in a wide variety of polypeptides. These individual peptide links may have completely different neighboring chemical environments from that of the model peptide link we have used to develop the "Karplus-like relationship" and one can question the validity of using the same values for *A*, *B* and *C*. Fortunately, the NMR chemical shifts and spin-spin coupling constants are local properties and the influence of the neighboring chemical environment is fairly small. Further support for this assertion comes from the NMR measurements of polypeptides having known X-ray crystallographic structures. It has been shown from those experimental measurements combined with relations similar to Eqn. 7.221 that the numerical errors introduced by using the same *A*, *B* and *C* is small [233, 223].

The third point is somewhat related to the one discussed earlier. This point concerns the fact that the effect of the other parameters such as bond angles, bond distances and substituent effects are not incorporated in a simple relation like the one given in Eqn. 7.221. For example, recently Barfield and Smith [234] have shown that the $^3J(^1H^1H)$ in H-C-C-H is dependent not only on the dihedral angle but also on the two bond angles of the hydrogen atoms. However, their conclusions are based on an oversimplified expression presented by Pople and Santry [95] to calculate the coupling constants. Edison *et al.* [223] studied the $^3J(^1H^1H)$ coupling surface of alanine dipeptide with respect to angles ϕ_i and ψ_i (see Fig. 6.1) by employing the uncoupled Hartree-Fock (UCHF) method. Their findings show that the coupling surface is almost flat in the direction of variation of ψ_i and support a simple relation as given in Eqn. 7.221 for wide range of values of ψ_i. Even for a smaller model system, a correlated *ab initio* study of a coupling surface demands an extensive use of computer resources and is not very practical.

Having considered a general picture of conformational analysis based on NMR spin coupling constants and the problems associated with it, we are now in a position to focus on the subject material specific to this chapter. We employ the newly developed EOM-CCSD method to study the variation of vicinal $^3J(^1H^1H)$ with the dihedral angle in N-methylacetamide. As mentioned, N-methylacetamide is widely used to mimic the peptide bond in polypeptides and more importantly, it is a medium-sized molecule which can be treated by current correlated *ab initio* methods. A fragment of a peptide chain is depicted in Fig. 6.1 and the angles ϕ_i and ψ_i shown define the conformation of the peptide link.

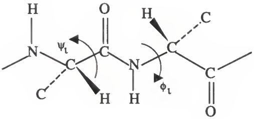

Figure 6.1

The conditions for the determination of the angle ϕ_i by measuring coupling constants are quite favorable because there is a pair of vicinal protons between which the coupling is large and *strongly dependent* on ϕ_i. However, the experimental condition for the NMR determination of the angle ψ is less favourable; there is no vicinal proton-proton coupling that can be used for this purpose. Here, our focus is mainly on the variation of the angle ϕ_i for a fixed value of ψ_i. We take advantage of Edison *et al.* [223] findings that the vicinal $^3J(^1H^1H)$ coupling constant has only a slight dependence on the angle ψ_i. In addition to NMR spin-spin coupling constants, we consider geometries, energetics and vibrational frequencies of the *cis* and *trans* forms of N-methylacetamide.

In the case of formamide, NMR spin-spin coupling constants are experimentally known. Therefore calculations on the formamide molecule provide us several usefull information which we could use in N-methylacetamide case. For example, formamide results give us a feel for the magnitude of the proton-proton coupling constants and the importance of non-contact contributions.

7.2 NMR Spin-Spin Coupling Constants of Formamide ($HCONH_2$) and N-methylacetamide ($CH_3NHCOCH_3$)

Amides provide the simplest models for the structure and conformational characteristics of the backbones of proteins. Formamide is the simplest amide and is considered as the parent molecule of all peptides. The cis and trans form of a generic peptide link are depicted in Fig. 6.2.

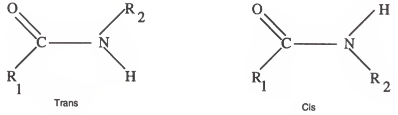

Trans

Cis

Figure 6.2

The characteristics of the peptide link are the coplanarity of the groups directly attached to it, its partial double bond nature evident from the shorter C-N bond length, substantial rotational barriers (ca. 20 kcal/mol) and preference for the trans configuration rather than the cis [235].

Geometry of formamide and N-methylacetamide is determined at the CCSD level using a DZP basis set that consists of the (9s,5p,1d)/[4s,2p,1d] contraction for C and (4s,1p)/[2s,1p] contraction for H. The sp set has been taken from Dunning [138]. Polarization exponents have been optimized locally at the correlated level [141]. In the case of N-methylacetamide both cis and trans configurations with respect to the C-N bond have been considered. We employ the same DZP basis set for the MBPT(2) vibrational frequencies, CCSD single point energy and EOM-CCSD NMR spin-spin coupling constant calculations at the CCSD/DZP optimized geometries. Spherical harmonic Gaussian basis functions have been used in geometry optimization, vibrational frequency calculations, and single point energy calculations. We employ Cartesian Gaussian basis functions for NMR spin-spin coupling constant calculations.

The CCSD/DZP geometry of formamide is depicted in Fig. 6.2 and the EOM-CCSD/DZP NMR spin-spin coupling constants are given in Table 7.28. As we can see from Table 7.28, large coupling constants such as ${}^1J({}^{15}N{}^1H)$, ${}^1J({}^{13}C{}^1H)$ show good agreement with experiment. Also, for such coupling constants the non-contact contributions are seemingly insignificant.

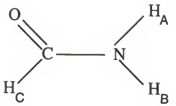

Figure 6.2. $r(CH_C) = 1.10931$ Å, $r(CN) = 1.36966$ Å, $r(NH_A) = 1.01006$ Å, $r(NH_B) = 1.00756$ Å, $r(CO) = 1.21705$ Å, $\alpha(H_ANC) = 119.33066°$, $\alpha(H_BNC) = 121.21279°$, $\alpha(OCH_C) = 123.15927°$

Table 7.28. The NMR spin-spin coupling constants of formamide (in Hz)[a].

Coupling	FC	SD	PSO	DSO	Total	Exp.
$^1J(^{15}N^1H_A)$	-82.98	-0.18	-1.63	-0.30	-85.09	±88.0[b], 88.3[c]
$^1J(^{15}N^1H_B)$	-83.11	-0.22	-1.80	-0.29	-85.42	±92.0[b], 90.7[c]
$^2J(^{15}N^1H_C)$	-18.54	0.00	0.26	0.15	-18.13	±19.0[b]
$^1J(^{13}C^1H_C)$	173.72	0.17	-0.72	1.07	174.24	
$^2J(^{13}C^1H_A)$	-1.20	-0.12	-0.63	-0.62	-2.57	
$^2J(^{13}C^1H_B)$	5.43	-0.05	-0.60	-0.63	4.15	
$^1J(^{13}C^{15}N)$	-18.30	-0.03	2.75	-0.09	-15.67	
$^2J(^1H_A{}^1H_B)$	3.52	-0.12	4.71	-6.03	2.08	±2.4[b]
$^3J(^1H_B{}^1H_C)$	0.48	0.13	0.27	-0.49	0.39	±2.1[b]
$^3J(^1H_A{}^1H_C)$	10.98	-0.04	2.39	-4.04	9.29	±12.9[b], 14.6[c]

[a] EOM-CCSD/DZP NMR spin-spin coupling constants at the CCSD/DZP optimized geometries.

[b] Sunners *et al.*, [236]. Corresponds to measurements carried out on a pure liquid sample.

[c] Marchal and Canet, [237]. Corresponds to measurements carried out on a pure liquid sample.

However, as we can see, the proton-proton couplings are relatively small and have large DSO and PSO contributions. Moreover, these non-contact contributions have opposite signs and nearly cancel with each other leaving the FC contribution approximately equal to the total coupling constant. As we can see from Table 7.28, the EOM-CCSD/DZP results for $^2J(^1H_A{}^1H_B)$, $^3J(^1H_B{}^1H_C)$ and $^3J(^1H_A{}^1H_C)$

including all the non-contact contributions are consistently lower compared to experiment while just the FC contributions are both larger and smaller compared to experiment and less systematic. On average, EOM-CCSD/DZP results for proton-proton coupling constants in formamide underestimate experiment by about 2 Hz. Large deviation from experiment can be attributed to the poor quality of the atomic basis set. In the following section we will employ calculated $^3J(HH)$ coupling constants of N-methylacetamide to develop a "Karplus like relation" which will eventually be used in the conformational analysis of peptides. Consequently, the accuracy of the EOM-CCSD/DZP proton-proton coupling constants is a primary concern.

The CCSD/DZP optimized geometries of the lowest energy cis and trans configurations of N-methylacetamide are given in Table 7.29 and depicted in Fig. 6.3 (I) and (II) respectively. As we can see bond lengths of cis and trans forms of N-methylacetamide are close to one another while the key bond angles $\alpha(NC_2O)$, $\alpha(H_CNC_2)$, $\alpha(C_3NC_2)$, $\alpha(H_BC_1C_2)$ and $\alpha(H_DC_3N)$ show a significant difference. Table 7.29 also contains experimental bond lengths and angles reported by Kitano *et al.* [238] from electron diffraction measurements. The experimental values for angles $\alpha(NC_2O)$ and $\alpha(C_3NC_2)$ are closer to the CCSD/DZP optimized

Table 7.29. The geometries of cis and trans N-methylacetamide[a].

	trans form (I)	cis form (II)	Exp.[b]
$r(C_1C_2)$	1.5241	1.5240	1.520
$r(C_2O)$	1.2250	1.2242	1.224
$r(C_2N)$	1.3688	1.3744	1.386
$r(C_3N)$	1.4551	1.4533	1.468
$r(NH_C)$	1.0077	1.0108	
$r(C_1H_A)$	1.0975	1.0936	
$r(C_1H_B)$	1.0967	1.0985	
$r(C_2H_D)$	1.0964	1.0960	
$r(C_2H_E)$	1.0979	1.0997	
$\alpha(NC_2O)$	122.1255	121.5906	121.8
$\alpha(C_1C_2O)$	122. 4773	122.7630	
$\alpha(C_1C_2N)$	115.3972	115.6464	115.2
$\alpha(H_CNC_2)$	119.4391	114.4531	
$\alpha(C_3NC_2)$	121.0514	126.6168	119.6
$\alpha(H_AC_1C_2)$	108. 6373	108.3853	
$\alpha(H_BC_1C_2)$	113.2287	110.7500	
$\alpha(H_CC_3N)$	110.8806	108.2697	
$\alpha(H_DC_3N)$	108.5418	112.1182	
$\tau(H_AC_1C_2H_B)$	121.4049	121.1501	
$\tau(H_DC_3NH_E)$	119.9316	118.8286	

[a] Bond lengths are in Angstroms and bond angles are in degrees. The reported geometries are obtained at the CCSD/DZP level.

[b] Kitano *et al.*, [238].

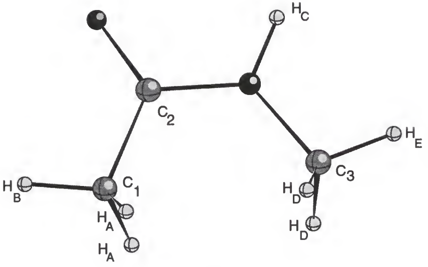

(I)

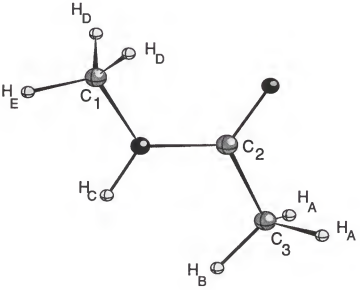

(II)

Figure 6.3

values of the trans, and hence it is clear that the experimental results of Kitano *et al.* [238] correspond to the trans configuration. The shorter bond length of r(C_2N) compared to r(C_3N) is an indication of the double bond character of the C_2N bond and reponsible for the larger barrier to internal rotation with respect to the C_2N axis. The CCSD/DZP optimized C_2N bond length is 0.0172 Å longer than the experimental result. The comparatively large difference between the calculated and experimental results is common to multiple bonds and can be improved by incorporating better basis sets and more electron correlation. Changes in angles $\alpha(C_1C_2N)$ and $\alpha(C_2NC_3)$ from 115.3972° and 121.0514° to 115.6464° and 126.6168° indicate that the principal changes upon rotation to the cis form appear to help accommodate the steric congestion. Further evidence for this assertion comes from changes in $\alpha(H_CNC_2)$ from 119.44° to 114.45°. The C_2-N bond length is indicative of the double bond character of the C_2-N bond and it is significantly shorter in the trans form compared to the cis form.

The stationary points are characterized by vibrational frequency calculations and the conformations shown in Fig. 6.3 for the cis and trans form are actual minima on their respective potential energy surfaces. Vibrational frequencies of the cis and trans minimum structures (Fig. 6.3 (I) and (II)) are similar and they cannot be distinguished from each other by vibrational spectroscopy alone. In the gas phase, the trans form (Fig 6.3, (II)) is 2.30 kcal/mol more stable than the cis form (Fig 6.3, (I)) at the CCSD/DZP level, at the CCSD/DZP geometries.

This includes the zero-point energy at 0 K calculated at the MBPT(2)/DZP level. Naturally, the zero-point energy differences are small; the cis isomer is favored by 0.026 kcal/mol at the MBPT(2)/DZP level.

Table 7.30 presents the EOM-CCSD NMR spin-spin coupling constants of the trans and cis form of N-methylacetamide. As we have seen from the EOM-CCSD/DZP results for formamide, it is advantageous to include non-contact contributions to have a consistent deviation from experiment. To have a better agreement with experiment a basis set better than DZP is required. However, for N-methylacetamide, due to limitations in computer resources we are not at liberty to improve upon atomic basis set beyond DZP. Moreover, even with a DZP basis set, we are not in a position to evaluate non-contact contibutions. Consequently, we estimate DSO and PSO contributions by employing a DZP basis on the heavy atoms and a DZ basis set on hydrogen atoms. As we have concluded in chapter 3, this will give us a fairly accurate estimate of these two contributions since these contributions are more or less insensitive to the choice of the atomic orbital basis set.

From the selection of calculated coupling constants given in Table 7.30, $^{1}J(^{15}N^{1}H)$ and $^{1}J(^{13}C^{1}H)$ the coupling constants are consistent with the literature values for sp^2 hybridized nitrogen and proton and sp^3 hybridized carbon and proton coupling constants [239–241].

Table 7.30. The NMR spin-spin coupling constants of cis and trans froms of N-methylacetamide (in Hz)[a].

	Trans	Cis	Exp.
$^1J(^{15}N^1H)$	-86.12	-85.90	±93.0[b]
$^1J(^{15}N^{13}C_2)$	-15.99	-15.80	
$^1J(^{15}N^{13}C_3)$	-13.27	-12.67	
$^2J(^{15}N^{13}H_E)$	0.84	1.47	
$^2J(^{15}N^{13}H_D)$	1.52	0.89	
$^3J(^{15}N^{13}H_B)$	-0.47	-2.08	
$^3J(^{15}N^{13}H_A)$	-1.00	0.39	
$^1J(^{13}C_1H_A)$	116.09	110.68	
$^1J(^{13}C_1H_B)$	111.49	122.86	
$^1J(^{13}C_3H_D)$	127.34	123.74	
$^1J(^{13}C_3H_E)$	116.38	118.19	
$^2J(^1H_AH_A)$	-17.41	-16.55	
$^2J(^1H_AH_B)$	-13.57	-13.88	
$^2J(^1H_DH_D)$	-13.33	-11.12	
$^2J(^1H_DH_E)$	-13.85	-15.10	
$^3J(^1H_DH_C)$	1.17	1.55	
$^3J(^1H_EH_C)$	5.36	6.67	
$^4J(^1H_AH_C)$	-0.81	-1.34	
$^4J(^1H_BH_C)$	0.83	0.59	

[a] The FC contributions are calculated using a DZP basis and the PSO and DSO contributions are calculated using a DZP basis on heavy atoms and a DZ basis on hydrogens.

[b] Marchal and Canet, [237, 242]. Corresponds to measurements carried out on a pure liquid sample.

As expected from the similar geometries and bonding character, these coupling constants have similar values in the cis and trans froms. Multiple bond character of the C_2-N bond is reflected by its relatively large negative value for the $^1J(^{13}C_2{}^{15}N)$ value compared to $^1J(^{13}C^{15}N)$ in CH_3NH_2 and shorter C_2-N bond length compared to C-N single bond length (ca. 1.46). As we have seen earlier, in the cis form H_C and H_E are further apart in the space compared to the corresponding atoms in the trans form. This is also reflected in the large $^3J(^1H_E{}^1H_C)$ value in the trans form compared to the cis form. Similarly, H_B and H_C are further apart in the trans form and have a smaller coupling constant compared to the cis form. Consequently, the relative magnitude of the $^3J(^1H^1H)$ may be used to assign the configuration (cis or trans) of the peptide link.

Several experiments have been carried out to measure the NMR spectrum of N-methylacetamide. The cis isomer of N-methylacetamide is in too small a proportion (ca. 3% in water) to observe in the NMR measurements. As a result, experimentally measured NMR chemical shifts and spin-spin coupling constants are mostly due to the trans isomer. The EOM-CCSD/DZP results of the $^1J(^{15}N^1H)$ coupling constant, when considered with the mean absolute error of such a method as reported in chapter 4 (ca. 12%) is in good agreement with experiment. As indicated on several occasions, the EOM-CCSD results almost always provide an unambiguous determination of the sign of the coupling constant and the $^1J(^{15}N^1H)$ is in fact negative. The long range $^3J(^{15}N^1H)$ coupling constant has been reported

---

to be ± 1.63 Hz [243] and subject to the error bars of the EOM-CCSD/DZP level compares very well with the rotationally averaged calculated result – 0.82 Hz for the trans isomer.

The coupling constant we are most interested in is $^3J(^1H_C{}^1H_D)$. The calculated $^3J(^1H_C{}^1H_D)$ coupling constant for several different values of the dihedral angle ϕ is given in Table 7.31. If it is assumed that the hydrogens of the methyl group occupy discrete rotational states with one of the methyl protons cis to the N-H proton (energetically preferred conformation), then the calculated average $^3J(^1H_C{}^1H_D)$ coupling constants for the trans and cis forms are 2.6 and 3.3 Hz respectively. The corresponding experimental values are 4.8 and and 5.3 respectively [244]. Similar to formamide, the calculated results underestimate experiment by about 2 Hz and also the coupling constants under consideration have similar magnitudes to those of the formamide and appears also to have a similar chemical environment. Consequently, it is fair to assume that the calculated results are systematically lower by about 2 Hz for the proton-proton coupling constants of interest in these molecules, and scale the calculated results by 2 Hz to have a better agreement with experiment. The scaled values are also presented in Table 7.31 (given in parenthesis). The range of $^3J(^1H_C{}^1H_D)$ as the dihedral angle varies from 0° to 180° is 7.36 to 10.25 Hz in the trans form and 8.67 to 11.31 Hz in the cis form.

Table 7.31. Variation of $^3J(^1H^1H)$ with dihedral angle (in degrees) of cis and trans N-methylacetamide (in Hz)[a].

Dihedral Angle	Trans	Cis
0	5.36 (7.36)	6.67 (8.67)
30	3.96 (5.96)	4.68 (6.68)
60	0.29 (2.29)	0.50 (2.50)
120	1.17 (3.17)	1.55 (3.55)
150	5.52 (7.52)	6.53 (8.53)
180	8.25 (10.25)	9.31 (11.31)

[a] The EOM-CCSD spin-spin coupling constants at the CCSD/DZP optimized geometries. The FC contributions are calculated using a DZP basis and the PSO and DSO contributions are calculated using a DZP basis on heavy atoms and a DZ basis on hydrogens.

The disadvantage of having such a small range for the $^3J(^1H_C{}^1H_D)$ is that the smaller errors in the calculated or experimentally measured $^3J(^1H_C{}^1H_D)$ will correspond to larger errors in the dihedral angle in question. In other words, to minimize these errors, the calculated $^3J(^1H_C{}^1H_D)$ results for different dihedral angles which we will employ to estimate A, B and C are required to be highly accurate. The scaled values for the $^1J(^1H^1H)$ coupling constants for different values of the dihedral angle ϕ presented in Table 7.31 are used to estimate the magnitudes of A, B and C in Eqn. 7.221.

Within the error bars of the statistical fit, the expressions

$$^{3}J(\mathrm{HH}) = (8.09 \pm 0.42)cos^{2}\phi - (1.17 \pm 0.16)cos^{2}\phi + (0.70 \pm 0.31) \quad (7.222)$$

$$^{3}J(\mathrm{HH}) = (9.27 \pm 0.20)cos^{2}\phi - (1.19 \pm 0.08)cos^{2}\phi + (0.69 \pm 0.15) \quad (7.223)$$

describe the variations of calculated vicinal ^{3}J(HH) spin-spin coupling constants with the dihedral angle for the trans and cis arrangement of the amide bond respectively. Respective equations are plotted as a function of the dihedral angle ϕ in Figs. 6.4 and 6.5.

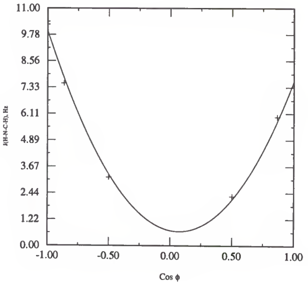

Figure 6.4. A plot of vicinal ^{3}J(^{1}H^{1}H) coupling constant as a function of dihedral angle for the trans arrangement of the amide bond.

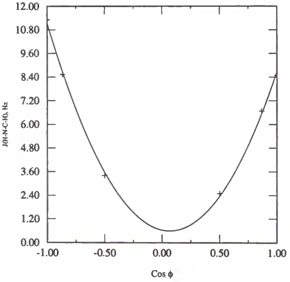

Figure 6.5. A plot of vicinal $^3J(^1H^1H)$ coupling constant as a function of dihedral angle for the cis arrangement of the amide bond.

In Table 7.32, we compare the proposed values for the constants *A*, *B* and *C* with several other sets of values reported in the literature. It has been shown that the coefficients proposed by Néel *et al.* [245–247] and Ramachandran [229, 230] give lower values for the $^3J(^1H^1H)$ coupling constant for the dihedral angles in the range of $0^o \leq \phi \leq 90^o$ [248]. The coefficients proposed by Barfield *et al.* [220] are based on the INDO (intermediate neglect of differential overlap) calculations on the model compound n-methylacetamide.

Table 7.32. Coefficients proposed for Eqn. 7.221.

Reference	Configuration	Coefficients (Hz)		
		A	*B*	*C*
Bystrov *et al.*, [249]		9.8	1.1	0.4
Néel *et al.*, [245, 246]		9.3	3.5	0.3
Néel *et al.*, [247]		9.4	3.2	0.0
Ramachandran *et al.*, [229]		8.6	1.7	1.5
Barfield *et al.*, [220]	trans	12.06	4.48	0.01
	cis	11.27	4.32	0.01
Present work	trans	8.09	1.17	0.70
	cis	9.27	1.19	0.69

The relations given by Barfield *et al.* [220] predicts larger $^3J(^1H^1H)$ for the trans configuration than the corresponding coupling for the cis configuration of the amide bond. This is contrary to the experimental results reported for model systems having cis and trans amide bonds and the dihedral angle ϕ in the region of $\sim 0^o$. Consistent with experiment, the relations derived in this study gives larger $^3J(HH)$ coupling constants for the cis arrangement compared to the trans arrangement of the amide bond in the region of $\phi \sim 0^o$. Our results also predict similar behaviour in the region of $\phi \sim 180^o$. However, it is, as yet impossible to verify experimentally that larger $^3J(HH)$ values for the cis than trans configuration of the amide bond holds for this region as well.

7.3 Conclusions

In this chapter, we have presented a preliminary study of the application of theoretically calculated EOM-CCSD NMR spin-spin coupling constants in conformational analysis. Here, our focus was on the determination of dihedral angle ϕ of a peptide link (Fig. 6.1) by using NMR spin-spin coupling constants.

For this purpose, we have presented a model mathematical relation which relates the vicinal $^3J(^1H\text{-}N\text{-}C\text{-}^1H)$ spin-spin coupling constant to the dihedral angle ϕ using n-methylacetamide as the model molecule. The structure and energetics of n-methylacetamide was itself found to be interesting. The trans configuration of the amide bond was shown to be (Fig. 6.3, (I)) 2.30 kcal/mol more stable than the cis configuration (Fig. 6.3, (II)) at the CCSD/DZP level, at the CCSD/DZP geometries. The eclipsed conformation of the methyl hydrogens with respect to the N-H and C=O bond was found to be the most stable conformation for the cis configuration of the amide bond. On the other hand for the trans configuration, the eclipsed conformation of the methyl hydrogen with respect to the N-H bond and staggered conformation with respect to C=O bond was found to be the most stable conformation. Relative magnitude of the $^3J(^1H\text{-}N\text{-}C\text{-}^1H)$ may be useful to assign the configuration of the peptide link.

The relations given in Eqns. 7.222 and 7.223 for variation of the vicinal coupling $^3J(^1H\text{-}N\text{-}C\text{-}^1H)$ with dihedral angle for the trans and cis configuration of the amide bond predicts the relative ordering of the $^3J(^1H\text{-}N\text{-}C\text{-}^1H)$ for the cis and trans configurations of the amide bond consistent with experiment in the range of $\sim 0^o$. This is a remarkable improvement over the relations that have been widely used in the literature. However, the absolute accuracy of the dihedral angle ϕ calculated by given relations need to be carefully assessed before widspread use of Eqns. 7.222 and 7.223 in conformational analysis.

In several previous occasions, we have emphasized the importance of having very accurate NMR spin-spin coupling constants to develop "Karplus like relations". We were also able to demonstrate the difficulties of obtaining accurate spin-spin coupling constants even for a small model system. Therefore it is absolutely essential to find alternative means for improvement, without relying so much on improving the level of theory (ie. method, basis set, *etc.*). An alternative way to look at Eqn. 7.221 is that the constants A and B describe the relative change in spin-spin coupling constants with respect to a base value C, with the variation of the dihedral angle. Due to the error cancellations, the relative changes in the NMR spin-spin coupling constants can be calculated accurately. Therefore, the constants A and B can be estimated fairly accurately by our EOM-CCSD/DZP results. The constant C being an absolute value difficult to compute accurately from theoretically calculated results. Therefore we suggest to obtain a better estimate for the constant C for given A and B by using a one experimentally measured spin-spin coupling constant for a known dihedral angle.

As illustrated in this chapter, the accurate calculations of NMR spin-spin coupling constant of conformers, regardless of the atoms involved, and which otherwise would not have been accessible experimentally, will enormously expand the applicablity of NMR spectroscopy in conformational analysis.

BIBLIOGRAPHY

1. K. Kamieńska-trela, Applications of spin-spin couplings, in *Nuclear Magnetic Resonance (A Specialist Periodical Report)*, edited by G. A. Webb, volume 23, pages 137–178, Royal Society of Chemistry, Cambridge, 1993.

2. W. G. Espersen and R. B. Martin, J. Phys. Chem. **80**, 741 (1976).

3. E. A. Salter, H. Sekino, and R. J. Bartlett, J. Chem. Phys. **87**, 502 (1987).

4. H. Sekino and R. J. Bartlett, Int. J. Quantum Chem. **21**, 487 (1987).

5. J. F. Stanton and R. J. Bartlett, J. Chem. Phys. **97**, 2299 (1993).

6. G. A. Olah, G. K. S. Prakash, M. Arvanaghi, and F. A. L. Anet, J. Am. Chem. Soc. **104**, 7105 (1982).

7. P. A. M. Dirac, Proc. Roy. Soc., Ser. A **117**, 610 (1928).

8. P. A. M. Dirac, Proc. Roy. Soc., Ser. A **117**, 351 (1928).

9. W. v. Pauli Jr., Z. f. Physik **43**, 601 (1927).

10. R. E. Moss, *Advanced Molecular Quantum Mechanics, An Introduction to Relativistic Quantum Mechanics and the Quantum Theory of Radiation*, Chapman Hall Ltd., London, 1973.

11. E. Merzbacher, *Quantum Mechanics*, John Wiley & Sons, London, second edition, 1970.

12. R. Shankar, *Principles of Quantum Mechanics*, Plenum Press, New York and London, 1985.

13. P. A. M. Dirac, *The Principles of Quantum Mechanics*, Oxford University Press, New York, fourth edition, 1958.

14. W. v. Gordon, Z. f. Physik **40**, 117 (1927).

15. O. v. Klein, Z. f. Physik **41**, 407 (1927).

16. H. A. Bethe and E. E. Salpeter, *Quantum Mechanics of One- and Two-Electron Atoms*, Academic Press Inc., New York, 1958.

17. S. Tomanaga, Phys. Rev. **74**, 224 (1948).

18. R. P. Feynman, Phys. Rev. **76**, 749 (1949).

19. R. P. Feynman, Phys. Rev. **76**, 769 (1949).

20. R. P. Feynman, Phys. Rev. **76**, 790 (1949).

21. F. J. Dyson, Phys. Rev. **75**, 486 (1949).

22. D. P. Craig and T. Thirunamachandran, *Molecular Quantum Electrodynamics An Introduction to Radiation-Molecule Interactions*, Academic Press, London, 1984.

23. J. Sucher, Physica Scripta **36**, 271 (1987).

24. G. Breit, Phys. Rev. **34**, 553 (1929).

25. G. E. Brown and D. G. Ravenhall, Proc. Roy. Soc., Ser. A **208**, 552 (1951).

26. J. Sucher, Phys. Rev. Lett. **55**, 1033 (1985).

27. B. Swirles, Proc. Roy. Soc., Ser. A **625**, 152 (1935).

28. I. P. Grant, Proc. Roy. Soc., Ser. A **162**, 555 (1961).

29. G. Malli and J. Oreg, J. Chem. Phys. **63**, 830 (1975).

30. J. Sucher, Foundation of the relativistic theory of atomic structure, in *Workshop on the Foundation of the Relativistic Theory of Atomic Structure*, edited by H. G. Berry, K. T. Cheng, W. R. Johnson, and Y. K. Kim, pages 2–26, Argonne National Laboratory, Illinois, 1980.

31. J. Sucher, Phys. Rev. A **22**, 348 (1980).

32. L. Visscher, *Relativity and Electron Correlation in Chemistry*, PhD thesis, Rijksuniversiteit Groningen, 1995.

33. J. Sucher, Int. J. Quantum Chem. **XXV**, 3 (1984).

34. A. A. Broyles, Phys. Rev. A **26**, 1181 (1982).

35. E. E. Salpeter and H. A. Bethe, Phys. Rev. **84**, 1232 (1951).

36. E. E. Salpeter, Phys. Rev. **87**, 328 (1951).

37. A. A. Broyles, Phys. Rev. A **38**, 1137 (1988).

38. A. A. Broyles, Int. J. Quantum Chem. Symp. **29**, 1181 (1995).

39. W. Kutzelnigg, Z. f. Physik **11**, 15 (1989).

40. W. Kutzelnigg, Z. f. Physik **15**, 27 (1990).

41. P. O. Löwdin, J. Mol. Struct. **14**, 131 (1964).

42. L. L. Foldy and S. A. Wouthuysen, Phys. Rev. **78**, 29 (1950).

43. I. Lindgren and J. Morrison, *Atomic Many-Body Theory*, Springer-Verlag, Berlin, 1982.

44. des Cloizeaux, Nucl. Phys. **20**, 329 (1960).

45. E. van Lenthe, E. J. Baerends, and J. G. Snijders, J. Chem. Phys. **99**, 4597 (1993).

46. C. Chang, M. Pelissier, and P. Durand, Physica Scripta **34**, 394 (1986).

47. E. van Lenthe, R. van Leeuwen, E. J. Baerends, and J. G. Snijders, Relativistic regular two-component hamiltonians, in *New Challenges in Computational Quantum Chemistry*, edited by R. Broer, P. J. C. Aerts, and P. S. Bagus, pages 93–111, University of Groningen, Netherlands, 1994.

48. R. van Leeuwen, E. van Lenthe, E. J. Baerends, and J. G. Snijders, J. Chem. Phys. **101**, 1272 (1994).

49. J. M. Levy-Leblond, Comm. Math. Phys. **6**, 286 (1967).

50. J. M. Levy-Leblond, Ann. Phys. (NY) **57**, 481 (1970).

51. G. A. Aucar and J. Oddershede, Int. J. Quantum Chem. **47**, 425 (1993).

52. Z. V. Chraplyvy, Phys. Rev. **91**, 388 (1953).

53. Z. V. Chraplyvy, Phys. Rev. **92**, 1310 (1953).

54. W. A. Barker and F. N. Glover, Phys. Rev. **99**, 317 (1955).

55. N. F. Ramsey, Phys. Rev. **91**, 303 (1953).

56. D. W. Davies, *The Theory of the Electric and Magnetic Properties of Molecules*, John Wiley & Sons, New York, 1967.

57. J. E. Harriman, *Theoretical Foundations of Electron Spin Resonance*, Academic Press, New York, 1978.

58. A. Messiah, *Quantum Mechanics II*, John Wiley & Sons, New York, 1962.

59. H. F. Hameka, *Advanced Quantum Chemistry*, Addison-Wesley Publishing Company, Reading, Massachusetts, 1965.

60. T. P. Das, *Relativistic Quantum Mechanics and Electrons*, Harper and Row, New York, 1973.

61. M. J. Lighthill, *Introduction to Fourier Analysis and Generalised Functions*, Cambridge University Press, London, 1958.

62. M. Born and R. Oppenheimer, Ann. Phys. **84**, 457 (1927).

63. J. I. Musher, Am. J. Phys. **34**, 267 (1966).

64. A. L. Fetter and J. D. Walecka, *Quantum Theory of Many Particle Systems*, McGraw-Hill, New York, 1971.

65. A. Isihara, *Statistical Physics*, Academic Press, New York, 1971.

66. R. D. Mattuck, *A Guide to Feynman Diagrams in the Many-Body Problem*, McGraw-Hill, New York, 1976.

67. N. Fukuda, Nucl. Phys. **44**, 553 (1963).

68. G. Y. Csanak, H. S. Taylor, and R. Yaris, Adv. Atom. Mole. Phys. **7**, 287 (1971).

69. J. Linderberg and Y. Öhrn, *Propagators in Quantum Chemistry*, Academic press, London and New York, 1973.

70. W. Kutzelnigg, Theor. Chim. Acta **83**, 263 (1992).

71. E. F. Hayes and R. G. Parr, J. Chem. Phys. **43**, 1831 (1965).

72. J. E. Rice and N. C. Handy, J. Chem. Phys. **94**, 4959 (1991).

73. J. E. Rice and N. C. Handy, Int. J. Quantum Chem. **43**, 91 (1992).

74. K. Sasagane, F. Aiga, and R. Itoh, J. Chem. Phys. **99**, 3738 (1993).

75. F. Aiga, K. Sasagane, and R. Itoh, J. Chem. Phys. **99**, 3779 (1993).

76. F. Aiga, K. Sasagane, and R. Itoh, Int. J. Quantum Chem. **51**, 87 (1994).

77. A. Szabo and N. S. Ostlund, *Modern Quantum Chemistry, Introduction to Advanced Electronic Structure Theory*, McGraw-Hill, Inc., New York, 1990.

78. M. Nooijen, *The Coupled Cluster Green's Function, A Perturbative Diagrammatic View on Many-Electron Theory*, PhD thesis, Vrije Universiteit, 1992.

79. N. H. March, W. H. Young, and S. Sampanthar, *The Many-body Problem in Quantum Mechanics*, Cambridge University Press, London, 1967.

80. J. Gerratt and I. M. Mills, J. Chem. Phys. **49**, 1719 (1968).

81. P. Pulay, Direct use of the gradient for investigation of molecular energy surfaces, in *Modern Theoretical Chemistry*, edited by H. F. Schaefer III, volume 4, pages 153–186, Plenum, New York, 1977.

82. P. Pulay, J. Chem. Phys. **78**, 5043 (1983).

83. F. London, J. Phys. Radium **8**, 397 (1937).

84. R. Ditchfield, Mol. Phys. **27**, 789 (1974).

85. T. Helgaker and P. Jørgensen, J. Chem. Phys. **95**, 2595 (1991).

86. P. Jørgensen and J. Simons, *Second Quantization-Based Methods in Quantum Chemistry*, Academic Press Inc., New York, 1981.

87. E. A. Salter, G. W. Trucks, and R. J. Bartlett, J. Chem. Phys. **90**, 1752 (1989).

88. H. Koch and P. Jørgensen, J. Chem. Phys. **93**, 3333 (1990).

89. P. B. Rozyczko, S. A. Perera, and R. J. Bartlett, In Preparation .

90. R. Kobayashi, H. Koch, and P. Jørgensen, Chem. Phys. Lett. **219**, 30 (1994).

91. H. Sekino and R. J. Bartlett, Chem. Phys. Lett. **225**, 486 (1994).

92. J. F. Stanton and R. J. Bartlett, J. Chem. Phys. **99**, 5178 (1993).

93. S. A. Perera, H. Sekino, and R. J. Bartlett, J. Chem. Phys. **101**, 2186 (1994).

94. J. A. Pople and D. P. Santry, Mol. Phys. **8**, 1 (1964).

95. J. A. Pople and D. P. Santry, Mol. Phys. **9**, 311 (1965).

96. M. Barfield and D. M. Grant, Theory of nuclear spin-spin coupling, in *Advances in Magnetic Resonance*, edited by J. S. Waugh, volume 1, pages 149–193, Academic Press, New York, 1965.

97. J. A. Pople, J. W. McIver Jr., and N. S. Ostuland, J. Chem. Phys. **49**, 2965 (1968).

98. G. E. Maciel, J. J. W. McIver, N. S. Ostlund, and J. A. Pople, J. Am. Chem. Soc. **92**, 1 (1970).

99. G. E. Maciel, J. J. W. McIver, N. S. Ostlund, and J. A. Pople, J. Am. Chem. Soc. **92**, 4497 (1970).

100. G. E. Maciel, J. J. W. McIver, N. S. Ostlund, and J. A. Pople, J. Am. Chem. Soc. **92**, 4506 (1970).

101. A. C. Blizzard and D. P. Santry, J. Chem. Phys. **55**, 1 (1971).

102. R. Ditchfield and L. C. Snyder, J. Chem. Phys. **56**, 5823 (1972).

103. W. S. Lee and J. M. Schulman, J. Chem. Phys. **70**, 1530 (1979).

104. O. Matsuoka, Int. J. Quantum Chem. **V**, 6229 (1971).

105. J. Kowalewski, Calculations of nuclear spin-spin couplings, in *Annual Reports on NMR Spectroscopy*, edited by G. A. Webb, volume 12, pages 81–176, Academic Press Inc., London, 1982.

106. M. F. Guest, V. R. Saunders, and R. E. Overill, Mol. Phys. **35**, 427 (1978).

107. E. J. M. C. J. Jameson, *Multinuclear NMR*, Plenum, New York, 1987.

108. J. Oddershede, Theoretical aspects of spin-spin couplings, in *Nuclear Magnetic Resonance (A specialist Periodical Report)*, edited by G. A. Webb, volume 18, pages 98–112, Royal Society of Chemistry, Cambridge, 1988.

109. J. Kowalewski, A. Laaksonen, B. Roos, and P. Siegbahn, J. Chem. Phys. **71**, 2896 (1979).

110. J. Kowalewski, A. Laaksonen, and V. R. Saunders, J. Chem. Phys. **74**, 2412 (1981).

111. H. Fukui, J. Chem. Phys. **65**, 844 (1976).

112. T. Itagaki and A. Saika, J. Chem. Phys. **71**, 4620 (1979).

113. M. Iwai and A. Saika, Phys. Rev. A **28**, 1924 (1983).

114. H. Fukui, K. Miura, and H. Matsuda, J. Chem. Phys. **94**, 533 (1991).

115. H. Sekino and R. J. Bartlett, J. Chem. Phys. **85**, 3945 (1986).

116. I. Carmichael, J. Phys. Chem. **97**, 1789 (1993).

117. H. Fukui, K. Miura, H. Matsuda, and T. Baba, J. Chem. Phys. **97**, 2299 (1992).

118. A. Dalgarno and G. A. Victor, Proc. Roy. Soc. (London) **A291**, 219 (1966).

119. J. Oddershede, Adv. Quantum Chem. **II**, 275 (1978).

120. C. W. McCurdy Jr., T. N. Rescigno, D. L. Yeager, and V. McKoy, Calculations of nuclear spin-spin couplings, in *The Equations of Motion Method: An Approach to the Dynamical Properties Atoms and Molecules*, edited by G. A. Webb, volume 12, pages 339–386, Academic Press, New York, 1982.

121. V. Galasso, J. Chem. Phys. **82**, 899 (1985).

122. J. Geertsen and J. Oddershede, Chem. Phys. **90**, 6652 (1984).

123. J. Geertsen, J. Oddershede, and G. E. Scuseria, J. Chem. Phys. **87**, 2138 (1987).

124. J. Oddershede, J. Geertsen, and G. E. Scuseria, J. Phys. Chem. **92**, 3056 (1988).

125. J. Geertsen, J. Oddershede, W. T. Raynes, and G. E. Scuseria, J. Magn. Res. **93**, 458 (1991).

126. J. Geertsen, J. Oddershede, and G. E. Scuseria, Int. J. Quantum Chem. Symp. **21**, 475 (1987).

127. J. Kowalewski, B. Roos, P. Siegbahn, and R. Vestin, Chem. Phys. **3**, 70 (1974).

128. J. Kowalewski, B. Roos, P. Siegbahn, and R. Vestin, Chem. Phys. **9**, 29 (1975).

129. B. Kirtman and K. B. Kirtley, J. Chem. Phys. **65**, 1357 (1976).

130. B. Kirtman and K. B. Kirtley, J. Phys. Chem. **83**, 1470 (1979).

131. P. Albertsen, P. Jørgensen, and D. L. Yeager, J. Chem. Phys. **76**, 354 (1980).

132. G. Fronzoni and V. Galasso, Chem. Phys. **103**, 29 (1986).

133. V. Galasso and G. Fronzoni, J. Chem. Phys. **85**, 5200 (1986).

134. O. Vahtras, H. Ågren, P. Jørgensen, H. J. A. Jensen, S. B. Padkjær, and T. Helgaker, J. Chem. Phys. **96**, 6120 (1992).

135. V. G. Malkin, O. L. Malkina, and D. R. Salahub, Chem. Phys. Lett. **221**, 91 (1994).

136. K. Kamieńska-trela, Applications of spin-spin couplings in structure elucidations, in *Nuclear Magnetic Resonace (A specialist Periodical Report)*, edited by G. A. Webb, volume 22, pages 159–175, Royal Society of Chemistry, Cambridge, 1992.

137. O. Matsuoka and T. Aoyama, J. Chem. Phys. **73**, 5718 (1980).

138. T. H. Dunning, Jr., J. Chem. Phys. **53**, 2823 (1970).

139. T. H. Dunning, Jr., J. Chem. Phys. **55**, 716 (1971).

140. D. M. Chipman, Theor. Chim. Acta **76**, 73 (1989).

141. L. T. Redmon, G. D. Purvis III, and R. J. Bartlett, J. Am. Chem. Soc. **101**, 2856 (1979).

142. D. M. Chipman, J. Chem. Phys. **91**, 5455 (1989).

143. A. Schäfer, H. Horn, and R. Ahlrichs, J. Chem. Phys. **97**, 2571 (1992).

144. S. G. Frankiss, J. Phys. Chem. **67**, 752 (1963).

145. W. McFarlane, Mol. Phys. **10**, 603 (1966).

146. L. Paolillo and E. D. Becker, J. Magn. Res. **3**, 200 (1970).

147. R. M. Lynden-Bell and N. Sheppard, Proc. Roy. Soc., Ser. A **269**, 385 (1962).

148. D. F. Gaines, R. Schaeffer, and F. Tebbe, J. Phys. Chem. **67**, 1937 (1963).

149. D. F. Gaines, R. Schaeffer, and F. Tebbe, J. Phys. Chem. **2**, 523 (1963).

150. R. A. Ogg Jr., J. Chem. Phys. **22**, 1933 (1954).

151. W. D. Phillips, H. C. Miller, and E. L. Muetterties, J. Am. Chem. Soc. **81**, 4496 (1959).

152. R. E. Williams, H. D. Fisher, and C. O. Wilson, J. Phys. Chem. **64**, 1583 (1960).

153. R. Schaeffer, D. F. Gaines, and F. Tebbe, Inorg. Chem. **3**, 904 (1964).

154. T. C. Farrar and G. R. Quinting, Inorg. Chem. **24**, 1941 (1985).

155. T. P. Onak, H. Landesman, R. E. Williams, and I. Shapiro, J. Phys. Chem. **63**, 1533 (1959).

156. L. E. Sutton, editor, *Tables of Interatomic Distances and Configuration in Molecules and Ions, Supplement*, The Chemical Society, London, 1965.

157. J. R. Beckett, *The Temperature and Density Dependence of the Nuclear Spin-Spin Interaction in HD Gas and Fluid*, PhD thesis, Rutgers University, 1979.

158. J. S. Muenter and W. Klemperer, J. Chem. Phys. **52**, 6033 (1970).

159. R. E. Wasylishen, J. O. Friedrich, S. Mooibroek, and J. B. Macdonald, J. Chem. Phys. **83**, 548 (1985).

160. J. O. Friedrich and R. E. Wasylishen, J. Chem. Phys. **83**, 3707 (1985).

161. J. R. Holmes, D. Kivelson, and W. C. Drinkard, J. Chem. Phys. **37**, 150 (1962).

162. A. E. Florin and M. Alei Jr., J. Chem. Phys. **47**, 4268 (1967).

163. D. L. Gray and A. G. Robiette, Mol. Phys. **37**, 1901 (1979).

164. B. Bennett, W. T. Raynes, and C. W. Anderson, Spectrochim. Acta. **45A**, 821 (1989).

165. F. A. L. Anet and D. J. O'leary, Tetrahedron Letters **30**, 2755 (1989).

166. D. Bethell and V. Gold, *Carbonium Ions: An Introduction*, Academic Press, New York, 1967.

167. P. Vogel, *Carbocation Chemistry*, Elsevier, Amsterdam, 1985.

168. G. A. Olah, Angew. Chem. Int. Ed. Engl. **34**, 1393 (1995).

169. P. D. Bartlett, *Non-classical Ions*, Benjamin, New York, 1965.

170. H. C. Brown and (with comments by P. v. R. Schleyer), *The Non-classical Ion Problem*, Plenum Press, New York, 1977.

171. G. A. Olah, Angew. Chem. Int. Ed. Engl. **2**, 629 (1963).

172. G. A. Olah, G. Liang, G. D. Mateescu, and J. L. Riemenschneider, J. Am. Chem. Soc. **95**, 8698 (1973).

173. G. A. Olah and J. A. Olah, Alkyl carbonium ions, in *Carbonium Ions*, edited by G. A. Olah and P. von R. Schleyer, volume 2, pages 715–782, John Wiley, New York, 1970.

174. G. A. Olah, G. K. S. Prakash, and J. Sommer, *Superacids*, Wiley-Interscience, New York, 1985.

175. G. A. Olah, J. R. DeMember, R. H. Schlosberg, and Y. Halpern, J. Am. Chem. Soc. **94**, 156 (1972).

176. J. H. Vorachek, G. G. Meisels, R. A. Geanangel, and R. H. Emmel, J. Am. Chem. Soc. **95**, 4078 (1973).

177. F. A. Houle and J. L. Beauchamp, J. Am. Chem. Soc. **101**, 4067 (1979).

178. B. Ruscic, J. Berkowitz, L. A. Curtiss, and J. A. Pople, J. Chem. Phys. **91**, 114 (1989).

179. W. Klopper and W. Kutzelnigg, J. Phys. Chem. **94**, 5625 (1990).

180. R. Glaser, G. S. C. Choy, and M. K. Hall, J. Am. Chem. Soc. **113**, 1109 (1991).

181. P. Buzek, P. v. R. Schleyer, H. Vancik, and D. E. Sunko, J. Chem. Soc., Chem. Commun. **115**, 1538 (1991).

182. T. H. Dunning, Jr., J. Chem. Phys. **90**, 1007 (1989).

183. J. Gauss, Chem. Phys. Lett. **191**, 614 (1992).

184. J. Gauss, J. Chem. Phys. **99**, 3629 (1993).

185. R. Boese, D. Blaeser, N. Niederpruem, M. Nuesse, W. A. Btett, P. v. R. Schleyer, M. Buehl, and N. J. R. van Eikema Hommes, Angew. Chem. Int. Ed. Engl. **31**, 314 (1992).

186. S. Sieber, P. Buzek, P. v. R. Schleyer, W. Koch, J. M. W. Carneiro, H. Vancik, and D. S. Sunko, J. Am. Chem. Soc. **115**, 259 (1993).

187. P. Buzek, P. v. R. Schleyer, W. Koch, J. M. W. Carneiro, H. Vancik, and D. S. Sunko, J. Am. Chem. Soc. **115**, 671 (1991).

188. A. K. Jameson and C. J. Jameson, Chem. Phys. Lett. **134**, 461 (1987).

189. G. Trinquier, J. Am. Chem. Soc. **114**, 6807 (1992).

190. R. T. Morrison and R. N. Boyd, *Organic Chemistry*, Allyn and Bacon, Inc. Massachusetts, fifth edition, 1971.

191. F. Sun and T. Sorenson, J. Am. Chem. Soc. **115**, 77 (1993).

192. J. E. McMurry and T. Lectka, J. Am. Chem. Soc. **115**, 10167 (1993).

193. R. P. Kirchen, N. Okazawa, K. Ranganayakulu, and T. S. Sorensen, J. Am. Chem. Soc. **103**, 597 (1987).

194. G. A. Olah, Acc. Chem. Res. **9**, 41 (1976).

195. H. C. Brown, Tetrahedron **179**, 179 (1976).

196. G. A. Olah, E. B. Barker, J. C. Evans, W. S. Tolgyesi, J. S. McIntyre, and I. J. Bastien, J. Am. Chem. Soc. **86**, 1360 (1964).

197. J. R. D. George A. Olah, Anthony M. White, A. Commeyras, and C. Y. Lui, J. Am. Chem. Soc. **92**, 4627 (1970).

198. M. Saunders, M. H. Jaffe, and P. Vogel, J. Am. Chem. Soc. **93**, 2558 (1971).

199. M. Saunders and M. R. Kates, J. Am. Chem. Soc. **102**, 6867 (1980).

200. C. S. Yannoni, V. Macho, and P. C. Myhre, J. Am. Chem. Soc. **104**, 907 (1982).

201. P. v. R. Schleyer and J. Chandrasekhar, J. Am. Chem. Soc. **46**, 225 (1981).

202. M. J. S. Dewar, R. C. Haddon, A. Komornicki, and H. Rzepa, J. Am. Chem. Soc. **99**, 377 (1977).

203. D. W. Goetz, H. B. Schlegel, and L. C. Allen, J. Am. Chem. Soc. **99**, 8118 (1977).

204. G. Wenke and D. Lenoir, Tetrahedron **35**, 489 (1979).

205. H. J. Köhler and H. Lischka, J. Am. Chem. Soc. **101**, 3479 (1979).

206. J. D. Goddard, Y. Osamura, and H. F. Schaefer III, J. Am. Chem. Soc. **104**, 3258 (1982).

207. S. Masamune, M. Sakai, A. V. K. Jones, and T. Nakashima, Can. J. Chem. **52**, 855 (1974).

208. S. Masamune, M. Sakai, A. V. K. Jones, and T. Nakashima, Can. J. Chem. **52**, 858 (1974).

209. G. A. Olah, G. K. S. Prakash, T. N. Rawdah, D. Whittaker, and J. C. Rees, J. Am. Chem. Soc. **101**, 3935 (1979).

210. P. v. R. Schleyer, D. L. P. Mison, G. L. G. K. Prakash, and G. A. Olah, J. Am. Chem. Soc. **102**, 683 (1980).

211. M. Saunders, P. von R. Schleyer, and G. A. Olah, J. Am. Chem. Soc. **86**, 5680 (1964).

212. T. Onak, J. Tseng, M. Diaz, D. Tran, J. Arias, S. Herrera, and D. Brown, Inorg. Chem. **32**, 487 (1993).

213. S. A. Perera, R. J. Bartlett, and P. V. R. Schleyer, J. Am. Chem. Soc. **117**, 8476 (1995).

214. S. A. Perera, M. Nooijen, and R. J. Bartlett, Accepted for publication .

215. M. Karplus, J. Am. Chem. Soc. **58**, 2870 (1963).

216. J. L. Marshall, *Carbon-Carbon and Carbon-Proton NMR Couplings: Applications to Organic Stereochemistry and Conformational Analysis*, Verlag Chemie International, Deerfield Beach, Florida, 1983.

217. M. Karplus, J. Phys. Chem. **30**, 11 (1959).

218. M. Barfield and D. M. Grant, Advan. Magn. Resonance **1**, 149 (1965).

219. M. Barfield and M. Karplus, J. Am. Chem. Soc. **91**, 1 (1969).

220. M. Barfield and H. L. Gearhart, J. Am. Chem. Soc. **24**, 641 (1973).

221. M. Barfield and H. L. Gearhart, Mol. Phys. **27**, 899 (1974).

222. P. Mohanakrishnan and K. R. K. Easwaran, Biopolymers **18**, 1769 (1979).

223. A. S. Edison, J. L. Markley, and F. Weinhold, J. Biomol. NMR **4**, 519 (1994).

224. G. W. Vuister, F. Delaglio, and A. Bax, J. Am. Chem. Soc. **114**, 9674 (1992).

225. L. E. Kay, B. Brooks, S. W. Sparks, D. A. Torchia, and A. Bax, J. Am. Chem. Soc. **111**, 5488 (1989).

226. A. P. Marchand, *Applications of NMR Studies in Rigid Bicyclic Systems*, Verlag Chemie International, Deerfield Beach, Florida, 1982.

227. V. F. Bystrov, S. L. Portnova, V. I. Tsetlin, V. I. Ivanov, and Ovchinnikov, Tetrahedron **25**, 493 (1969).

228. A. E. Tonelli and F. A. Bovey, Macromolecules **3**, 410 (1970).

229. G. N. Ramachandran and R. Chandrasekaran, Biopolymers **10**, 935 (1971).

230. G. N. Ramachandran, R. Chandrasekaran, and K. D. Kopple, Biopolymers **10**, 2113 (1971).

231. A. E. Tonelli, J. Am. Chem. Soc. **94**, 346 (1972).

232. G. Wagner, S. G. Hyberts, and T. F. Havel, Annu. Rev. Biophys. Biomol. Struct. **21**, 167 (1992).

233. A. S. Edison, F. Weinhold, W. M. Westler, and J. L. Markley, J. Biomol. NMR **4**, 543 (1994).

234. M. Barfield and W. B. Smith, J. Am. Chem. Soc. **114**, 1574 (1992).

235. G. E. Schulz and Schirman, *Principles of Protein Structure*, Springer-Verlag, New York, 1979.

236. B. Sunners, L. H. Piette, and W. G. Schneider, Can. J. Chem. **38**, 681 (1960).

237. J. P. Marchal and D. Canet, J. Am. Chem. Soc. **97**, 6581 (1975).

238. M. Kitano, T. Fukuyama, and K. Kuchitsu, Bull. Chem. Soc. Jpn. **46**, 384 (1973).

239. E. Breitmaier and W. Voelter, *Carbon-13 NMR Spectroscopy*, VCH Publishers, New York, 1988.

240. G. Binsch, J. B. Lambert, B. W. Roberts, and J. D. Roberts, J. Am. Chem. Soc. **86**, 5564 (1964).

241. A. J. R. Bourn and E. W. Randall, Mol. Phys. **8**, 567 (1964).

242. J. P. Marchal and D. Canet, Org. Mag. Res. **15**, 6581 (1981).

243. D. G. Davis, W. C. Agosta, and D. Cowburn, J. Am. Chem. Soc. **105**, 5680 (1983).

244. M. Lier, J. Chem. Soc. Perkin Trans. **2**, 720 (1972).

245. J. Néel, Pure. Appl. Chem. **201**, 201 (1972).

246. M. T. Cung, M. Marraud, and J. Néel, Ann. Chim. Paris **7**, 183 (1972).

247. M. T. Cung, M. Marraud, and J. Néel, Macromolecules **7**, 606 (1974).

248. V. F. Bystrov, Progress in NMR Spectroscopy **10**, 41 (1976).

249. V. F. Bystrov, V. T. Ivanov, S. L. Portnova, T. A. Balashova, and Y. A. Ovchinnikov, Tetrahedron **29**, 873 (1973).

BIOGRAPHICAL SKETCH

S. Ajith D. Perera was born in 1962 in Weedagama, a hamlet 22 miles south of Colombo, Sri-Lanka. After earning a B. Sc. in chemistry from University of Sri-Jayewardenapura, Sri-Lanka, he spent three years as an assistant lecturer at his alma mater. As an assistant lecturer, in addition to teaching classes he was enthusiastically involved in natural product chemistry research. He took a big turn in his professional life by deciding to attend graduate school at University of Florida and pursue *ab initio* quantum chemistry under the guidance of Professor Rod Bartlett.

At Florida, in addition to the usual course of study and research for the Ph. D., he learned a lot about life in general and was able to interact with many interesting people from various parts of the world. In his graduate student career he was involved in several different research projects and one of these is the content of this dissertation. He feels that his time in Florida was fruitfully spent and well worth leaving home.

In his free time, though he has not had much of it lately, he would like to participate in social service activities, follow college sports and listen to music. After graduation he plans to continue theoretical chemistry research, once again at his new alma mater, the University of Florida with Professor Rod Bartlett.

I certify that I have read this study and that in my opinion it conforms to acceptable standards of scholarly presentation and is fully adequate, in scope and quality, as a dissertation for the degree of Doctor of Philosophy.

Rodney J. Bartlett

Rodney J. Bartlett Chair
Professor of Chemistry

I certify that I have read this study and that in my opinion it conforms to acceptable standards of scholarly presentation and is fully adequate, in scope and quality, as a dissertation for the degree of Doctor of Philosophy.

Michael C. Zerner

Michael. C. Zerner
Professor of Chemistry

I certify that I have read this study and that in my opinion it conforms to acceptable standards of scholarly presentation and is fully adequate, in scope and quality, as a dissertation for the degree of Doctor of Philosophy.

Samuel B. Trickey

Samuel B. Trickey
Professor of Physics

I certify that I have read this study and that in my opinion it conforms to acceptable standards of scholarly presentation and is fully adequate, in scope and quality, as a dissertation for the degree of Doctor of Philosophy.

Willis B. Person

Willis B. Person
Professor of Chemistry

I certify that I have read this study and that in my opinion it conforms to acceptable standards of scholarly presentation and is fully adequate, in scope and quality, as a dissertation for the degree of Doctor of Philosophy.

Daniel R. Talham
Associate Professor of Chemistry

This dissertation was submitted to the Graduate Faculty of the Department of Chemistry in the College of Liberal Arts and Sciences, and to the Graduate School and was accepted as partial fulfillment of the requirements for the degree of Doctor of Philosophy.

May 1996

Dean, Graduate School